INHIBITION OF CALCIUM-INDEPENDENT PHOSPHOLIPASE A_2 INDUCES PROSTATE CANCER CELL CYTOSTASIS

by

BIN SUN

(Under the Direction of Brian S. Cummings)

ABSTRACT

The goal of this work was to identify mechanisms by which inhibition of calcium-independent phospholipase A2 ($iPLA_2$) induces cytostasis in human LNCaP (p53 wild-type and androgen-sensitive) and PC-3 (p53 negative and androgen-insensitive) prostate cancer cells. Both the $iPLA_2$ selective inhibitor bromoenol lactone (BEL) and $iPLA_2\beta$ siRNA induced cytostasis. Cytostasis correlated to a G_1/G_0 arrest in LNCaP cells and a G_2/M arrest in PC-3 cells. In LNCaP cells, G_1 arrest was preceded by increases in tumor suppresser protein p53 and p21. In contrast, neither p53 nor p21 was detectable in PC-3 cells, suggesting that BEL activates p21 independently of p53. Further, the $iPLA_2\beta$ selective inhibitor *S*-BEL had greater affects on cytostasis, phosphorylated (P)-p53 (Ser15), p53 and p21 expression than the $iPLA_2\gamma$ inhibitor *R*-BEL, suggesting that $iPLA_2\beta$ plays more important roles in cytostasis and p53/p21 epxression than $iPLA_2\gamma$.

BEL decreased cell growth correlated to activation of p38MAPK in both cells. In contrast, BEL only transiently induced ERK in PC-3 cells but not in LNCaP and did not activate

JNK in either cell line. Pharmacological inhibition of p38 inhibited BEL-induced increases in P-p53 (Ser15), p53 and p21 as well as G1 arrest in LNCaP cells. BEL treatment also induced reactive species (RS) in PC-3 and LNCaP cells. The antioxidant NAC inhibited BEL-induced RS, p38, p53 and cytostasis in LNCaP cells and attenuated BEL induced RS and cytostasis in PC-3 cells, supporting the hypothesis that RS mediated cytostasis induced by $iPLA_2$ inhibition.

Cytostasis induced by $iPLA_2$ inhibition was not reversed by lysophosphatidic acids (LPA) or polyunsaturated fatty acids (PUFA). Thus we tested the hypothesis that $iPLA_2$ inhibition induces cytostasis in prostate cancer cells by altering phospholipid profiles. BEL treatment increased the abundance of unsaturated phosphatidylcholine (PtdCho) and decreased saturated PtdCho without altering phosphatidylserines (PtdSer) or phosphatidylethanolamines (PtdEtn). These results demonstrate that $iPLA_2$ inhibition alters the phospholipid profile of human prostate cancer cells in correlation with induction of cytostasis and identifies the specific phospholipids involved.

In conclusion, novel roles of $iPLA_2$ in prostate cancer cell growth and signaling are demonstrated, suggesting that $iPLA_2$ represent a novel therapeutic target for treatment of prostate cancer.

INDEX WORDS: Phospholipase A_2, Phospholipids, p53, Mitogen Activated Protein Kinases, Reactive species, Phospholipid Profiles

INHIBITION OF CALCIUM-INDEPENDENT PHOSPHOLIPASE A_2 INDUCES PROSTATE CANCER CELL CYTOSTASIS

by

BIN SUN

B.S., East China Normal University, China, 2001

M.S., East China Normal University, China, 2004

A Dissertation Submitted to the Graduate Faculty of The University of Georgia in Partial Fulfillment of the Requirements for the Degree

DOCTOR OF PHILOSOPHY

ATHENS, GEORGIA

2010

INHIBITION OF CALCIUM-INDEPENDENT PHOSPHOLIPASE A_2 INDUCES PROSTATE CANCER CELL CYTOSTASIS

by

BIN SUN

Major Professor:	Brian S. Cummings
Committee:	Michael G. Bartlett James Franklin Julie Coffield Robert Arnold

Electronic Version Approved:

Maureen Grasso
Dean of the Graduate School
The University of Georgia
August 2010

ACKNOWLEDGEMENTS

Firstly, I thank my advisor Dr. Brian Cummings, for his continuous support throughout my Ph.D. training at The University of Georgia. Dr. Cummings is an excellent advisor. He was responsible for bring me in this PhD program and the iPLA$_2$-prostate cancer project in the first place. When I had problems with experiments, he was always there to listen patiently and to give constructive advice to me. In the last four years, he has been teaching me the way of scientific thinking and effective writing, and he has been always encouraging me to develop my own ideas. In my mind, he is not only a good teacher but also a good friend I can always trust and rely on.

Secondly, I thank my wife-Shirley, who has been consistently supporting me in my research for eight years and will also be supportive for the rest of my life, regardless of success or failure. She is always encouraging me to stick with my objectives of my research. I also want to thank my parents for bringing me to the world, doing their best to develop and educate me into a good person. They are always standing behind me in my path to obtaining the PhD degree.

Last but not least, I would like to thank all of the professors in my committee for excellently advising me on my research, including Dr. Michael Bartlett, Dr. James Franklin, Dr. Julie Coffield and Dr. Robert Arnold. I also want to say thanks to all my lab mates Jason Mock, Narendababu Kolisetty, Darren Gullick, Leah Costyn and Krelin Naidu as well as people from other labs such as Dr. Jillian Hurst, Philip Callahan, Ibrahim Aljufalli and Guodong Zhu. All of them have contributed to the research work during my PhD training at The University of Georgia.

TABLE OF CONTENTS

Page

LIST OF TABLES

Page

LIST OF FIGURES

Page

ABBREVIATIONS

2D-HP-TLC-ESI/MS = two dimensional high performance thin layer liquid chromotagraphy tandem with electrospray ionization mass spectrometry

AA = arachidonic acid

AAOCF3 = arachidonyl trifluoromethylketone

ASA = ascorbic acid

ATR = ataxia telangiectasia and rad-3-related kinase

BEL = bromoenol lactone

CM-H2DCFDA = 5-(and-6)-chloromethyl-2 7 -dichlorodihydrofluorescein diacetate acetyl ester

COX = cyclooxygenase

$cPLA_2$ = cytosolic phospholipase A_2

CTB = celltiter blue

DHA = docosahexaenoic acid

EGF = epidermal growth factor

EGFR = epidermal growth factor receptor

ER = endoplasmic reticulum

ERK = extracellular-signal-regulated kinases

GAPDH = glyceraldehyde-3-phosphate dehydrogenase

$iPLA_2$ = Ca^{2+}-independnt phospholipase A_2

JNK/SAPK = c-jun N-terminal kinase/stress-activated protein kinase

LA = linoleic acid

LOX = lipoxygenase

LPA = lysophosphatidic acid

$LPLA_2$ = lysosomal phospholipase A_2

LysoPC = lysophosphatidylcholine

MAFP = methyl arachidonyl fluorophosphonate

MAPK = mitogen activated protein kinase

MEK = mitogen activated protein kinase/extracellular signal-regulated kinase kinase

MEKK= mitogen activated protein kinase kinase kinase

MMP = matrix metalloproteinase

mTOR = mammalian target of rapamycin

MTT = 3-(4, 5-Dimethylthiazol-2-yl)-2,5-diphenyltetrazolium bromide

MUFA = monounsaturated fatty acid

NAC = N-acetyl-cysteine

PAF-AH = platelet activating factor-acetylhydrolase

PGE_2 = prostaglandin E_2

PI = propidium iodide

PLA_2 = phospholipase A_2

PtdCho = phosphatidylcholine

PtdSer = phosphatidylserine

PtdEtn = phosphatidylethanolamine

PUFA = polyunsaturated fatty acid

PUPC = polyunsaturated phosphatidylcholine

$sPLA_2$ = secretory phospholipase A_2

RS = reactive species

SFA = saturated fatty acid

SPC = saturated phosphatidylcholine

SRB = sulforhodamine B

CHAPTER 1

INTRODUCTION

Phospholipase A_2

Phospholipase A_2 (PLA_2) are a diverse class of esterases that hydrolyze the *sn*-2 ester bond of glycerophospholipids, releasing a free fatty acid and a lysophospholipid (Dennis, 1997) (**Fig. 1.1)**. PLA_2 are involved in both physiological and pathological events. The best-known roles for PLA_2 are in the facilitation of arachidonic acid-mediated inflammation (Capper et al, 2001) and the sequelae following this event, such as cell proliferation, injury, death and carcinogenesis.

PLA_2 are broadly classified into five major classes; secretory PLA_2 ($sPLA_2$), cytosolic PLA_2 ($cPLA_2$), Ca^{2+}-independent PLA_2 ($iPLA_2$), platelet activating factor acetylhydrolase (PAF-AH) and lysosomal PLA_2 ($LPLA_2$) (Schaloske et al, 2006). $sPLA_2$ are the oldest known class of PLA_2, ranging in size from 3 to 19 kDa, and typically require millimolar concentrations of Ca^{2+} for their activity, and utilize histidine to hydrolyze the *sn*-2 ester bond of the glycerol backbone.

$cPLA_2$ and $iPLA_2$ are larger in size than $sPLA_2$, typically 66–90 kDa, and utilize serine to facilitate the hydrolytic cleavage of the *sn*-2 fatty acid (Ackermann et al, 1994; Balsinde et al, 2002A). The major difference between these two enzymes is that $cPLA_2$ require Ca^{2+} to facilitate translocation to membrane, while $iPLA_2$ do not require Ca^{2+} for either activity or translocation to membranes (Balsinde et al, 2002A). PAF-AH and $LPLA_2$ are the two newest members of the

PLA_2 superfamily. PAF-AH range from 26-45 kDa, while $LPLA_2$ is 45 kDa. Both PAF-AH and $LPLA_2$ are Ca^{2+}-independent.

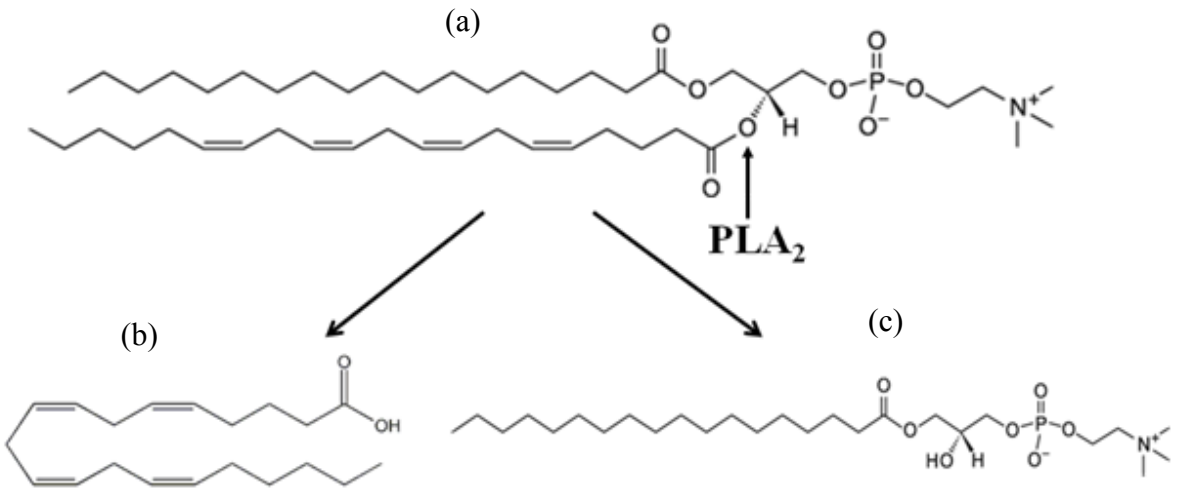

Figure 1.1. Basic glycerophospholipid structure. Phospholipase A_2 acts on the ester bond at the *sn*-2 position of the glycerol backbone (a) to release a fatty acid (b) and a lysophospholipid (c).

Classification of phospholipase A_2

Recently, a new classification system has been introduced that organizes PLA_2 based on their genetic sequence into 15 distinct groups (designated by a roman numeral), encompassing over 34 individual members (designated by arabic letters). This organization system comprises the five main types of PLA_2 mentioned above (Balsinde et al, 2002B; Cummings, 2007; Schaloske et al, 2006; Burke et al, 2009). (**Table 1. 1**). $sPLA_2$ are represented by Groups I–III, V, and IX–XIV. $cPLA_2$ are represented by Group IV PLA_2 including six isoforms: Group IVA, B, C, D, E and F in which Group IVC is unique because it is membrane-associated (Stewart et al, 2002). $iPLA_2$ are defined as Group VI and is comprised of at five known members (Balsinde et al, 2002A). Group VIA, also known as $iPLA_2\beta$, is expressed in the cytosol and has two splice variants-Group VIA-1 and A-2 (Ma et al, 1999). In contrast, Group VIB, also known as $iPLA_2\gamma$, is localized to the endoplasmic, peroxisomal, and mitochondrial membranes (Mancuso et al, 2000; Mancuso et al, 2004; Cummings et al, 2002). In order to avoid confusion, the traditional names $iPLA_2\beta$ and $iPLA_2\gamma$ will be used instead of Group VIA and VIB in the following chapters.

Unlike $cPLA_2$, which have preference for arachidonic acid at the *sn*-2 position, $iPLA_2$ have no preference for fatty acids at the *sn*-2 position (Tang et al, 1997); however, $iPLA_2$ prefer phospholipids that contain a vinyl ether linkage at the *sn*-1 position (Hazen et al, 1990; Hazen et al 1991). In 2004, three novel calcium-independent PLA_2, named $iPLA_2\varepsilon$, $iPLA_2\zeta$, and $iPLA_2\eta$, were identified (Jenkins et al, 2004). These were subsequently designated as GroupVID, E and F .

Groups VII and VIII PLA_2 are Ca^{2+}-independent, and range in size from 26 to 45 kDa. These are the aforementioned PAF-AH (Kell et al, 2003). Like $iPLA_2$ or $cPLA_2$, PAF-AH utilize a catalytic serine to hydrolyze the *sn*-2 ester bond, but they typically act to deacetylate, and inactivate PAF, as opposed to cleaving glycerophospholipids.

Table 1. 1 Classification of Phospholipase A_2*

Class	Active site	Group	Ca^{2+}	Molecular Weight	Subcellular Locaion	Sources
$sPLA_2$	Histidine	IA-B	mM	13-15	Secretory	Cobras and kraits (A) Human pancreas (B)
		IIA-F		13-17	Secretory	Rattlesnakes/gaboon viper/human/rodent
		III		15-18	Secretory	Human/murine/lizard/bee
		V		14	Secretory	Human/murine heart/lung/macrophage
		IX		14	Secretory	Snail venom
		X		14	Secretory	Human spleen/thymus/leukocyte
		XIA-B		12-13	Secretory	Green rice shoots
		XII		18-19	Secretory	Human/murine
		XIII		<10	Secretory	Parvovirus
		XIV		13-19	Secretory	Symbiotic fungus/ bacteria
$cPLA_2$	Serine	IVA(α)	μM	85	Cytosolic	Human/murine
		IVB(β)	μM	114	Cytosolic	Human
		IVC(γ)	none	61	Cytosolic	Human
		IVD(δ) IVF(ζ)	μM	100	Cytosolic	Human/murine
$iPLA_2$	Serine	VIA (β)	none	84-85	Cytosolic	Human/murine
		VIB (γ)		63-88	Membrane	Human/murine
		VIC (δ)		146	Membrane	Human/murine
		VID (ε)		53	Membrane	Human
		VIE (ζ)		57	Membrane	Human
		VIF (η)		28	Membrane	Human
PAF-AH	Ser/His/ Asp	VIIA	none	40-45	Secretory	Human/murine/porcine/bovine
		VIIB		40	Cytosolic	Human/bovine
		VIIIA-B		26	Membrane	Human
Lysosomal PLA_2	Ser/His/ Asp	XV	none	45	Lysosomes	Human/murine/bovine

*Adapted from (Schaloske, et al 2006 and Cummings, 2007)

$LPLA_2$ is a 45 kDa protein that is exclusively located in lysosomes. This enzyme possesses Ca^{2+}-independent activities and, interestingly, exhibits transacylase and O-acylceramide synthase activities as well as PLA_2 activitity (Hiraoka et al, 2002). Recently, $LPLA_2$ has been demonstrated to have preference for the hydrolysis of phosphatidylcholine (PtdCho) and phosphatidylethanolamine (PtdEtn) (Hiraoka et al, 2006).

General functions of Group VI Calcium-Independent PLA_2

The first defined role of Ca^{2+}-independent PLA_2 ($iPLA_2$) involved cellular phospholipid remodeling (Balsinde et al, 1995). This resulted in $iPLA_2$ as being labeled a "housekeeping" protein, only important for generating substrates for the Lands Cycle. This cycle is a reacylation/deacylation pathway used for altering the free fatty acids present in phospholipids. This cycle is integral to the maintenance of normal cell membrane homeostasis (Lands, 1965). Basically, it involves the cleavage of a fatty acid by $iPLA_2$ at the *sn*-2 position of a phospholipid. This creates a lysophospholipid that is reesterified with another fatty acid by acyl-CoA: lysophosphatidic acyltransferase (**Figure 1.2)**.

$iPLA_2$ are not the only PLA_2 involved in the Lands Cycle. $cPLA_2$ can also be involved: however, $cPLA_2$ preferentially cleave glycerophospholipids that contain arachidonic acid (20:4) at the *sn-2* position. (Balsinde et al, 2000; Ramanadham et al, 1997; Balsinde et al, 1997A; Balsinde et al, 1997B). In contrast, $iPLA_2$ participate in the Lands cycle by releasing relatively low levels of arachidonic acid, or facilitating LPA formation. This is important because it causes limited inflammation and cell death.

It should be noted that $iPLA_2$ roles as housekeeping enzymes might not apply to all cells. In fact, studies in insulinoma INS-1 cells suggest that $iPLA_2$ may play more significant roles in

cell signaling than phospholipid remodeling (Balsinde et al, 2000; Balsinde et al, 1997A; Balsinde et al, 1996). Thus, the functions of $iPLA_2$ appear to be cell-dependent.

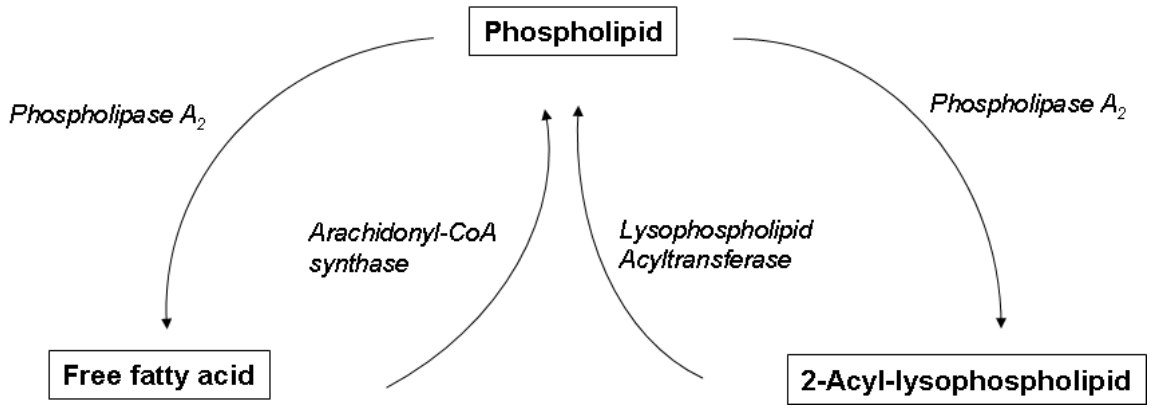

Figure 1.2. Lands Cycle (Peterson, 2007).

Methods for inhibition of $iPLA_2$

Diverse chemical inhibitors of $iPLA_2$ are characterized (**Table 1.2**). One of the most widely used is the selective inhibitor bromoenol lactone (BEL or (E)-6-(1-bromoethyl) tetrahydro-3-(1 naphthalenyl)-2H-pyran-2-one)) (Hazen et al, 1991). BEL inhibits $iPLA_2$ irreversibly in a mechanism that involves covalent interactions. The mechanism of inhibition is unique and has been recently described (Song et al, 2006B). Briefly, serine-mediated hydrolysis of BEL results in ring opening of the chemical. This hydrolyzed product is believed to form a diffusible bromomethyl keto acid that alkylates and inactivates functional cysteine groups located in the $iPLA_2$ active site.

BEL also inhibits phosphatidate phosphohydrolase (PAP-1) at relatively high concentrations (IC_{50} approximately 25 μM (Balsinde et al, 1996)). In contrast, BEL does not inhibit $cPLA_2$ or $sPLA_2$ at similar doses. As a result, concentrations of BEL of 2 μM to 10 μM

are used to distinguish between events mediated by $cPLA_2$ and $iPLA_2$, and to eliminate roles for PAP-1.

Other inhibitors of $iPLA_2$ include methyl arachidonyl flourophosphonate (MAFP) and arachidonyl triflouromethylketone ($AAOCF_3$). Unlike BEL, MAFP and $AAOCF_3$ also inhibit Group IV PLA_2 ($cPLA_2$) at similar concentrations that they inhibit $iPLA_2$ (5-10 μM) (Cummings et al, 2000).

Recently *R*- and *S*-enantiomers of BEL were developed and validated to selectively inhibit $iPLA_2\gamma$ and β respectively (Jenkins et al, 2002; Kinsey et al, 2005). The mechanisms involved in their selectivity are under study; however, they have similar IC_{50} in cells as racemic BEL (50:50 mixture of *R*- and *S*-BEL, 2–5 μM). *R*- and *S*-BEL have proven extremely useful as tools to distinguish between $iPLA_2\beta$ and $iPLA_2\gamma$.

Several molecular techniques have been developed for inhibition of $iPLA_2$. Multiple studies have used siRNA or anti-sense oligonucleotides to knockdown $iPLA_2$ (Zhang et al, 2006; Herbert et al 2006; Saavadra G et al, 2006; Yellatulu et al, 2003), as well as $iPLA_2\gamma$ (Saavadra et al, 2006, Kinsey et al, 2008). Further, studies using $iPLA_2\beta$-null mice (Bao et al, 2004; Ramandaham et al, 2008) and $iPLA_2\gamma$-null mice (Song et al, 2010) have recently been published.

Table 1.2 Pharmacological inhibitors of PLA_2*

Enzyme	Inhibitor	IC_{50}	Reference
General	Manoalide	30-500 mM	(Farooqui et al, 1999)
$sPLA_2$	3-(3-Acetamide-1-benzyl-2-ethylindolyl-5-oxy) propane sulfonic acid (LY311727)	20-40 nM	(Balsinde et al, 1999)
$cPLA_2$, $iPLA_2$ PAF-AH	Methyl arachidonyl fluorohosphonate (MAFP)	0.5 μM	(Lio et al, 1996) (Kell et al, 2003)
$cPLA_2$, $iPLA_2$	Arachidonyl trifluoromethyl ketone ($AACOCF_3$)	0.3 μM 15 μM	(Ackermann et al, 1995)
$iPLA_2\gamma$	*R*-Bromonel lactone (*R*-BEL)	2 μM	(Jenkins et al, 2002)
$iPLA_2\beta$	*S*-Bromoenol lactone (*S*-BEL)	1 μM	(Jenkins et al, 2002)
PAF-AH	Diisopropylfluorophosphate (DFP)	1mM	(Meyer et al, 2004)
	Phenylmethylsulfonylfluoride (PMSF)	1mM	(Jarvi et al, 1993)

*Adapted from (Cummings, 2007)

Role of Ca^{2+}-independent phospholipase A_2 in cell growth and signaling

Recent studies demonstrate that $iPLA_2$ mediate cell growth, cell cycle regulation and cell signaling in both cancerous and non-cancerous cell models including insulinomas, ovarian cancer, colon cancer, human embryo kidney (HEK293) cells, fibroblasts, macrophages and endothelial cells (HEVUC and HDMEC) (Saavedra et al, 2006; Zhang et al, 2006; Song et al, 2007; Herbert et al, 2006).

Although several studies, including our own, suggest that both $iPLA_2\beta$ and γ are involved in cell growth (Jenkins et al, 2002; Murakami et al, 2005; Cummings et al, 2004), a majority of these studies focused on $iPLA_2\beta$. These studies suggest that $iPLA_2$ inhibition induces cytostasis and p53-dependent G1 cell cycle arrest rather than cell death in insulinoma cells (Zhang et al, 2006). In contrast, other studies report $iPLA_2$ inhibition induces moderate levels of cell death and G2/M arrest in ovarian cancer cells, independent of p53 (Song et al, 2007). Further, $iPLA_2$ inhibition also alters cyclin A/CDK2, induces G1 arrest, decreases growth and angiogenesis in HUVEC cells (Herbert et al, 2006). Thus, the above studies suggest that inhibition of $iPLA_2$ induces cytostasis, cell death and cell cycle arrest in multiple cell types; however, the intrinsic mechanisms involved are not well understood. One of the goals of this work is to determine the cellular and molecular signaling mechanisms involved in cytostatis induced by $iPLA_2$ inhibitors.

Mitogen activated protein kinases and Ca^{2+}-independent phospholipase A_2

Mitogen activated protein kinases (MAPK) are serine-threonine kinases activated by a cascade of protein-protein interactions. They are crucial mediators of proliferation, adhesion, differentiation, gene expression and apoptosis in several types of cancer cells (Chen et al, 2001). They also mediate the activation of the tumor suppressor protein p53 in several studies

(Reinhardt et al, 2007; Bae et al, 2006). The most extensively studied MAPK are extracellular signal-regulated kinase 1 and 2 (ERK1/2), p38 MAPK and c-jun N-terminal kinase/stress-activated protein kinase (JNK/SAPK). MAPK are activated by kinases called MAPK/extracellular signal-regulated kinase or MEK (Seger et al, 1995).

The mitogenic ability of ERK1/2 correlates to their translocation to the nucleus and activation of transcription factors such as AP-1, Elk-1 and c-Myc (Campbell et al, 1998), however, ERK 1/2 can also mediate apoptosis. For example, ERK 1/2 is needed for oxidant-induced cell death in oligodendrocytes and cisplatin-induced apoptosis in HeLa cells (Wang et al, 2000; Bhat et al, 1999). The role of ERK1/2 in mitogenic or cell death processes depends on both the cell types and stimuli of activation. ERK1/2 can be activated through the epidermal growth factor receptor (EGFR), which is mediated by a small G-protein Ras (Sabbatini et al, 2006; Morrison et al, 1997; Avruch et al, 1994; Williams et al, 1994). EGFR mediated activation of Ras, and subsequent activation of ERK1/2 is dysregulated in several types of cancers including prostate cancer (Gioeli et al, 1999), suggesting the hypothesis that this pathway is a target for therapeutic intervention of prostate cancer cell growth.

p38 MAPK and JNK/SAPK are activated in response to cellular stress, inflammation and apoptosis (Kyriakis et al, 1994; Frasch et al, 1998). In contrast to ERK, p38 and JNK are commonly known as stress activated protein kinase (SAPK) as they are activated by diverse cell stresses including irradiation, heat shock, reactive oxygen species, LPS, TNF and IL-1 (Krishina et al, 2008). The mechanism of activation differs from ERK1/2 as p38 and JNK are activated by a different small G-protein called Rac, which activates distinct MEKK and MEK than those involved in ERK1/2 activation (Frasch et al, 1998).

Recent evidence suggests that p38 and JNK play key roles in anticancer pathways in prostate cancer cells, including cytostasis, cell cycle arrest and apoptosis (Reinhardt et al, 2007; Fan et al 2001; Chang et al, 2008; Bradham et al, 2006). The mechanisms involved are linked to the activation of the tumor suppressor protein p53, which activates proteins involved in cell cycle arrest (Reinhardt et al, 2007; Brown et al 2006), apoptosis (Kim et al, 2006) and proteins linked to DNA damage such as GADD153 (Woo et al, 2007; Oh-Hashi et al, 2001).

To our knowledge, no study has reported on links between $iPLA_2$ and MAPK activation in cancer cells. Recent studies show that thrombin stimulates both MAPK and $iPLA_2$ activity in ventricular myocytes and vascular smooth muscle cells (Yellaturu et al, 2003). One of these studies showed that $iPLA_2$ inhibition decreased agonist-stimulated MAPK activation (Beckett et al, 2006). Another study showed that MAPK mediated $iPLA_2$ activity during hypoxia in mouse neural cells (Aoto et al, 2009). It should be noted that several studies demonstrate links between MAPK and $cPLA_2$ (Xu et al, 2002; Han et al, 2003; Hassan et al, 2006), however, $iPLA_2$ and $cPLA_2$ are different proteins, with different substrate preferences, locations within the cell and Ca^{2+} requirements.

Oxidant stress and Ca^{2+}-independent phospholipase A_2

Several oxidants such as H_2O_2, NO, and HOCl inactivate $iPLA_2\beta$ by oxidizing multiple Cysteine residues. During oxidative stress $iPLA_2\beta$ will be oligomerized and inactivated by forming intermolecular disulfide bonds, and this process can be partially reversed by dithiothreitol (DTT) (Song et al, 2006). Other researchers report that oxidants such as *tert*-butylhydroperoxide (TBHP) also inactivate $iPLA_2\gamma$ which is also reversed by DTT as well (Cummings et al, 2004). Recently it was suggest that $iPLA_2$ prefer to catalyze the hydrolysis of

oxidized phospholipids (Kinsey et al, 2008). This finding suggests the novel hypothesis that cells utilize $iPLA_2$ as an antioxidant to fight against phospholipid peroxidation and maintain the integrity of cell membrane.

Lipidomics and Ca^{2+}-independent phospholipase A_2

Lipidomics may be defined as the large-scale study of pathways and networks of cellular lipids in biological systems (Wenk, 2005). A majority of studies solely investigate arachidonic acid-containing lipids (Green et al, 2008, Wilkins et al, 2008).

In contrast to $cPLA_2$ and $sPLA_2$, $iPLA_2$ have some unique characteristics with regards to their catalytic activities and preference for phospholipids. For example, unlike $cPLA_2$, $iPLA_2$ have no preference for the *sn*-2 fatty acid, but appear to have preferences for phospholipids with choline and ethanolamine groups other than inositol groups (Tang et al, 1997; Yang et al, 1999) as substrates. With regards to the *sn-1* linkage of the glycerol backbone, $iPLA_2$ can metabolize all phospholipids, but prefers those with an alkenyl linkage as opposed to an alkyl linkage (McHowat et al, 2001).

As mentioned above, the first-characterized function of $iPLA_2$ is phospholipid remodeling, which is supported by two key pieces of evidence; 1) $iPLA_2$ mediate the incorporation of exogenous arachidonic acid into cell membranes (Balsinde et al, 2000; Ramanadham et al, 1997; Balsinde et al, 1997A; Balsinde et al, 1997B) and regulate exogenous phospholipid metabolism to generate lysophospholipids (Baburina et al, 1999); 2) and in some cell types, $iPLA_2\beta$ activity maintains the steady-state level of cellular lysophosphatidylcholine. For example, treatment of $P388D_1$ macrophages with BEL, or antisense oligonucleotides reduces, cellular lysoPC levels by 50–60% (Balsinde et al,1997A). In pancreatic islets, which naturally contain exceedingly high

levels of lysoPC, BEL lowers lysoPC levels by approximatley 20–25% (Ramanadham et al, 1999). Another study reports that iPLA$_2$β inhibition increases phosphatylcholines containing omega-3 polyunsaturated fatty acids in insulinoma cells (Zhang et al, 2006), suggesting iPLA$_2$β may favor this particular type of phospholipid.

Recently, it has been reported that iPLA$_2$ is involved in lipid raft regulation (Nakano et al, 2009). This study suggests that cells utilize inverted cone-shaped lysophospholipids generated by iPLA$_2$ to modulate plasma membrane structure and assist the budding of raft-associated plasma membrane particles, which virus utilizes in budding. These brush borders are enriched with membrane-rafts and undergo rapid turnover, suggesting that iPLA$_2$ may be involved in the regulatory mechanism of membrane dynamics.

Prostate cancer and phospholipase A$_2$

Prostate cancer is the most common cancer in man, excluding skin cancer, and is the second leading cause of cancer-related death in men in the United States (www.cancer.gov). Mortality from prostate cancer is associated with progression of tumors to androgen-independent growth and metastasis. Eicosanoid products of both the cyclooxygenase (COX) and lipoxygenase (LOX) pathways are important mediators of prostate cancer cell proliferation in vitro and regulate tumor vascularization and metastasis in animal models (Vijayakrishnan, 2009). PLA$_2$'s role in this is believed to be the provision of arachidonic acid, which leads to COX- and LOX-derived eicosanoids (Dong et al, 2006).

It is reported that Group IIA sPLA$_2$ is elevated in prostate cancer tissues compared with either benign tumors or normal tissues (Graff et al, 2001, Sved et al, 2004). Further, cPLA$_2$α is expressed in both androgen-sensitive and –insensitive prostate cancer cells lines, but increased in

androgen-insensitive cells (Patel et al, 2008). Inhibition of Group IIA $sPLA_2$ or $cPLA_2\alpha$ decreases prostate cancer cell growth in both in vitro models and in vivo xenograft models (Graff et al, 2001, Sved et al, 2004, Patel et al, 2008). However, to our knowledge, no study has reported the expression of $iPLA_2$ in prostate cancer cells and or demonstrated the relationship of between $iPLA_2$ and prostate cancer cell growth.

Conclusion

$iPLA_2$ functions are not only to maintain phospholipid remodeling, but also to mediate cell growth and signaling in numerous cancer and non-cancer cells. Previous studies suggest important roles for $iPLA_2$ in agonist activated MAPK pathways and cellular redox regulations. Owing to the fact that there are strong correlations between RS, MAPK and p53, we hypothesize that $iPLA_2$ may be involved in these particular pathways in prostate cancer. However, the expression of $iPLA_2$ in prostate cancer cells and their roles in cell proliferation are not fully understood. Therefore, this disseratation tests the novel hypothesis that inhibition of $iPLA_2$ decreases prostate cancer cell growth, using pathways involving RS and MAPK. These studies will aid in our understanding of the mechanism of $iPLA_2$ mediated cell growth and determine if $iPLA_2$ is a novel therapeutic target for prostate cancer.

CHAPTER 2

MATERIALS AND METHODS METHODS

Materials

Reagents and antibodies

PC-3 cells (p53 negative, androgen-independent human prostate cancer), LNCaP cells (p53 positive, androgen-dependent human prostate cancer), Ham's F-12K medium, RPMI-1640 and fetal bovine serum (FBS) were purchased from American Type Culture Collection (Manassas, VA). Penicillin, streptomycin, lipofectamine2000 and Optimum I® media were obtained from Invitrogen (Carlsbad, CA). Mouse anti p53, p21, Mdm2 and GAPDH monoclonal antibodies, rabbit anti JNK/SAPK antibodies and goat anti $iPLA_2$ were purchased from Santa Cruz Biotechnology (Santa Cruz, CA). Mouse anti phospho-p38 (Thr180/Tyr182) and phospho-JNK/SAPK (Thr183/Tyr185) rabbit anti p38, phospho-ERK1/2 (Thr202/Tyr204) and ERK1/2 antibodies were purchased from Cell Signaling Technology (Danvers, MA). Horseradish peroxidase (HRP)-linked anti-mouse, anti-rabbit and anti-goat IgG were obtained from Promega (Madison, WI). Racemic bromoenol lactone (BEL), *S*-BEL ($iPLA_2\beta$ inhibitor) and *R*-BEL ($iPLA_2\gamma$ inhibitor) were obtained from Cayman Chemical Co. (Ann Arbor, MI). SB202190, SB203580, AG1478 and GM6001 were purchased from Calbiochem (San Diego, CA). CM-H2DCFDA was obtained from Invitrogen (Calsbad, Ca), Propidium iodide (PI), Trypan blue, the Bicinchoninic Acid Assay kit, and all other chemicals not mentioned were obtained from Sigma-Aldrich (St. Louis, MO).

Methods

Cell culture

PC-3 and LNCaP cells were grown under the conditions recommended by ATCC for each cell line. PC-3 cells were cultured in F-12K media supplemented with 10% (v/v) heat inactivated FBS, 100 mg/L streptomycin and 100 U/mL of penicillin G at 37ºC in a humidified atmosphere of 95% air and 5% CO_2. LNCaP cells were grown under the same conditions except that RPMI 1640 media was used. The passages of both cell lines were no more than 30 during all experiments. Cells were grown in 12-well plates for immunoblot analysis and in 48-well plates for cell growth studies. All cells were seeded at 64,000 or 128,000 cells/mL for 24 hr prior to pharmacological treatment. For inhibitor studies, cells were treated with the respective inhibitors for 30 min prior to treatment.

Measurement of iPLA$_2$ activity

After treatment, cells were collected, and subcellular fractions were isolated using differential centrifugation. Arachidonoyl thio-phosphatidylcholine was used as a synthetic substrate to detect PLA_2 activity. Hydrolysis of the arachidonoyl thioester bond at the *sn*-2 bond by PLA_2 releases a free thiol that can be detected by 5,5′-dithiobis(2-nitrobenzoic acid). PLA_2 activity was measured in cytosolic and microsomal fractions in the absence and presence of racemic, *R*-or *S*-BEL, and 4 mM EGTA. Samples were treated for 30 min at room temperature before the assay. Activity was calculated by measuring the absorbance of 5,5′-dithiobis(2-nitrobenzoic acid) ($\varepsilon = 10.66$) at 404 nm and normalized with the protein content of each sample.

Assessment of cell morphology

Cell morphology was determined using a Nikon AZ100 fluorescence microscope (Nikon, Melville, NY).

RNA interference

At 40% confluence, cells were transfected with 40 nM annealed iPLA$_2$-VIA siRNA (Sense: 5′-GGAUCUCAUGCACAUCUCATT-3′, antisense: 5′-UGAGAUGUGCAUGAGAUCCTG-3′ siRNA; 139141; Ambion, Austin, TX) or 40 nM non-targeting control siRNA (mock-transfection; 12935-300; Invitrogen, Carlsbad, CA), which were diluted in serum-free Opti-MEM I Medium, for 6 hr using the Lipofectamine2000 transfection reagent (Invitrogen, Carlsbad, CA). After 6 hr the siRNA-containing media was replaced with fresh growth media. iPLA$_2$ mRNA and protein levels were determined after 72 and 96 hr.

Real time-PCR

Real time-PCR for assessment of iPLA$_2\beta$ expression was performed as previously described (Saavedra, et al, 2006). Briefly, total RNA was isolated using TRIzol® reagent as directed by the manufacturer (Invitrogen, Carlsbad, CA). cDNA was prepared using Omniscript RT Kit (Qiagen, Valencia, CA) for 60 min at 37°C, diluted in the range of 0.1 to 1.0 x 10^{-6} μg/μL in sterile H_2O, and 25 μL of SuperMix SYBR (Bio-Rad, Hercules, CA) was added along with 1 μL of forward and reverse primers for glyceraldehyde-3-phosphate dehydrogenase (GAPDH) of iPLA$_2\beta$ and 5 μL of each cDNA reaction along with sterile H_2O. Negative controls included the absence of cDNA. Each sample was run in duplicate (20 μL per reaction) using a Bio-Rad ICycler sequencer in 96-well PCR plates under the conditions of 95°C for 3 min, followed by 40

cycles at 95°C for 10 s and 55°C for 1 min. For all of the cells, a separate GAPDH reaction was performed for normalization. A standard curve was generated for each set of primers and each set of cells. PCR efficiency was determined by analysis of serial dilutions of cDNA for each primer set. Quantification of RNA was based on comparison of the number of cycles required to reach reference and target threshold values (Ct) as normalized against GAPDH. The primers used for real-time PCR are as follows: GAPDH sense = 5'-AAGGTCGGAGTCAACGGAT-3', GAPDH antisense = 5'-TGGAAGATGGTGATGGGATT-3'; iPLA$_2$β sense = 5'-TCCTGAAGCGGGAGTTTG-3', iPLA$_2$β antisense = 5'-GACAGTTTCTGGAGCATCGTA-3'.

Immunoblot analysis

After treatment, cells were washed three times using PBS and collected using a rubber policeman in immunoblot buffer ((0.25 M TrisHCl (pH 6.8), 4% SDS, 10% glycerol, 1 mg/mL bromophenol blue and 0.5% (v/v) 2-mercaptoethanol)). Protein levels were determined in duplicate wells using a lysis buffer that contained 1% (v/v) Triton X-100. Following isolation, cell lysates containing 20 μg total protein were heated to 70°C for 10 min, separated under reducing conditions on a 12% SDS-polyacrylamide gel, and transferred to a nitrocellulose membrane. Non-specific binding was blocked by incubating the membrane with 3% (w/v) bovine serum albumin in TBS buffer (10 mM Tris-HCl, pH 7.5, 150 mM NaCl) overnight at room temperature. Membranes were then incubated with the indicated primary antibody for 2 hr followed by a 2 hr incubation in the appropriate secondary antibody. Bands were detected by enhanced chemiluminescence (GE Healthcare, Chalfont St. Giles, UK).

Cell counting

Cells were seeded at 64,000 cells/mL in 12 well plates (1mL per well). After appropriate treatment, cells were trypsinized and constituted in 1 mL cell suspensions. Cell suspensions were then stained with trypan blue and living cells (trypan blue unstained) were counted under a microscope using a hemocytometer.

MTT staining

Cells were seeded in 48-well plates at the indicated concentration and allowed to attach for 24 hr before treatment. At the desired time points, 20 μL of 5 mg/mL MTT was added to each well; the cells were incubated for 2 hr, after which the medium was removed; 400 μL of dimethyl sulfoxide was added to dissolve the resulting purple formazan; and absorbance was read at 544 nm with a FLUOstar OPTIMA plate reader (BMG Labtechnologies, Inc., Durham, NC).

Sulforhodamine B (SRB) staining

Cells were seeded in 48-well plates 24 hr prior to treatment. After an incubation period, cell monolayers were fixed with 10% (w/v) trichloroacetic acid on ice for at least 1 hr and then stained with 0.4% SRB (1% acetic acid) for 30 min, after which the excess dye was removed by washing repeatedly with 1% (vol/vol) acetic acid. The protein-bound dye was dissolved in 10 mM Tris base solution for OD determination at 544 nm using a FLUOstar OPTIMA plate reader (BMG Labtechnologies, Inc., Durham, NC).

CellTiter Blue staining

Cells were seeded in 48-well plates 24 hr prior to treatment. After an incubation period, media was replaced with fresh growth media and then 14 μL celltiter blue staining agent (G8080, Promega, Madison, WI) was added to each well. Plates were incubated in dark at 37 ºC for 4 hr, after which 100 μL aliquots were used to measure fluorescence at 560 nm excitation and 590 nm emission with a SpectraMax M2 Microplate Reader (Molecular Devices, Sunnyvale, CA)

Cell cycle analysis

Cell cycle was assessed using methods previously described (Cummings, 2002). In brief, cells were washed twice with sample buffer [PBS plus glucose (1 g/L)], dislodged using Cellstripper (Mediatech, Herndon, VA), centrifuged at 400 g for 10 min, and suspended in sample buffer. Cells were fixed in ice-cold ethanol (70% v/v) and stained with PI (50 μg/mL) in sample buffer containing RNase A (100 U/mL) for 30 min at room temperature with gentle shaking. Samples were analyzed within 24 hr by flow cytometry with a FACSCalibur flow cytometer located in the Center for Tropical and Emerging Diseases at the University of Georgia.

Reactive species measurement

The generation of reactive species, including those containing oxygen, was measured using CM-H2DCFDA, which is a non-fluorescent chemical whose fluorescence increases as reactive species production increases. It should be noted that CM-H2DCFDA can be used to detect several reactive species, including hydrogen peroxide, hydroxyl radical, peroxyl radical and peroxynitrite anion; however it cannot be applied to all species, most notably superoxide

(Murrant , et al, 2001; Oyama et al, 1994). LNCaP and PC-3 cells were seeded in 48 well plates at a concentration of 64,000-128,000 cells/mL (400 μL per well) and allowed to grow for 24 hr. Cultures in 48-well plates were preloaded with 10 μM CM-H2DCFDA for 30 min at 37°C. After incubation, the medium was replaced with fresh serum free media for 10 min. Cells were pretreated with either NAC or ascorbic acid for 1 hr and then exposed to 10 μM BEL or 5 μM *S*-BEL or 5 μM *R*-BEL for 2 hr. After treatment, medium was aspirated and cells detached using 0.01M Tris–HCl with 0.5% Triton X-100 (pH 7.4). A 100 μL aliquot was used to measure fluorescence at 485 nm excitation and 520 nm emission with a FLUOstar OPTIMA plate reader.

Protein determination

Protein concentrations were determined using the Bicinchoninic acid assay kit provided by Sigma-Aldrich (Sigma procedure TRPO-562) with bovine serum albumin as a standard.

Bligh-Dyer lipid extraction

Cellular or tissue phospholipids were extracted using chloroform and methanol according to the method of Bligh and Dyer (Bligh and Dyer, 1959). 1×10^7 Cells or 50 mg tissue was washed with PBS. Then 2 mL methanol: water (2.0:0.8 v/v) was added and cells were suspended or tissues were homogenized by sonication. The liquid was transferred to a glass test tube and 1.5 mL chloroform was added. Tubes were vortexed for 30 seconds and allowed to sit for 10 min on ice. Tubes were centrifuged at 213 *g* for 1 min and the bottom chloroform layer was transferred to a new test tube. The extraction steps were repeated a second time and the chloroform layers combined. The collected chloroform layers were dried under argon, reconstituted with 50 μL of methanol: chloroform (2:1 v/v), and stored at -20°C.

Lipid phosphorus assay

Lipid phosphorus was quantified using malachite green (Zhou et al, 1992). Lipid extract (20 μL) was dried down under argon in a test tube. Perchloric acid (200 μL) was added to the tube, and heated at 130°C for 2-3 hours. After this time, 1 mL of deionized H_2O was added to the tube while vortexing. Reagent C (1.5 mL) (4.2 grams Ammonium Molybdate Tetrahydrate in 100 mL 5 N HCl and 0.15 grams Malachite Green Oxalate in 300 mL deionized H_2O) was added and vortexed. 1.5% (v/v) Tween-20 (50 μL) was added and vortexed. After 25 min of sitting at room temperature, a 200 μL aliquot was used to measure the absorbance at 590 nm.

Two-Dimensional High-Performance Thin-Layer Chromatography (2D-HP-TLC)

Extracted lipids (100 nMole) were dried under nitrogen and separated by two-dimensional high-performance thin-layer chromatography (2D-HP-TLC) on silica G plates (Merck, Germany). The plates were first developed with a solvent system consisting of chloroform/methanol/28% ammonium hydroxide (65:25:5, v/v). After drying the plates with a forced-air blower to remove the solvent, the plates were developed in the second dimension with a solvent system consisting of chloroform/acetone/methanol/glacial acetic acid/water (50:20:10:10:5, v/v). The phospholipids were visualized by exposure to iodine vapors and identified by comparison with migration of authentic phospholipid standards. The spots identified by iodine staining were scraped, and the silica was transferred to tubes. The identity of each phospholipid was established by comparison with the Rf values (The distance travelled by lipids divided by distance travelled by the solvent front in chromatography) measured for authentic standards.

Characterization and quantitation of cellular phospholipids using electrospray ionization-mass spectrometry (ESI/MS)

Lipid extract samples (20 pmol/μl) were prepared by reconstituting in chloroform: methanol (2:1, v/v). Samples were analyzed using an Agilent Trap XCT ion-trap mass spectrometer equipped with an electrospray ion source (Agilent, Santa Clara, CA). Samples (5 μL) were introduced by means of a flow injector into the ESI chamber at a rate of 0.2 mL/min. The elution solvent was acetonitrile:methanol:water (2:3:1, v/v/v) containing 0.1% (w/v) ammonium formate (pH 6.4). The mass spectrometer was operated in both positive and negative ion scanning mode. The flow rate of the nitrogen drying gas was 8 L/min at 350°C. The capillary and cone voltages were set at 2.5 kV and 30 V respectively. Qualitative identification of individual phospholipid molecular species was based on their calculated theoretical monoisotopic mass values and quantification was done by comparison to the total ion count in each sample.

Statistical analysis

Cells isolated from a distinct passage represented one experiment (n = 1). Data are represented as the mean ± SD of at least three separate experiments (n = 3). The appropriate analysis of variance was performed for each data set using SAS software (SAS Institute, Cary, NC). Individual means were compared using Fisher's protected least significant difference test or a student *t*-test with $P < 0.05$ considered as indicative of a statistically significant difference between mean values.

CHAPTER 3

INHIBITION OF $iPLA_2$ INDUCES CYTOSTASIS IN A p53-DEPENDENT AND -INDEPENDENT MANNER IN PROSTATE CANCER CELLS[1]

[1] Bin Sun, Xiaoling Zhang, Sonia Talathi, Brian S. Cummings (2008)
J Pharmacol Exp Ther. **326**: 59-68. Reprinted with permission of publisher.

Introduction

Prostate cancer forms from a gland of the male reproductive system found below the bladder and in front of the rectum. In 2009, prostate cancer had the second highest incidence of male cancer and caused the second most deaths in The United States (www.cancer.gov). Due to the apparent limitations of prostatectomy and androgen deprivation, which are two most popular therapies for prostate cancer, novel chemotherapeutic targets have attracted more and more attention.

LNCaP and PC-3 cells are two of the most widely used prostate cancer cell lines for in vitro studies. LNCaP cells represent a relatively early stage of prostate cancer, which are p53 positive and androgen-sensitive. In contrast, PC-3 cells represent an advanced prostate cancer cell line, negative for p53 and are androgen insensitive.

Prostate cancer expresses relatively high levels of cPLA$_2\alpha$ and sPLA$_2$ (Group IIA), compared with benign prostatic tumors (Graff et al, 2001; Sved et al, 2004). Further, androgen-insensitive prostate cancer cells have higher activities of cPLA$_2\alpha$ and Group IIA sPLA$_2$ than androgen-sensitive prostate cancer cells (Patel et al, 2008). However, to present, no one has reported if iPLA$_2$ are expressed in any prostatic tissues. Further, the role of iPLA$_2$ in prostate cancer cell growth is not known. Thus, in Chapter 3 we will test the hypothesis that iPLA$_2$ are expressed in prostate cancer cells and that inhibition of iPLA$_2$ decreases cell growth.

Results

Expression of iPLA$_2\beta$ and iPLA$_2\gamma$ in LNCaP and PC-3 Cells

Whole cell lysates of LNCaP and PC-3 cells were separated by SDS PAGE. Immunoblot analysis using a polyclonal antibody against cytosolic iPLA$_2\beta$ resulted in the detection of bands

at approximately 85 kDa in both PC-3 and LNCaP cells (**Fig. 3.1 A**). Immunoblot analysis using a peptide antibody against iPLA$_2\gamma$ resulted in the detection of two bands at approximately 63 and 78 kDa in both PC-3 and LNCaP cells (**Fig. 3.1 B**). PC-3 cells contained both cytosolic and microsomal iPLA$_2$ activity as indicated by the cleavage of the synthetic substrate arachidonoyl thio-phosphatidylcholine (**Fig. 3.1 C**). Treatment of cells with racemic 5 μM BEL, a selective iPLA$_2$ inhibitor (Cummings et al, 2002; Kinsey et al, 2005), decreased activity in both cytosolic and microsomal fractions, compared to control cells. Treatment of cells with 2.5 μM *R*-BEL, a selective inhibitor of microsomal iPLA$_2\gamma$ (Jenkins et al, 2002; Kinsey et al, 2005), did not decrease cytosolic iPLA$_2\beta$ activity but did decrease iPLA$_2\gamma$ activity in microsomes. In contrast, treatment of cells with 2.5 μM *S*-BEL, a selective inhibitor of cytosolic iPLA$_2\beta$ (Jenkins et al, 2002; Kinsey et al, 2005), decreased cytosolic but not microsomal iPLA$_2\gamma$ activity. Collectively, these data demonstrate that PC-3 and LNCaP cells express both iPLA$_2\beta$ and γ and that these activities are inhibited by BEL and its enantiomers.

Effect of Inhibition of iPLA$_2$ on LNCaP and PC-3 Cell Growth

The effect of iPLA$_2$ inhibition on prostate cancer cell growth was assessed by measurement of MTT and cell number in LNCaP and PC-3 cells after exposure to racemic, *R*- and *S*-BEL. Both cell lines were seeded in 48-well plates at 64,000 cells/mL, allowed to attach for 24 hr, and then exposed to 0–10 μM BEL for 24 or 48 hr. Treatment with racemic BEL significantly decreased MTT staining in both cell lines in a concentration- and time-dependent manner (**Fig. 3.2 A** and **C**). MTT staining was decreased 50% in both cell lines after a 48-hr exposure to 10 μM racemic BEL. Significant decreases in MTT staining were detected at earlier time points in LNCaP cells, compared with PC-3 cells. Treatment of cells with *R*- and *S*-BEL

also decreased MTT staining, but only after 48 hr (**Fig. 3.2 B** and **D**). Racemic BEL (5 μM) was more effective than 2.5 μM *R*- or *S*-BEL at decreasing MTT staining in both cell lines, while the effects of *S*-BEL were slightly higher than *R*-BEL. To further confirm the differential roles of iPLA$_2$β and iPLA$_2$γ the effects of 10 μM racemic BEL, 5 μM *R-BEL* and *S*-BEL were compared. The results showed that 5 μM *S*-BEL decreased MTT staining to the similar extent as 10 μM racemic BEL, which exhibited a greater affect than *R*-BEL (**Fig. 3.2 E**). Taken together, these data suggest that iPLA$_2$β plays more important roles than iPLA$_2$γ in prostate cancer cell growth.

The effect of BEL on nuclear morphology was studied to confirm the effect of BEL on cell growth and to rule out the presence of cell death (**Fig. 3.3 A–D**). Nuclear morphology in untreated LNCaP (**Fig. 3.3 A**) and PC-3 cells (**Fig. 3.3 B**) was normal with a minimal number of nuclei displaying chromatin condensation or nuclear fragmentation. Treatment of cells with BEL for 24 hr did not significantly increase either type of apoptotic morphology (**Fig. 3.3 C** and **D**). However, a decrease in the number of nuclei was observed. This decrease correlated to a decrease in cell number after 48 hr of exposure (**Fig. 3.3 E** and **F**).

To further test the hypothesis that BEL did not induce cell death at the concentrations used, annexin V and PI staining were determined using flow cytometry (**Fig. 3.4**). In the presence of serum, treatment of cells with concentrations of BEL as high as 20 μM did not increase annexin V (**A** and **B**) or PI (**C**) staining above control levels after 48 hr (**Fig. 3.4 A** and **B**). However, in the absence of serum, concentrations of BEL over 10 μM BEL modestly increased annexin V staining only in LNCaP cells, while 20 μM BEL significantly increased PI staining in both cells. Based on these data we conclude that concentrations of BEL of 10 μM or less decreases prostate cancer cell growth in the absence of cell death.

Effect of $iPLA_2$ Inhibition on Cell Cycle

Treatment of LNCaP cells with 2.5 to 10 μM racemic BEL for 24 hr modestly, but significantly, increased the percentage of cells in the G_1 phase of the cell cycle compared with control cells (**Fig. 3.5 A**). In contrast, treatment of PC-3 cells with similar doses of BEL caused S- and G_2/M-phase arrest (**Fig. 3.5 B**) compared with control cells.

Effect of Inhibition of $iPLA_2$ on p53, p21 and Mdm2 Expression

Cell cycle arrest and decreased cell growth can be mediated by alterations in cyclin-dependent kinase complexes, which are mediated by p21 and p53 (Zhang et al, 2006). Not unexpectedly, treatment of PC-3 cells with BEL did not induce p53 or p21 expression at any concentration or time point tested (data not shown). In contrast, treatment of LNCaP cells with 5 μM racemic BEL increased p53 expression compared with controls as early as 2 hr after exposure (**Fig. 3.6 A** and **B**). These increases were more rapid than those induced by cisplatin. The expression of p53 began to decrease after 21 hr of exposure to BEL (**Fig. 3.6 A**) and was reduced to control levels by 48 hr (**Fig. 3.6 C**).

Treatment of LNCaP cells with BEL increased p21 expression after 16 hr (**Fig. 3.6 A)**. Like p53, the ability of BEL to induce p21 expression was concentration-dependent (**Fig. 3.6 B**). Increases in p21 expression occurred after increase in p53 and were more rapid than increases induced by cisplatin. Increases in p53 and p21 were not a result of differences in loading as demonstrated by the expression of GAPDH.

To study the expression of p53 at greater length of time, cells were exposed to 5 μM BEL for periods up to 48 hr (**Fig. 3.6 C**). As expected, treatment of cells with BEL increased

expression of p53 at 6 and 12 hr. By 24 hr p53 expression decreased, and by 48 hr p53 expression almost returned to control levels.

To verify the expression of p53, LNCaP cells were treated with either solvent control or BEL and p53 expression was assessed using fluorescence microscopy (**Fig. 3.6 D** and **E**). Little, if any, p53 staining was detected in control cells (**Fig. 3.6 D**) or cells incubated with the IgG control (data not shown). In contrast, treatment of cells with 5 μM BEL for 16 hr resulted in clear punctate staining, which was mainly perinuclear as determined by the comparison with the nuclear dye DAPI (**Fig. 3.6 E**). Collectively, these data demonstrate that inhibition of $iPLA_2$ using BEL increases the expression of p53 and p21 in LNCaP cells.

We tested the hypothesis that $iPLA_2$ inhibition also regulates expression of the p53 antagonist Mdm2 expression. Treatment of LNCaP cells with BEL decreased Mdm2 expression as early as 30 min after exposure (**Fig. 3.7 F**). Mdm2 expression was decreased in LNCaP cells at 0.5 and 1 hr after exposure to BEL, but rebounded after 2 hr and continued to increase at later time points. Mdm2 expression was not detected in PC-3 cells at any time point or concentration of BEL tested (data not shown).

Differential Effects of Inhibition of $iPLA_2\beta$ and $iPLA_2\gamma$ on P-p53, p53 and p21 Expression

To further demonstrate differential roles for $iPLA_2\beta$ and $iPLA_2\gamma$ in p53 activation, we utilized racemic BEL, *R*-BEL and *S*-BEL to study the effect of $iPLA_2$ inhibition on p53 and p21 activation in LNCaP cells. Both racemic BEL and *S*-BEL increased the expression of phosphorylated p53 (P-p53 at Ser15), total p53 and p21 after 9 hr (**Fig. 3.7**). Treatment of cells

with *R*-BEL only slightly increased the expression of these proteins compared to controls. The levels of induction seen with *S*-BEL were comparable to racemic BEL. These results demonstrate that inhibition of iPLA$_2$β, rather than iPLA$_2$γ, predominantly activates p53 pathway in prostate cancer cells, suggesting iPLA$_2$β is more involved in prostate cancer cell growth than iPLA$_2$γ.

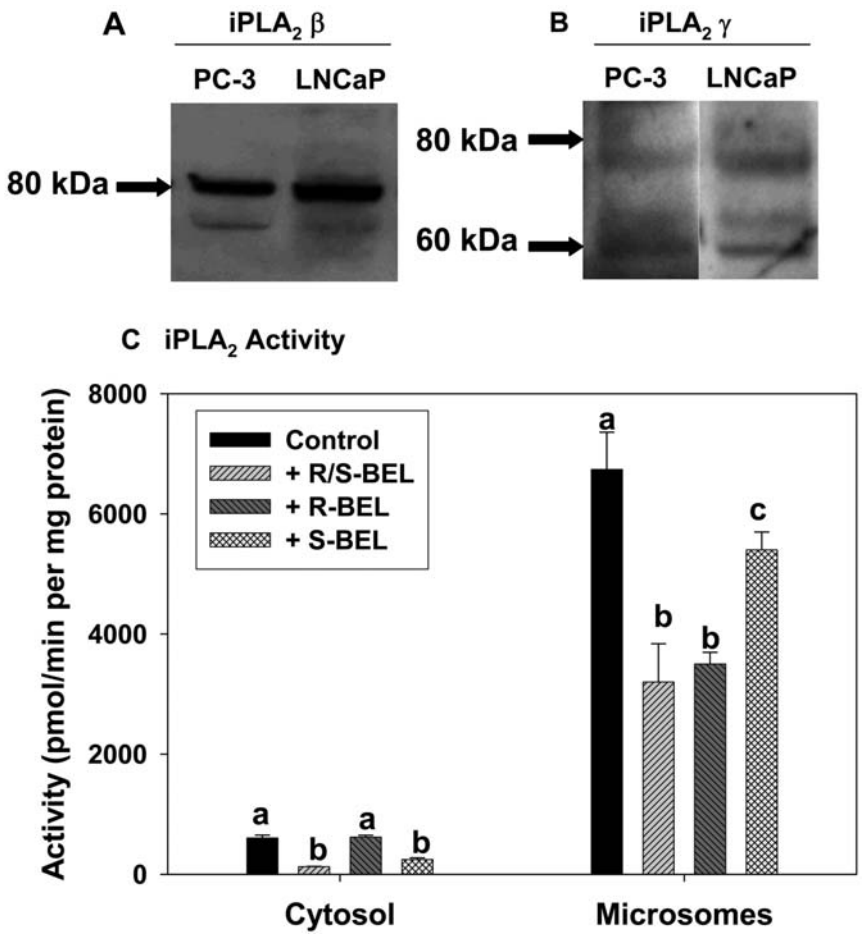

Figure 3.1 Expression of $iPLA_2$ isoforms in LNCaP and PC-3 cells. Whole cell lysates from LNCaP and PC-3 cells were separated by SDS-polyacrylamide gel electrophoresis and analyzed for expression of $iPLA_2\beta$ (**A**) or γ (**B**). Cell lysates from PC-3 cells were also separated into microsomes and cytosolic fractions, and $iPLA_2$ activity was assessed in the presence or absence of 5 μM racemic BEL or 2.5 μM *R*- and *S*-BEL (**C**). Data are presented as the mean ± SD of at least three separate experiments. Means with different subscripts are significantly different from each other ($P < 0.05$).

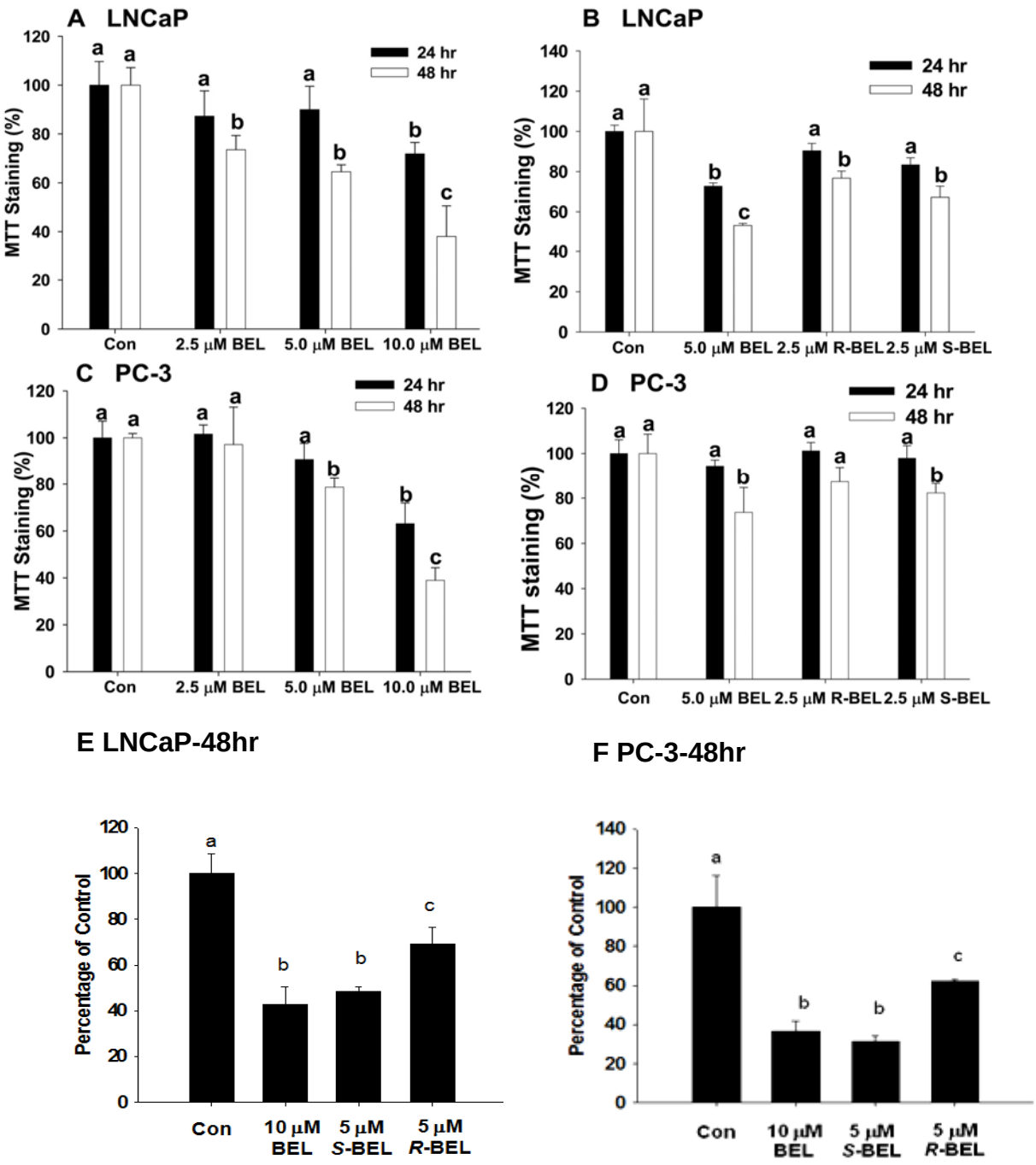

Figure 3.2 Effect of iPLA$_2$ inhibitors on MTT staining in LNCaP and PC-3 cells. LNCaP (**A** and **B**) and PC-3 (**C** and **D**) cells in log-phase growth were exposed to 0 to 10 μM racemic BEL (**A** and **C**) or *R*- and *S*-BEL (**B, D, E** and **F**) for either 24 or 48 hr before analysis of MTT staining. Data are presented as the mean ± SD of at least three separate experiments. Means with different subscripts are significantly different from each other ($P < 0.05$).

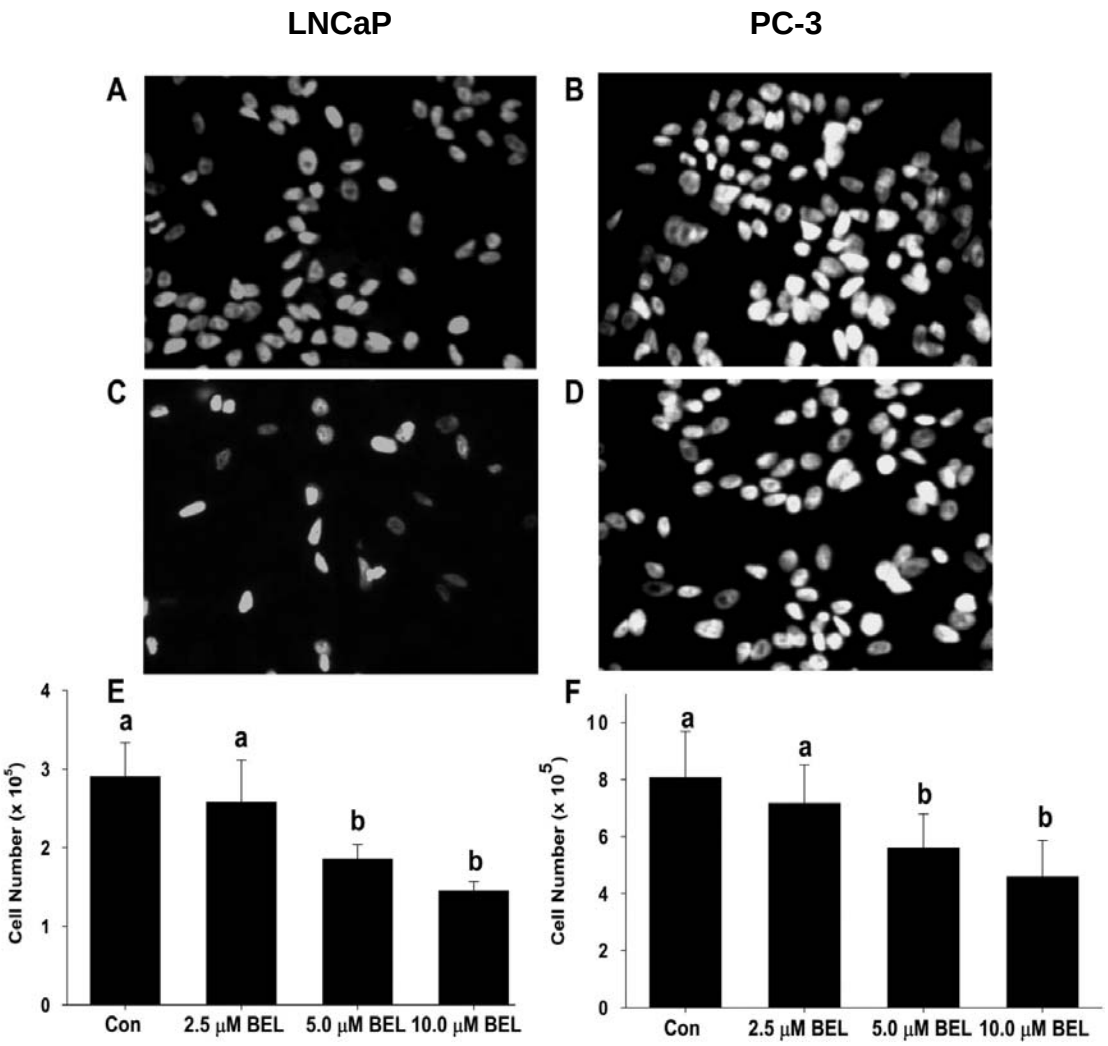

Figure 3.3 Effect of BEL on nuclear morphology and cell number in LNCaP and PC-3 cells. LNCaP (**A, C,** and **E**) and PC-3 (**B, D,** and **F**) cells were treated with 5 μM BEL for 24 (**A–D**) and 48 hr (**E** and **F**) before analysis of nuclear morphology (**A–D**) using fluorescence microscopy at 25X magnification or analysis of cell number (**E** and **F**). Data in **A–D** are representative of at least three different experiments. Data in **E** and **F** are presented as the mean ± SD of at least three separate experiments. Means with different subscripts are significantly different from each other ($P < 0.05$).

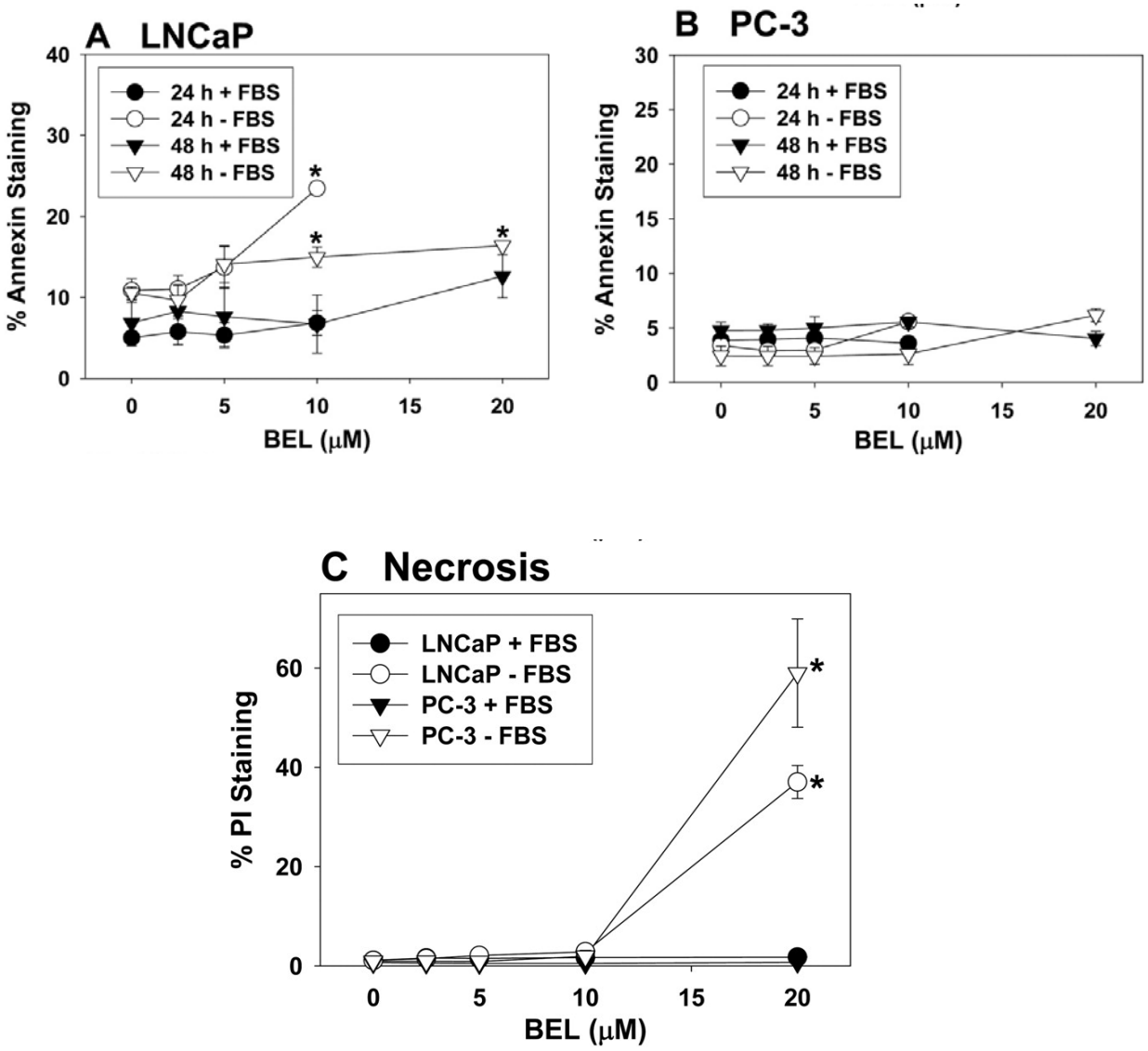

Figure 3.4 Effect of BEL and FBS on annexin V-FITC and PI staining in LNCaP and PC-3 cells. LNCaP and PC-3 cells were exposed to 0 to 20 μM racemic BEL for 24 and 48 hr in the presence or absence of 10% FBS. After exposure, cells were harvested and analyzed for annexin V-FITC (**A** and **B**) and PI (**C**) staining using flow cytometry. Data are presented as the mean ± SD of at least three separate experiments. *Significant difference ($P < 0.05$) from paired control.

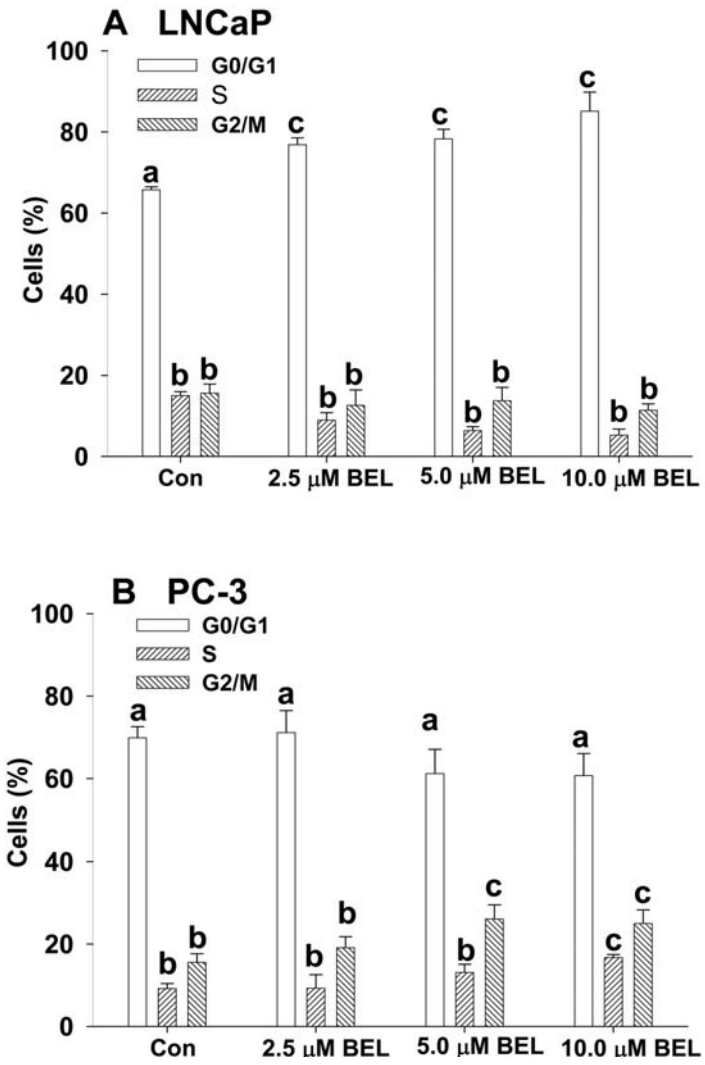

Fig. 3.5 Effect of BEL on LNCaP and PC-3 cell cycle. LNCaP (**A**) and PC-3 (**B**) cells were exposed to 0 to 10 μM racemic BEL for 24 hr. After exposure, cells were harvested, and cell cycle was assessed using PI staining and flow cytometry. Data are presented as the mean ± SD of at least three separate experiments. Means with different subscripts are significantly different from each other (P <0.05).

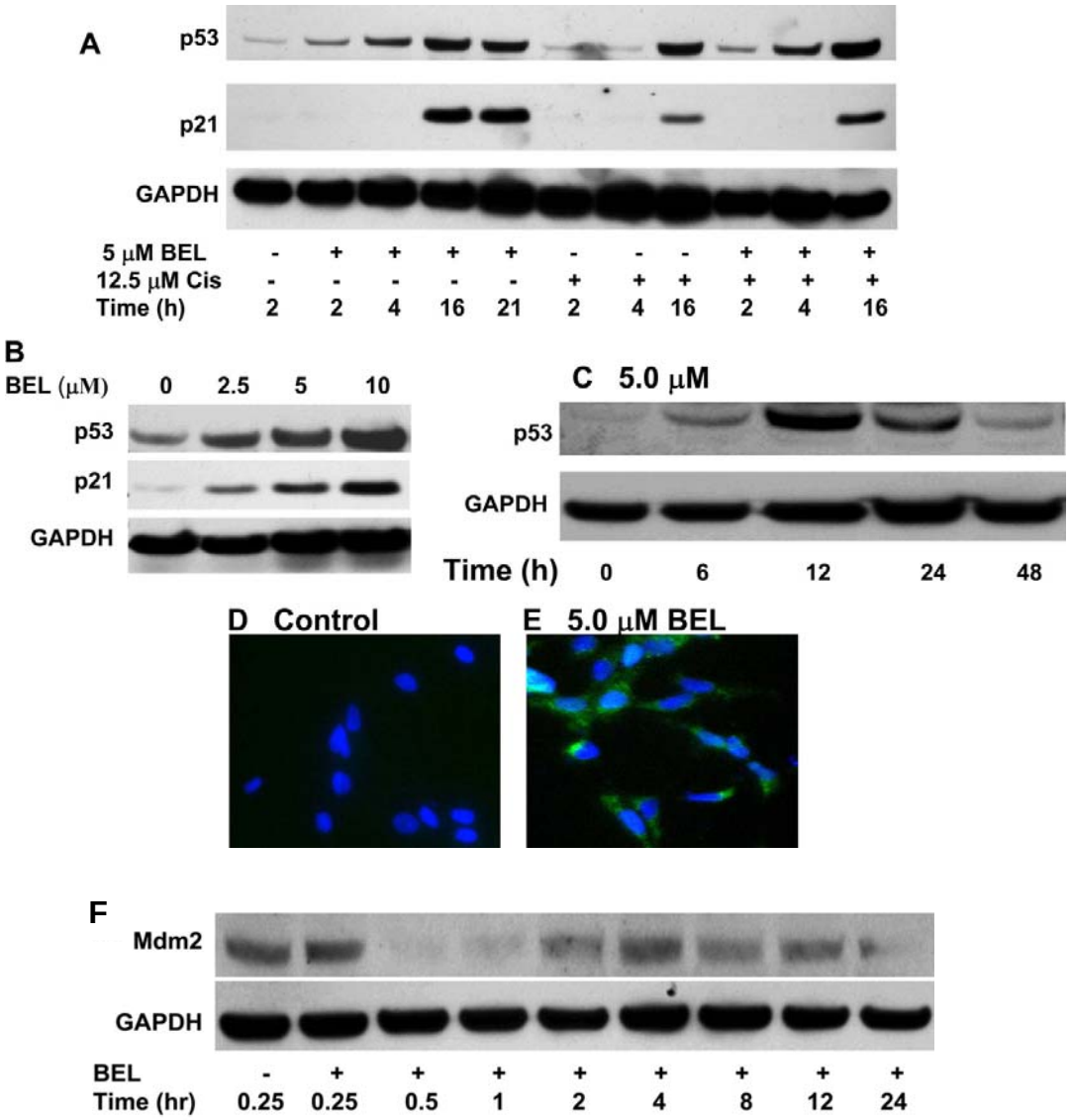

Fig. 3.6 Effect of BEL on p53, p21 and Mdm2 expression in LNCaP cells. LNCaP cells were exposed to racemic BEL, 12.5 μM cisplatin, or both for the indicated time points before isolation and analysis of p53 and p21 expression (**A**). Furthermore, LNCaP cells were treated with 0 to 10 μM racemic BEL for 12 hr (**B**) or with 5 μM BEL for 0, 6, 12 and 24 hr (**C**) before analysis of p53 and p21 expression. The expression of GAPDH is shown as a loading control. All blots are representative of at least three different experiments. The staining of p53 (green staining) in LNCaP cells was also determined after exposure to solvent control (**D**) or 5.0 μM BEL (**E**) for 16 hr using fluorescence microscopy. Blue staining represents DAPI staining of nuclei. Data in **D** and **E** are presented at 30X magnification and are representative of at least three different experiments. For Mdm2 expression (**F**) LNCaP cells were exposed to 5 μM racemic BEL for 0 to 24 hr followed by isolation and analysis of Mdm2 expression.

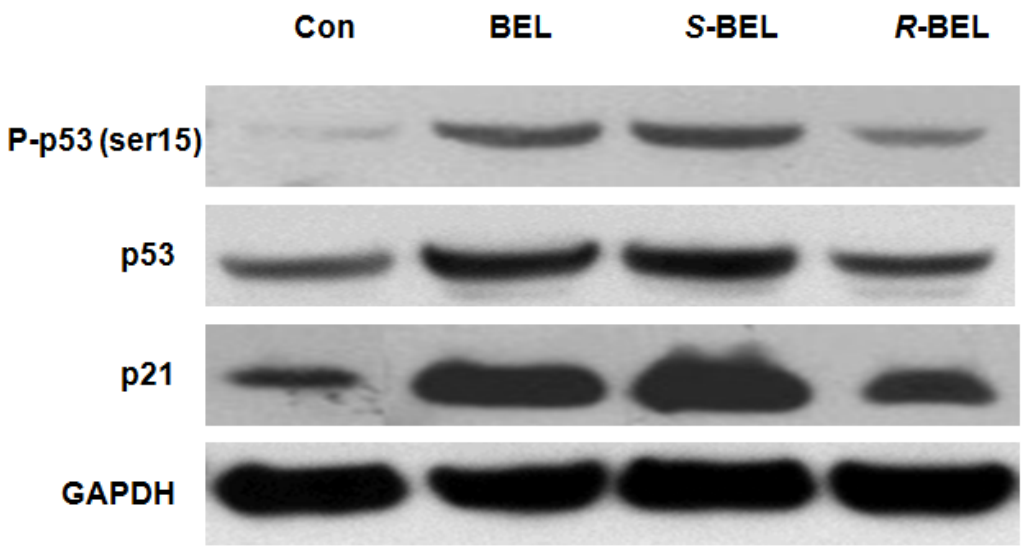

Fig. 3.7 The differential effects of BEL, *R*-BEL and *S*-BEL on P-p53 (Ser15), p53 and p21 expression in LNCaP cells. LNCaP cells were exposed to 10 μM racemic BEL, 5 μM R-BEL and 5 μM *S*-BEL for 9 hr before isolation and analysis of P-p53 (Ser15), p53 and p21 expression. The expression of GAPDH is shown as a loading control. All blots are representative of at least three different experiments.

Discussion

Inhibition of $iPLA_2$ decreases proliferation in several types of cancer and noncancerous cells (Saavedra et al, 2006; Zhang et al, 2006, Herbert et al, 2006). Decreased INS-1 cell growth correlated to p53-mediated G_1 arrest (Zhang et al, 2006). In contrast, decreased ovarian cancer cell growth correlated to G_2/M arrest and is p53-independent (Song et al, 2007). Although these studies suggest that the effect of $iPLA_2$ inhibition on cell growth is cell-dependent, they did not identify the roles of individual $iPLA_2$ isoforms in cell growth or identify the mechanisms involved in p53 induction.

We studied the effect of $iPLA_2$ inhibition in PC-3 and LNCaP cells lines, which represent two of the most common used cell models for studying prostate cancer. Furthermore, LNCaP cells are androgen-sensitive and express wild-type p53, whereas PC-3 cells are androgen-insensitive and p53-null. We demonstrated that LNCaP and PC-3 cells expressed $iPLA_2\beta$ and γ based on immunoblot analysis and activity assays. The expression of $iPLA_2\beta$ was higher than $iPLA_2\gamma$ in both cell lines, although direct comparisons are difficult due to differences in antibody specificities. Regardless, these data demonstrate the novel finding that $iPLA_2\beta$ and γ are both expressed in prostate cancer cells.

Racemic-BEL (5 μM) decreased MTT staining and cell number to a greater extent than 2.5 μM *S*-BEL or *R*-BEL, and 2.5 μM *S*-BEL had a slightly greater effect on MTT staining than R-BEL in both cell lines. However, 10 μM racemic BEL inhibited prostate cancer cell growth as effective as 5 μM *S*-BEL, which were both more effective than 5 μM R-BEL. These data suggest that both $iPLA_2\beta$ and γ are involved in prostate cancer cell growth, and that $iPLA_2\beta$ may play a more prominent role.

The ability of BEL to induce G_1-phase arrest in LNCaP cells agrees with data from INS-1 cells (Zhang et al, 2006) where 10 to 15% increases in cells in G_1 were reported. G_1 arrest and p53 induction in LNCaP cells occurred in the absence of DNA hypoploidy (data not shown), alterations in nuclear morphology, or increases in annexin V or PI staining. Thus, we do not believe that G_1 arrest is a result of DNA damage or cell death. Most likely, BEL-induced G_1 arrest is mediated by p53, which is activating p21. Checkpoints exist within the G_1 phase of the cell cycle to ensure that phospholipid levels and metabolism are adequate to ensure cell entry into S phase (Manguikian, et al, 2004; Zhang et al, 2006). It is possible that $iPLA_2$ inhibition decreases phospholipid levels and activates these checkpoints. Further, we tested the hypothesis that the p53 antagonist Mdm2 regulates p53 expression in our system. These data showed that Mdm2 was decreased 2 hr prior to p53 activation, suggesting that decrease of Mdm2 levels correlate to p53 activation. However, Mdm2 was also increased at late time points. This result is not surprising because p53 activates transcription of Mdm2 in a negative feedback manner (Lu X et al, 2007).

Similar to ovarian cancer cells (Song et al, 2007), $iPLA_2$ inhibition in PC-3 cells induced G_2/M- and S-phase arrests independently of p53. In contrast to ovarian cancer cells, $iPLA_2$ inhibition using BEL did not induce death at low concentrations, even in the absence of serum. Increases in cell death in the absence of serum at high doses suggest that BEL-induced cell death is serum-dependent. This may explain conflicting data concerning cell death in several studies (Fuentes et al, 2003; Zhang et al, 2006; Song et al, 2007). It is also possible that differences in $iPLA_2$ activities account for such differences.

Our cell growth data demonstrated that both *S*-BEL and *R*-BEL, which selectively inhibit $iPLA_2\beta$ and $iPLA_2\gamma$ respectively, decrease prostate cancer cell growth, while *S*-BEL had a

greater effect than *R*-BEL. In order to further address their differential roles on cell signaling, we compared the differential roles of racemic BEL, *R*-BEL and *S*-BEL on P-p53, p53 and p21 expression in LNCaP cells. Results from this study support the conclusions that *S*-BEL has a more potent effect on p53 and p21 expression than *R*-BEL. These results support the hypothesis that $iPLA_2\beta$ is more involved in prostate cancer cell growth signaling than $iPLA_2\gamma$. Therefore we chose to study $iPLA_2\beta$ in molecular knockdown experiments in Chapter 4.

CHAPTER 4

INHIBITION OF $iPLA_2$ INDUCES P38 MAPK DURING CYTOSTASIS IN PROSTATE CANCER CELLS[2]

[2] Bin Sun, Xiaoling Zhang, Christopher Yonz and Brian S. Cummings (2010). *J Biochem Pharmacol.* **79:** 1727-1735. Reprinted here with permission of publisher.

Introduction

Mitogen-activated protein kinases (MAPK) are serine-threonine kinases activated by a cascade of protein-protein interactions. The most extensively studied MAPK are ERK1/2 (p42/44MAPK), p38 MAPK and c-jun N-terminal kinase/stress-activated protein kinase (JNK/SAPK). All these three types of MAPK, especially p38 and JNK, are suggested to phosphorylate and activate p53 in several studies (Reinhardt et al, 2007; Bae et al, 2006). p38 and JNK are activated in response to cellular stress such as irradiation, heat shock, reactive oxygen species, LPS, TNF, IL-1, inflammation and apoptosis. Recent evidence suggests that p38 and JNK play key roles in anticancer pathways in prostate cancer cells, including cytostasis, cell cycle arrest and apoptosis (Reinhardt et al, 2007; Fan et al, 2001; Chang et al 2008; Bradham et al, 2006). The mechanisms involved are linked to the activation of the tumor suppressor protein p53, which activates proteins involved in cell cycle arrest (Reinhardt et al, 2007; Brown et al, 2006), apoptosis (Kim et al, 2006) and proteins linked to DNA damage such as GADD153 (Woo et al, 2007; OH-Hashi et al, 2001).

To our knowledge, no study has reported on links between $iPLA_2$ and MAPK activation in cancer cells. Recent studies show that thrombin-stimulates both MAPK and $iPLA_2$ activity in ventricular myocytes and vascular smooth muscle cells (Yellaturu et al, 2003; Beckett et al, 2006). One of these studies shows that $iPLA_2$ inhibition decreases agonist stimulated MAPK activation (Beckett et al, 2006). Another study shows that MAPK mediate $iPLA_2$ activity during hypoxia in mouse neural cells (Aoto et al, 2009). However, all these studies were conducted in presence of an agonist. Thus, the response of MAPK to $iPLA_2$ inhibition in the absence of agonist stimulation is not known.

Chapter 3 demonstrated that pharmacological inhibition of $iPLA_2$ induced cytostasis in prostate cancer cells; however these findings were not validated molecularly. Our previous data also showed that *S*-BEL increased the expression of phosphorylated p53 (P-p53), total p53 and p21, to levels comparable to that of racemic BEL, while treatment with *R*-BEL only slightly increased the expression of these proteins. Thus we chose to study $iPLA_2\beta$ in molecular knockdown experiments as our studies suggested that this was the predominate isoform involved in cytostatic signaling.

Results

Molecular knockdown of $iPLA_2\beta$ inhibits LNCaP and PC-3 cell growth

Transfection of siRNA against $iPLA_2\beta$ into PC-3 and LNCaP cells resulted in 70-80% reductions in the relative mRNA abundance compared to cells transfected with negative control siRNA (**Fig. 4.1 A**). The overall level of $iPLA_2\beta$ mRNA expression did not differ significantly between these cells (data not shown). Treatment of both LNCaP and PC-3 cells with $iPLA_2\beta$ siRNA also decreased $iPLA_2\beta$ protein expression as detected using immunoblot analysis (**Fig. 4.1 B**). Decreases in $iPLA_2\beta$ expression correlated to 50% decreases in cell growth after 72 hr as assessed by cell number (**Fig. 4.1 C**).

$iPLA_2$ inhibition induces p38 activation in PC-3 and LNCaP cells

We tested the hypothesis that $iPLA_2$ inhibition alters p38 activation by treating LNCaP and PC-3 cells with racemic BEL, *R*-BEL, *S*-BEL or $iPLA_2\beta$ siRNA, and assessing p38 phosphorylation (**Fig. 4.2**). Treatment of both PC-3 and LNCaP cells with racemic BEL caused concentration- and time-dependent increases in the phosphorylation of p38 (P-p38) (**Fig 4.2 A-**

D). P-p38 was induced as early as 5 min after exposure to BEL, and remained elevated after 2 hr. BEL concentrations as low as 2.5 μM also increased p38 phosphorylation after 30 min (**Fig. 4.2 B** and **D**). These data were confirmed by siRNA studies demonstrating that transfection of cells with iPLA$_2$β siRNA increased p38 phosphorylation, compared to cells transfected with negative control siRNA (**Fig. 4.2 E**).

To further study the differential roles of iPLA$_2$β in these processes we assessed p38 phosphorylation in cells treated with racemic BEL, *S*-BEL or *R*-BEL. *S*-BEL induced significantly higher levels of P-p38 compared to *R*-BEL (**Fig. 4.2 F** and **G**). The level of p38 phosphorylation seen with *S*-BEL was similar to that seen with racemic BEL, Collectively, these data demonstrate the novel finding that inhibition of iPLA$_2$ alone induced p38 activation in prostate cancer cells.

iPLA$_2$ inhibition does not significantly activate ERK1/2 and JNK in PC-3 and LNCaP cells

In contrast to p38, BEL only transiently increased ERK1/2 phosphorylation in PC-3 cells (**Fig. 4.3 A**), and did not induce ERK1/2 in LNCaP cells (**Fig. 4.3 B**). siRNA against iPLA$_2$β induced slight increases in P-ERK after 96 hr in PC-3 cells (**Fig. 4.7 A**). In contrast, BEL didn't significantly induce JNK activation in either cell type after 4 hr (**Fig. 4.3 C** and **D**). Based on these data, we chose to focus our studies on p38.

Inhibition of p38 alters BEL-induced p53 and p21 activation and cell cycle arrest

To investigate the functional role of p38 on p53 and p21 expression we exposed LNCaP cells to the p38 specific inhibitors SB202190 or SB203580 prior to exposure to BEL. LNCaP cells were used, as opposed to PC-3 cells, because PC-3 cells do not express p53. As previously

demonstrated, treatment of LNCaP cells with BEL (10 μM) increased p53 expression, compared to control cells (**Fig. 4.4 A**). BEL also induced p53 phosphorylation based on increases in phospho-p53 (Ser15) (**Fig. 4.4 A**). In contrast, exposure of cells to SB202190 (10 μM) or SB203580 (10 μM) for 30 min prior to BEL treatment decreased p53 and phosho-p53 (Ser15) expression, compared to cells treated with BEL alone (**Fig. 4.4 A**). Similar results were seen for p21 expression. Interestingly, SB202190 did not alter the basal level of p53 or p21 expression, while SB203580 slightly decreased these levels.

To test the functional role of p38 in cell cycle arrest induced by $iPLA_2$ inhibition we exposed cells to either solvent controls or SB202190 for 30 min prior to exposure to BEL (10 μM) for 24 hr. BEL treatment caused a small, but significant increase in cells in G1 in LNCaP cells (**Fig. 4.4 B**). Interestingly, there the number of cells in the G1 phase also increased after exposure to SB202190 alone. In contrast, treatment of cells with both SB202190 and BEL decreased the percent cells in G1 phase, compared to cells exposed to either BEL or SB202190 alone.

Even though PC-3 cells don't express p53, we still determined the effect of SB202190 on BEL-induced G2/M arrest (**Fig. 4.4 C**). PC-3 cells treated with BEL (10 μM) for 24 hr exhibited an increase in cells in both the S and G2/M phases of the cell cycle, compared to control (**Fig. 4.4 C**). Interestingly, treatment of cells with SB202190 prior to exposure to BEL, actually increased the percent cells in S-phase compared to cells exposed to BEL alone, but had no effect on BEL-induced increase in the G2/M phase. Zhang et al reported that ataxia telangiectasia mutated and rad3-related kinase (ATR) plays important roles in p53 phosphorylation during $iPLA_2$ inhibition in insulinoma cells (Zhang et al, 2008). Therefore, we tested the hypothesis that ATR also mediate p53 phophorylation in prostate cancer cells. Data (**Fig. 4.4 D)** shows that the

ATR inhibitor caffeine attenuated BEL induced P-p53 (Ser15), p53 and p21 as well as SB202190, but neither of them completely reversed the effect of BEL. However, a combination of caffeine and SB202190 completely abolished BEL induced p53 activation, suggesting both p38 and ATR are involved in p53 phosphorylation induced by $iPLA_2$ inhibition in prostate cancer cells

Inhibition of $iPLA_2$ induces reactive species in prostate cancer cells

We investigated the hypothesis that $iPLA_2$ inhibition activates p38 by reactive species (RS)-mediated mechanisms because several studies demonstrate that MAPK are activated by RS (Seger et al, 1995; Jing et al, 1999; Bhat et al, 1999). In doing so, LNCaP and PC-3 cells were exposed to 10 μM BEL for 2 hr and intracellular RS were assessed using CM-H2DCFDA staining. BEL treatment alone significantly increased RS levels in both cell lines (**Fig. 4.5 A**). Treatment of both cells with NAC prior to exposure to BEL significantly decreased RS formation (**Fig. 4.5 A**). In contrast, ascorbic acid (ASA) did not significantly alter the formation of RS in the presence of BEL. Larger decreases were seen in LNCaP cells compared to PC-3 cells; however, the decreases in PC-3, albeit small, were still statistically significant. Additionally, treatment of LNCaP cells with NAC prior to BEL exposure, decreased BEL induced increases in phosphorylated p38, phosphorylated-p53 (Ser15) and p53 (**Fig. 4.5 B**). NAC treatment also reversed BEL mediated decrease in the p53 antagonist Mdm2 in LNCaP cells (**Fig. 4.5 C**) and inhibited the ability of BEL to induce p38 phosphorylation in PC-3 cells (**Fig.4.5 D**). *S*-BEL significantly induced RS to levels comparable to racemic BEL (**Fig. 4.5 E**). In contrast, *R*-BEL only had a marginal effect on RS formation, suggesting that $iPLA_2\beta$ is more involved in RS induction than $iPLA_2\gamma$ as well as P-p38, as we just showed above.

Treatment with NAC partially reverses the effect of BEL and iPLA$_2\beta$ siRNA on cell growth

To test the functional consequence of NAC on cell growth we exposed LNCaP and PC-3 cells in log phase growth to 2.5 mM NAC for 30 min prior to exposure to 5 μM BEL for 48 hr. Analysis of cell morphology showed that BEL decreased growth in both cell types (**Fig. 4.6 A** and **C**). This finding was supported by cell counts (**Fig. 4.6 B** and **D**). Treatment with 2.5 mM NAC alone did not significantly alter cell morphology or growth; however, NAC reduced the ability of BEL to reduce cell number. We also tested the ability of NAC on cytostasis induced by iPLA$_2\beta$ siRNA. Cell counting results (**Fig. 4.7**) showed that treatment with 2.5 mM NAC significantly attenuated decreases in LNCaP and PC-3 cell growth induced by iPLA$_2\beta$ siRNA.

Inhibition of ERK1/2 augments the effect of BEL on cell growth

iPLA$_2\beta$ siRNA was used to assess the activation of ERK1/2 in PC-3 cells. PC-3 Cells transfected with siRNA for 72 hr exhibited slightly increased levels of P-ERK1/2 (**Fig. 4.8 A**). Further, the ERK1/2 specific inhibitor PD98059 was used to determine the functional consequence of ERK1/2 activation on prostate cancer cell growth after iPLA$_2$ inhibition. This compound did not alter MTT staining in control cells, but decreased MTT staining in cells exposed to BEL (**Fig. 4.8 B**) , suggesting that ERK1/2 may act as a survival signal.

Mechanisms of ERK1/2 activation in PC-3 cells during iPLA$_2$ inhibition

The above data suggests that activation of ERK1/2 in PC-3 cells during iPLA$_2$ inhibition mediates cell growth. EGFR is known to activate ERK1/2 (Sabbatini et al, 2006). Thus, we tested the hypothesis that iPLA$_2$ inhibitors activate ERK using EGFR.

Treatment of PC-3 cells with 10 μM BEL induced a time-dependent increase in EGFR phosphorylation as determined by immunoblot analysis (**Fig. 4.9 A**). Maximum activation occurred after 30 min of exposure. BEL treatment also induced ERK1/2 phosphorylation after 30 min, which was inhibited by 10 μM PD98059 (**Fig. 4.9 B**). Further, EGF (100 ng/mL) also induced ERK1/2 phosphorylation after 30 min, and this event was inhibited by pretreatment with PD98059 as well (**Fig. 4.9 B**).

To determine if EGFR pathways activate ERK1/2 during $iPLA_2$ inhibition we tested the effect of the EGFR inhibitor AG1478 (1.25 μM), or the matrix metalloproteinase (MMP) inhibitor GM6001 (10 μM), on BEL-induced ERK1/2 phosphorylation in PC-3 cells (**Fig. 4.9 C**). AG1478 and GM6001 are previously demonstrated to inhibit agonist stimulated EGFR activation in several cell types (Xu et al, 2007; Zhao et al, 2006). Treatment of cells with AG1478 for 30 min prior to exposure to BEL (10 μM) decreased ERK1/2 phosphorylation compared to cells exposed to BEL only. Further, AG1478 pretreatment also reduced BEL-induced EGFR phosphorylation. Similar results were seen with GM6001. These data suggest that ERK1/2 activation in PC-3 cells during $iPLA_2$ inhibition is mediated by EGFR associated pathways.

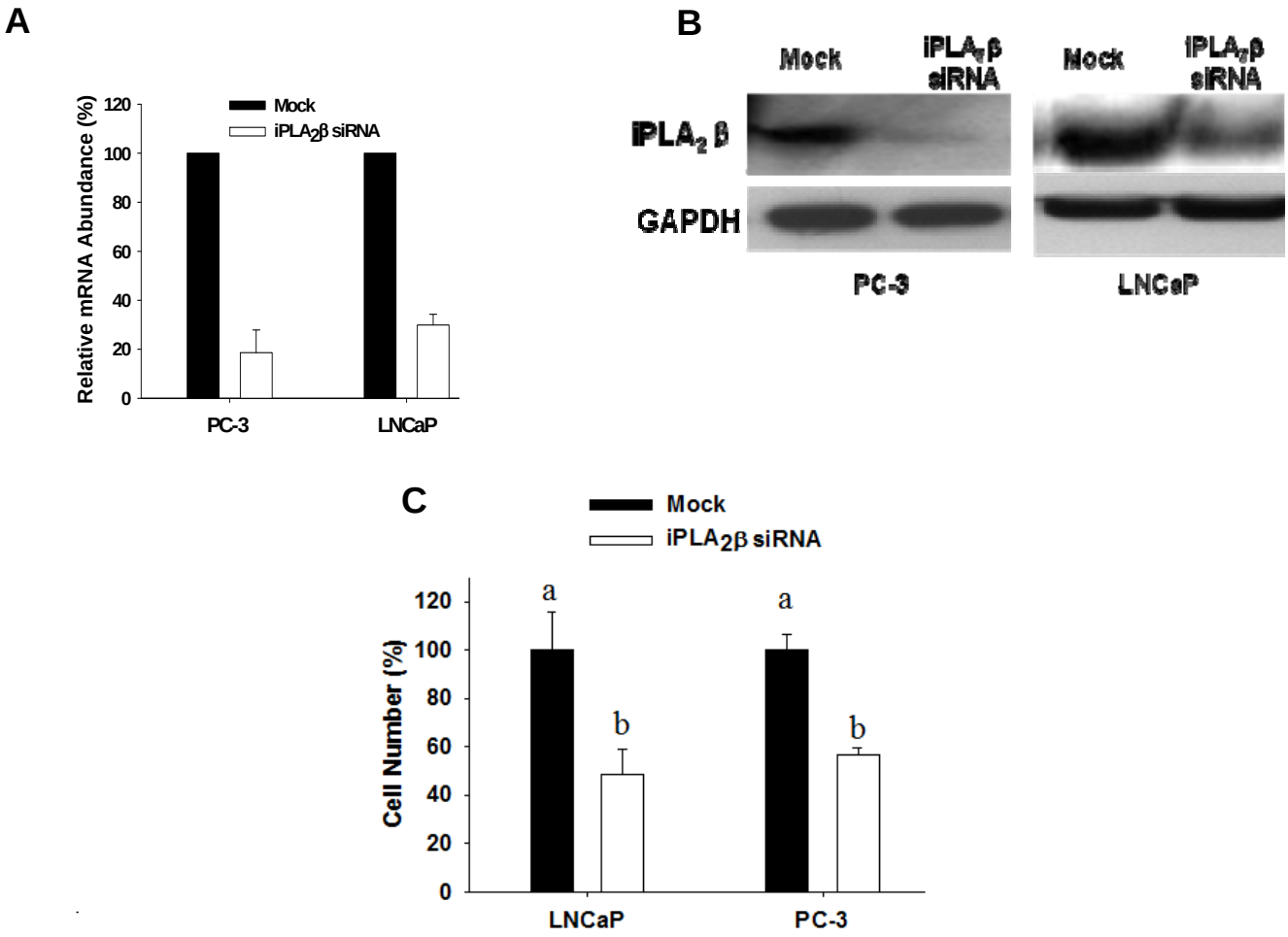

Fig 4.1. iPLA$_2$β knockdown decreases prostate cancer cell growth. iPLA$_2$β siRNA was transfected into PC-3 and LNCaP cells for 72 hr followed by real-time PCR analysis (**A**) or analysis of protein expression after 96 hr using immunoblot analysis (**B**). GAPDH expression is shown as a loading control. All blots are representative of at least three different experiments. **C.** iPLA$_2$β siRNA was transfected into PC-3 and LNCaP cells and cells were sub-cultured into 24 well plates and allowed to grow for 72 hr prior to cell counting. Data in **C** are presented as the mean ± SD of at least three separate experiments. Means with different subscripts are significantly different from each other ($P < 0.05$).

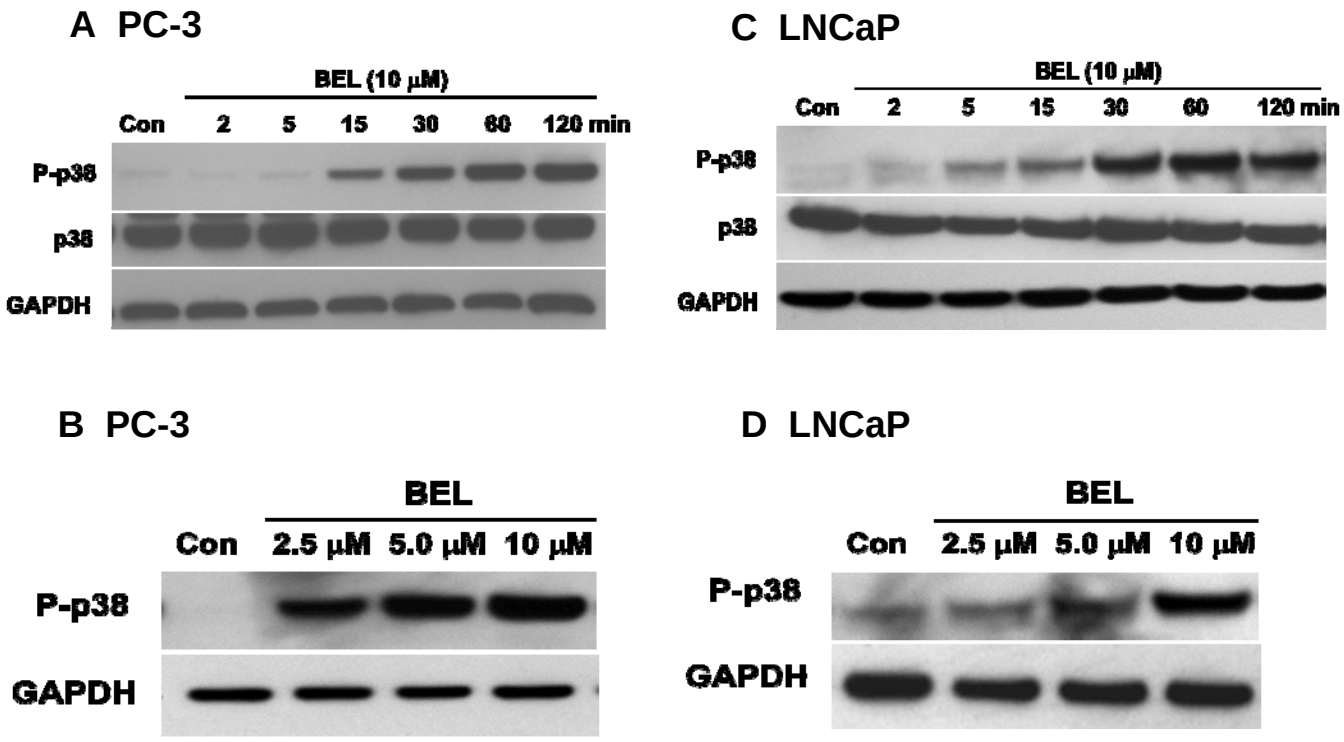

Figure. 4.2 (A-D) Effect of $iPLA_2$ inhibition on p38 activation in PC-3 and LNCaP cells. PC-3 (**A and B**) or LNCaP cells (**C** and **D**) were exposed to either 10 μM BEL for 0- 120 min (**A** and **C**) or to 0-10 μM BEL for 30 min (**B** and **D**), prior to analysis of p38 phosphorylation (P-p38 at Thr180/Tyr182) using immunoblot analysis. All blots are representative of at least three different experiments.

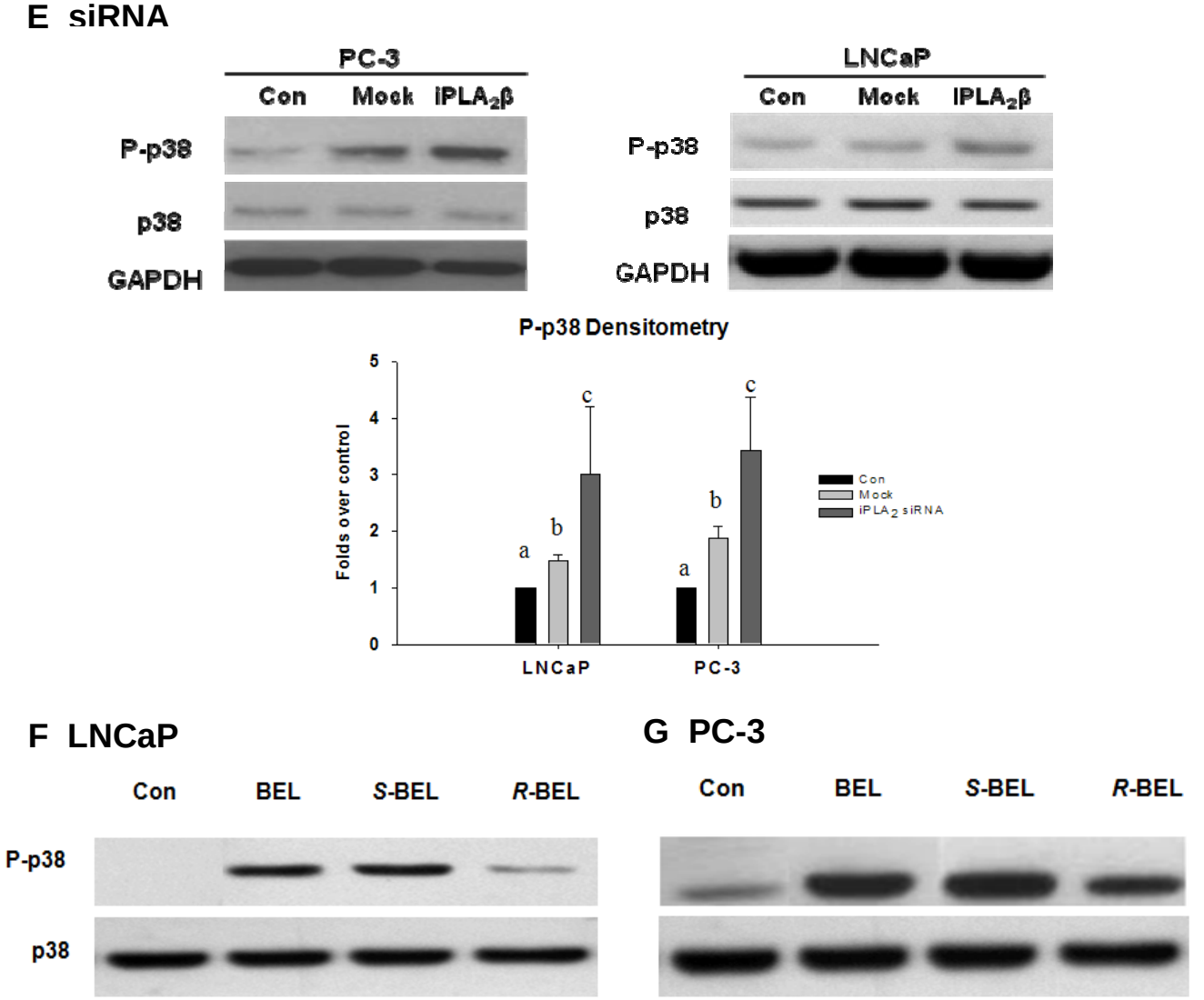

Figure. 4.2 (E-G) Effect of $iPLA_2$ inhibition on p38 activation in PC-3 and LNCaP cells. E. $iPLA_2\beta$ siRNA was transfected into PC-3 and LNCaP cells for 96 hr prior to isolation of cell lysate and analysis of P-p38 and p38 expression. GAPDH expression is shown as a loading control. The densitometry of P-p38 is also shown with regular p38 as normalization. **F** and **G**. LNCaP cells (**F**) and PC-3 cells (**G**) were treated with 10 μM BEL, 5 μM *S*-BEL or 5 μM *R*-BEL respectively for 2 hr followed by analysis of p38 and P-p38 using immunoblot analysis, All blots are representative of at least three different experiments. Densitometry data are presented as the mean ± SD of at least three separate experiments. Means with different subscripts are significantly different from each other ($P < 0.05$).

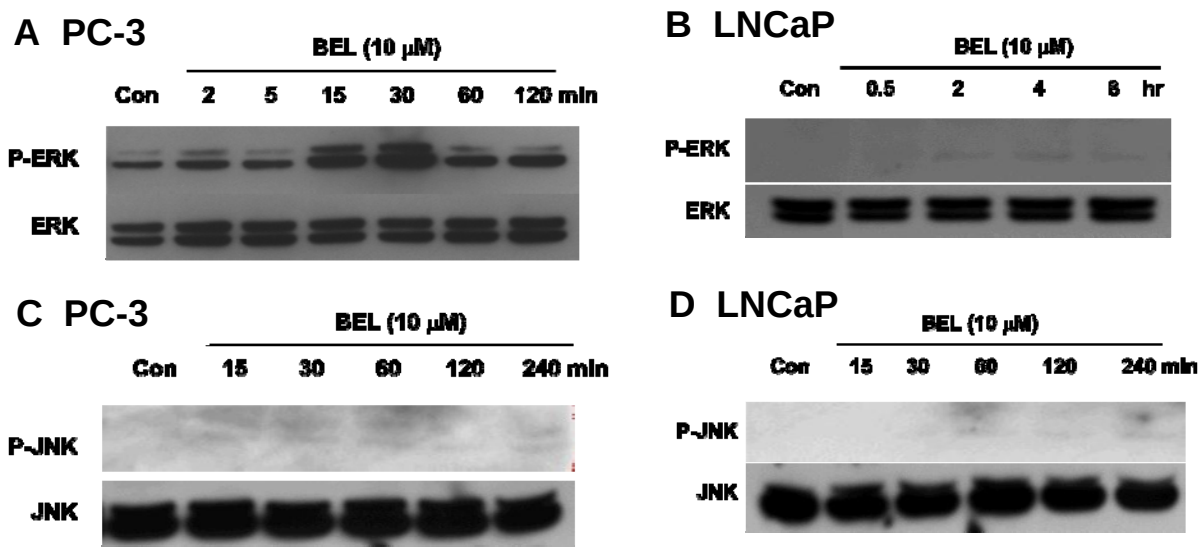

Figure 4.3 Effect of $iPLA_2$ inhibition on ERK1/2 and JNK activation in PC-3 and LNCaP cells. PC-3 (**A**) and LNCaP cells (**B**) were exposed to 10 μM BEL for 0-120 min (PC-3 cells) or 0-8 hr (LNCaP cells only), followed by analysis of P-ERK1/2 (Thr202/Tyr204) expression using immunoblot analysis. Total ERK1/2 expression is shown as a loading control. PC-3 cells (**C**) and LNCaP (**D**) were exposed to 10 μM BEL for 0, 15, 30, 60, 120 or 240 min followed by analysis of P-JNK (Thr183/Tyr185) expression using immunoblot analysis. Total JNK expression is shown as a loading control. The two observable bands are JNKI (46kD) and JNKII (54kD) respectively. All blots are representative of at least three different experiments.

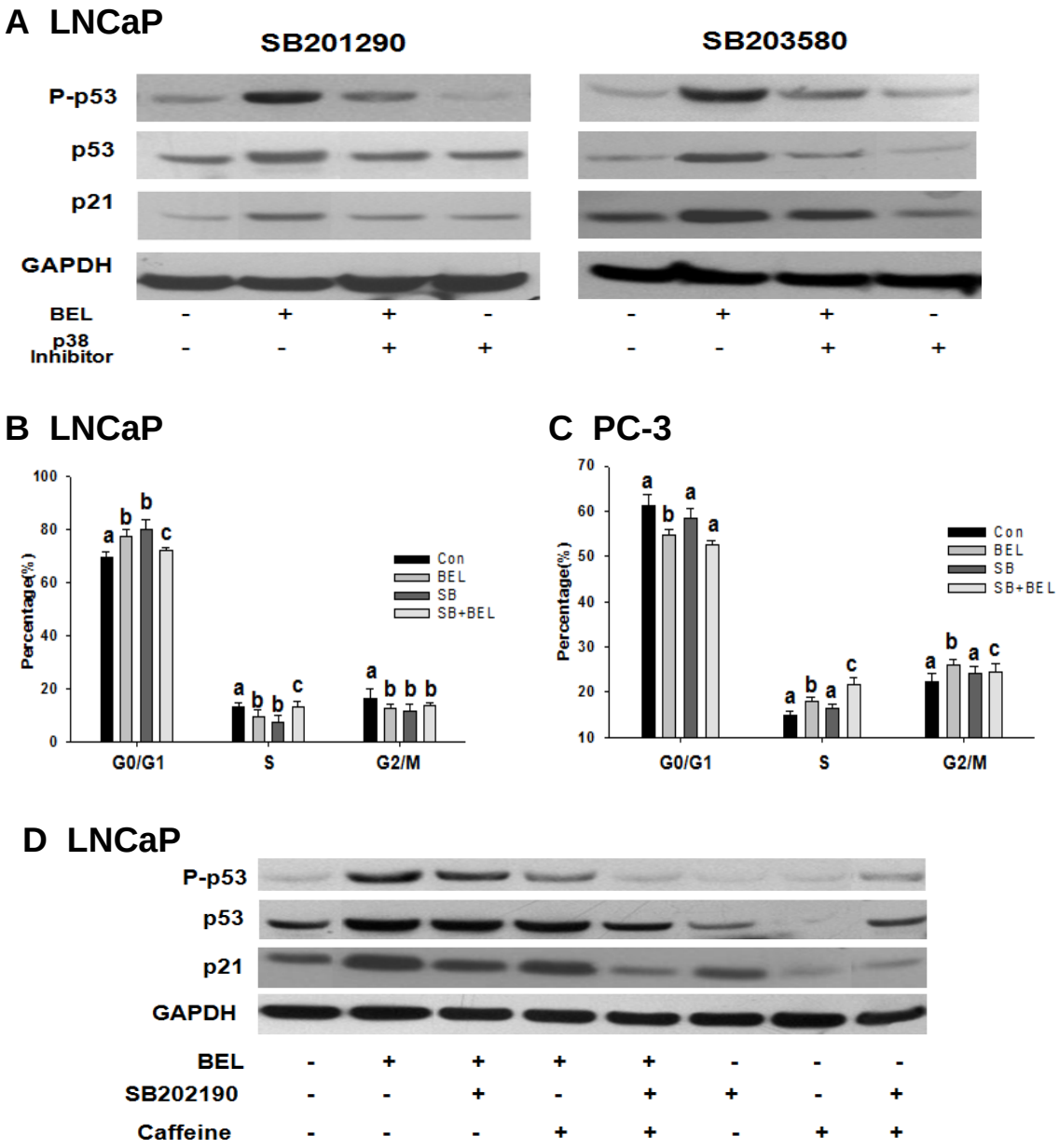

Figure 4.4 Effect of p38 inhibitors on BEL induced p53 and p21 expression and cell cycle in PC-3 and LNCaP cells. A. LNCaP cells were treated with SB202190 (10 μM) or SB203580 (10 μM) for 30 min prior to exposure to 10 μM BEL for 12 hr, followed by analysis of P-p53 (Ser15) p53 and p21 expression using immunoblot analysis. GAPDH expression is shown as a loading control. **B** and **C**. LNCaP (**B**) and PC-3 cells (**C**) were treated with SB202190 (10 μM) for 30 min prior to exposure to 10 μM BEL for 24 hr, followed by analysis of cell cycle using flow cytometery. **D.** LNCaP cells were pretreated with 10 μM SB202190, or 0.5 mM caffeine or both for 30 min prior to exposure to 10 μM BEL followed by immunoblot analysis of P-p53 (Ser15), p53 and p21 expression. All blots are representative of at least three different experiments. Densitometry data are presented as the mean ± SD of at least three separate experiments. Means with different subscripts are significantly different from each other ($P < 0.05$).

A

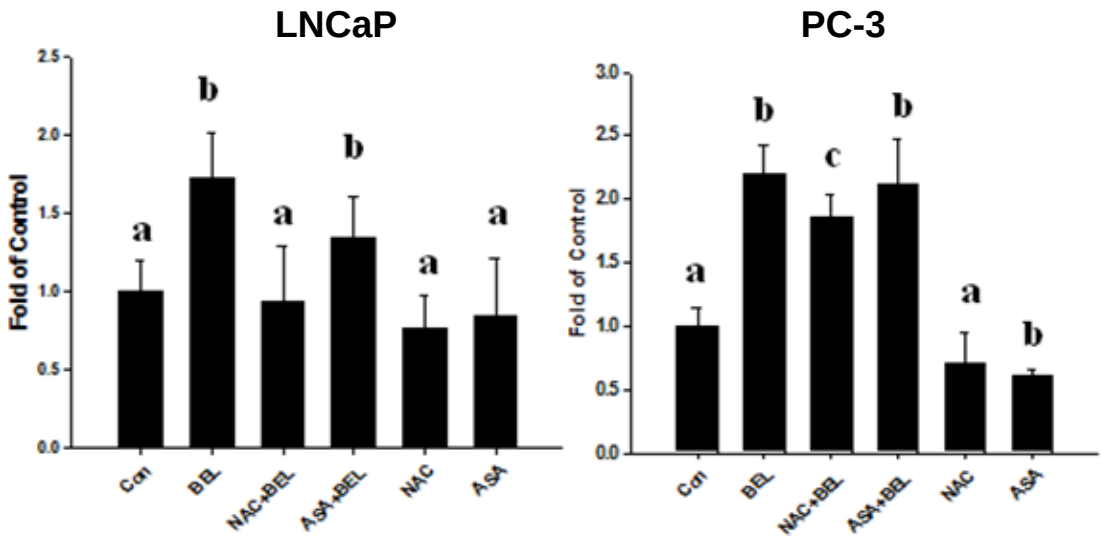

Figure 4.5 (A) BEL treatment induces RS in prostate cancer cells. **A.** LNCaP and PC-3 cells were loaded with CM-H2DCFDA for 30 min, followed by exposure to 2.5 mM NAC or 0.5 mM ascorbic acid (ASA) for 30 min prior to exposure to 10 μM BEL for 2 hr and analysis of fluorescence at 485 nm excitation and 520 nm emission. Data are presented as the mean ± SD of at least three separate experiments. Means with different subscripts are significantly different from each other (P <0.05).

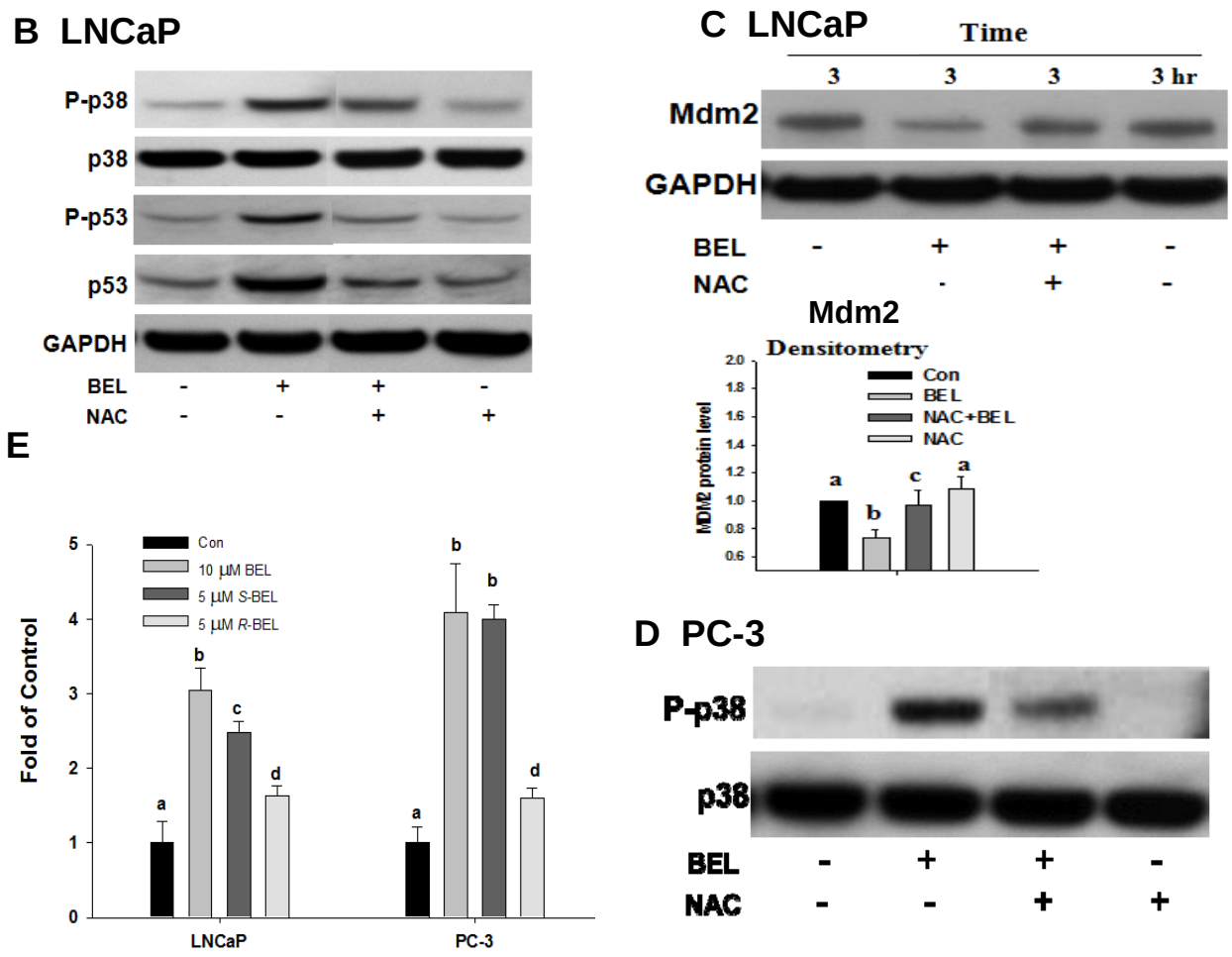

Figure 4.5 (B-E) BEL treatment induces RS in prostate cancer cells. **B.** LNCaP cells were treated with NAC for 30 min prior to exposure to 10 μM BEL and analysis of p38, P-p38, P-p53 (Ser15), p53 and GAPDH expression after 2 hr (p38 and P-p38) or 8 hr (P-p53, p53 and GAPDH). **C.** LNCaP cells were treated with 2.5 mM NAC for 30 min prior to exposure to BEL for 3 hr and analysis of Mdm2 expression. **D.** PC-3 cells were treated with 2.5 mM NAC for 30 min prior to treatment with 10 μM BEL and analysis of p38 and P-p38 expression after 2 hr. **E.** LNCaP and PC-3 cells were loaded with CM-H2DCFDA for 30 min, followed by exposure to 10 μM BEL, 5 μM *R*-BEL or 5 μM *S*-BEL for 2 hr and analysis of fluorescence at 485 nm excitation and 520 nm emission. Data are presented as the mean ± SD of at least three separate experiments. Means with different subscripts are significantly different from each other. (P <0.05). All blots are representative of at least three different experiments.

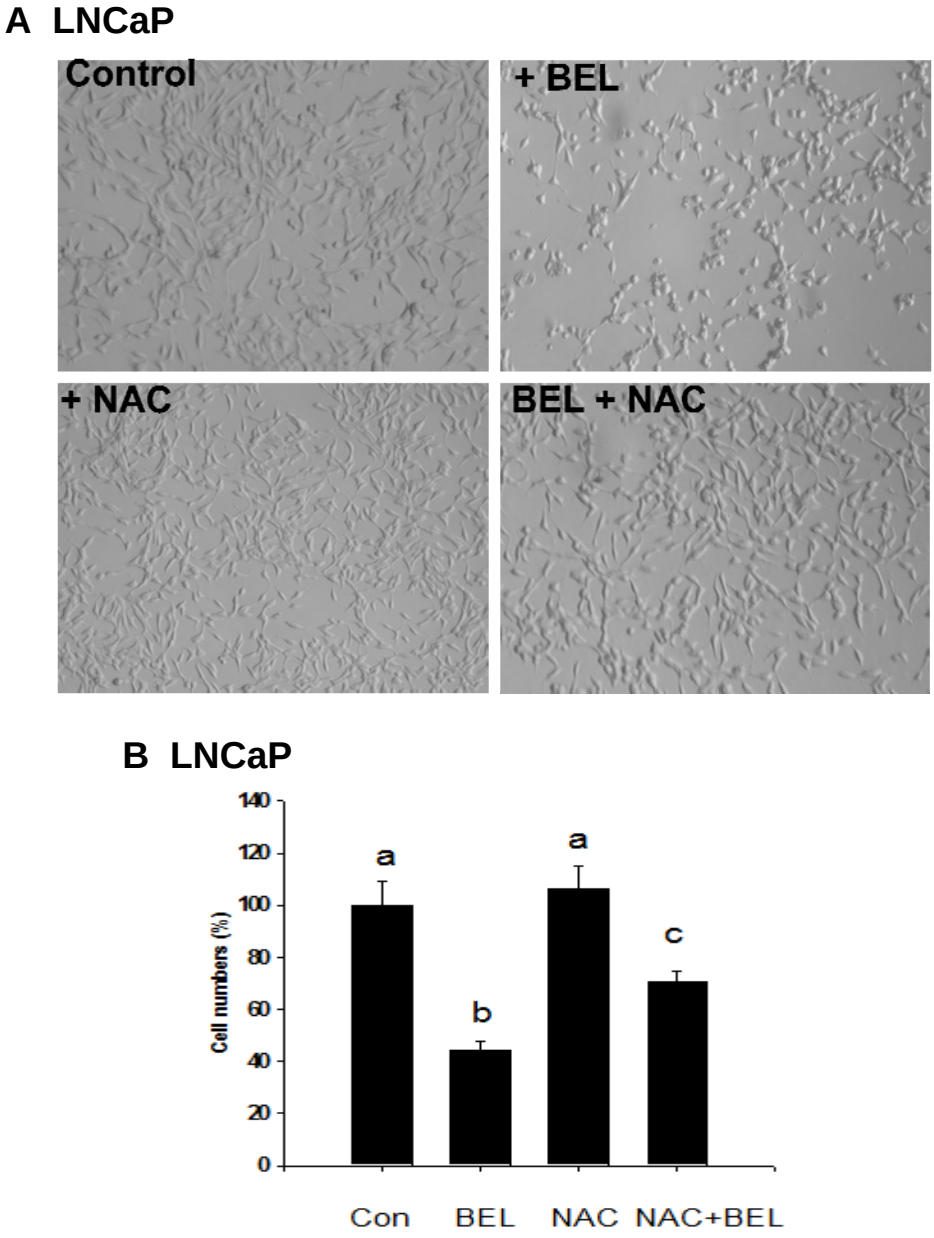

Figure 4.6 (A and **B) Treatment with NAC reverses the effect of BEL on cell growth and morphology.** LNCaP cells were seeded in 12-well plates for 24 hr after which media was replaced with serum-free media. After 2 hr, cells were treated with vehicle (DMSO), 5 μM BEL, 2.5 mM NAC, or NAC plus BEL. After 48 hr, the cells were visualized using microscopy at 25X magnification (**A**), followed by analysis of cell number (**B**). Data in **B** are presented as the mean ± SD of at least three separate experiments. Means with different subscripts are significantly different from each other ($P < 0.05$).

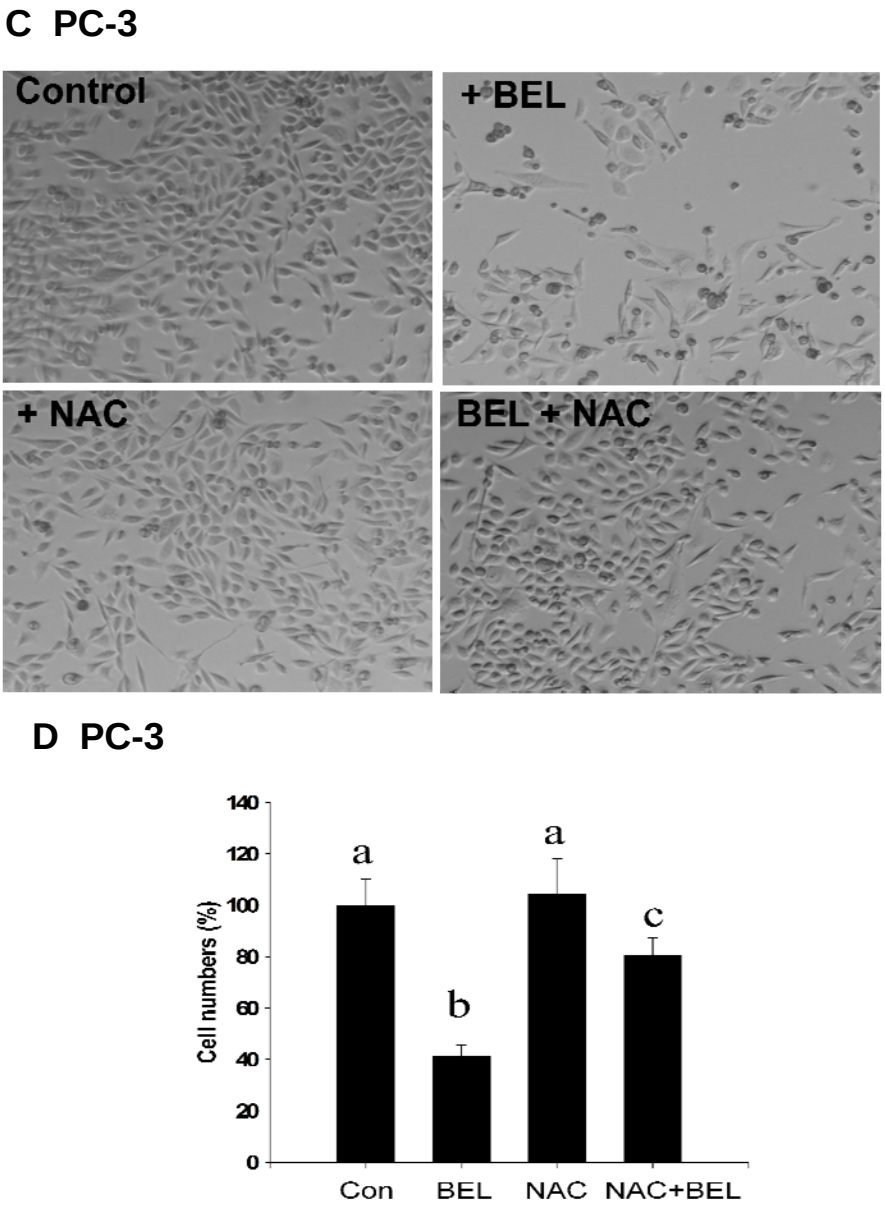

Figure 4.6 (C and D). Treatment with NAC reverses the effect of BEL on cell growth and morphology. PC-3 cells were seeded in 12-well plates for 24 hr after which media was replaced with serum-free media. After 2 hr, cells were treated with vehicle (DMSO), 5 μM BEL, 2.5 mM NAC, or NAC plus BEL. After 48 hr, the cells were visualized using microscopy at 25X magnification (**C**), followed by analysis of cell number (**D**). Data in **D** are presented as the mean ± SD of at least three separate experiments. Means with different subscripts are significantly different from each other ($P < 0.05$).

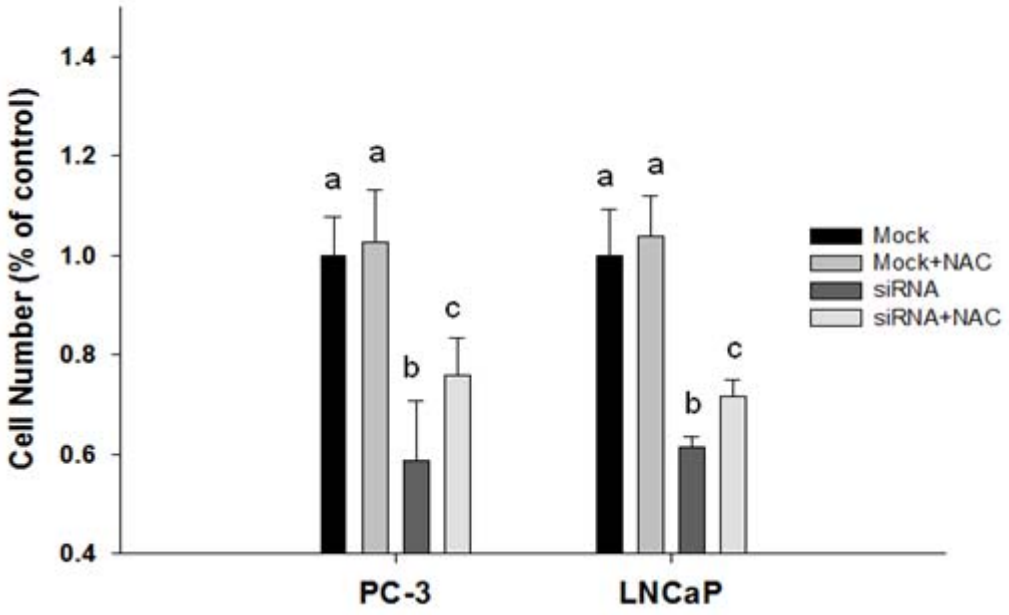

Figure 4.7 Treatment with NAC reverses the effect of $iPLA_2$ siRNA on cell growth. LNCaP and PC-3 cells were seeded in 24-well plates for 24 hr after which siRNA against 40nM $iPLA_2\beta$ siRNA was transfected into cells, after 6 hr, siRNA containing media was replaced with fresh growth media with or without 2.5 mM NAC. After 72 hr, cell number in each well was analyzed. Data in **E** are presented as the mean ± SD of at least three separate experiments. Means with different subscripts are significantly different from each other ($P < 0.05$).

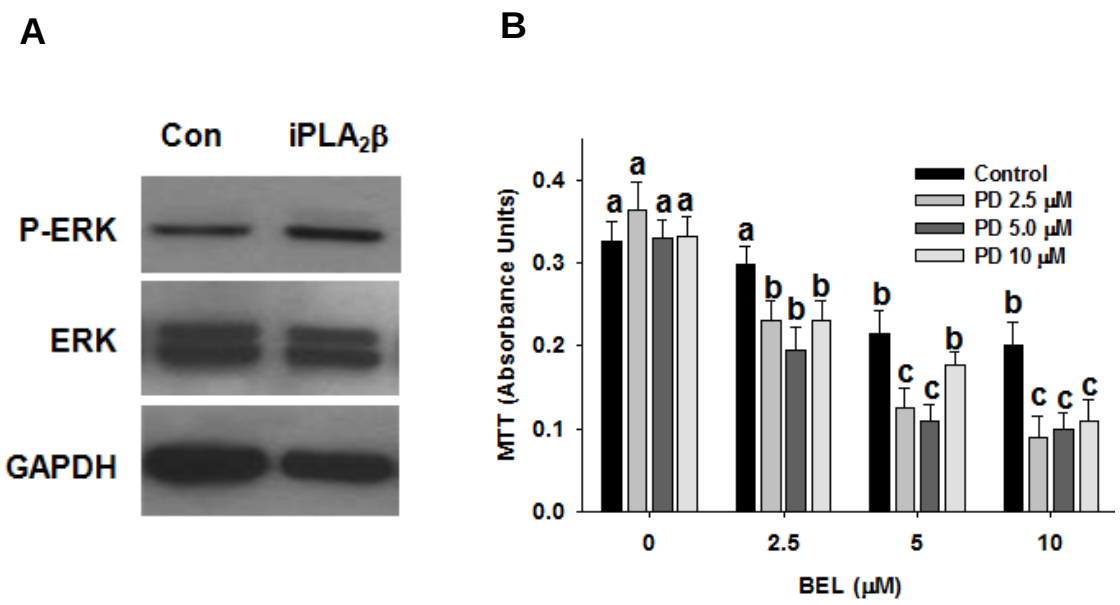

Figure 4.8 Effect of $iPLA_2$ inhibition on ERK 1/2 activation and ERK1/2 inhibitor on BEL-induced cytostasis in PC-3 cells. **A.** PC-3 cells were transfected with $iPLA_2\beta$ siRNA or negative control siRNA for 96 hr followed by immunoblot analysis of total ERK and phosphorylated ERK. **B.** PC-3 cells were pretreated with 0-10 μM PD98059 prior to 0-10 μM BEL exposure for 48 hr. After treatment, MTT assays were conducted to determine cell growth. Data are presented as the mean ± SD of at least three separate experiments. Means with different subscripts are significantly different from each other ($P < 0.05$).

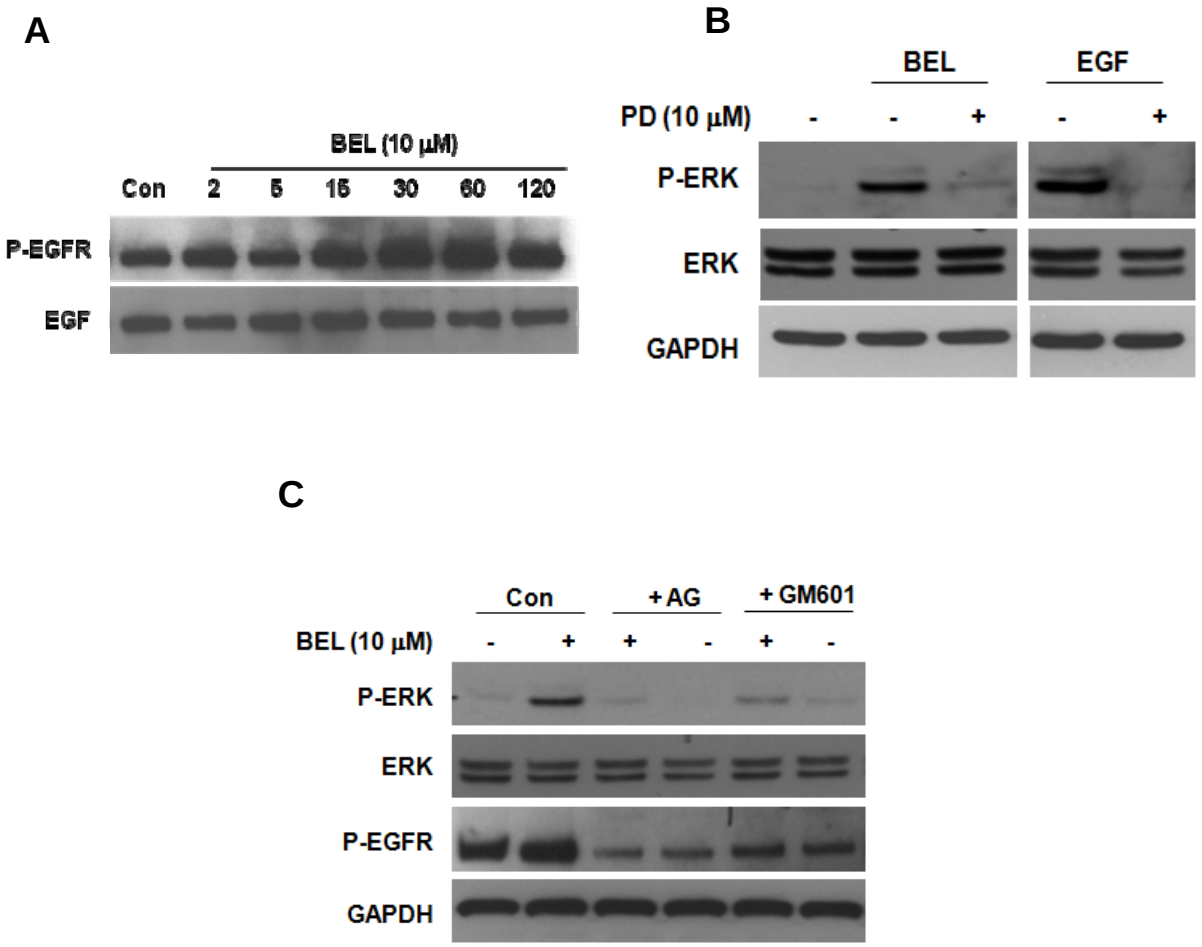

Figure 4.9 iPLA$_2$ inhibition induced ERK 1/2 activation is mediated by EGFR and MMP in PC-3 cells. **A.** Serum-deprived PC-3 cells were treated with 10 μM BEL for 2-120 min prior to analysis of phosphorylated EGFR (P-EGFR), total EGFR and GAPDH expression using immunoblot analysis. **B.** Serum-deprived PC-3 cells were exposed to 10 μM PD980589 for 30 min prior to treatment with 10 μM BEL or 100 ng/mL EGFR for 30 min, followed by analysis of P-ERK, ERK and GAPDH expression. **C.** Serum deprived PC-3 cells were exposed to 1.25 μM of the EGFR inhibitor AG1478 or 10 μM of the MMP inhibitor GM6001 for 30 min prior to treatment with 10 μM BEL for 30 min, followed by analysis of P-ERK, ERK, P-EGFR and GAPDH using immunoblot analysis. All blots are representative of at least three different experiments.

Discussion

Combined results from Chapter 3 and Chapter 4 support the conclusions that *S*-BEL has a more potent effect on p53, p38 MAPK and p21 expression, and RS formation, than *R*-BEL. The effect of *S*-BEL on cell signaling was validated using siRNA against iPLA$_2\beta$. These results support the hypothesis that iPLA$_2\beta$ is more involved in prostate cancer cell signaling than iPLA$_2\gamma$. This hypothesis is supported by studies in other cell types (Saavedra et al, 2006; Zhang et al, 2006; Herbert et al, 2006).

It is important to point out that these data do not suggest that iPLA$_2\gamma$ has no roles in cytostatic signaling. That fact that *R*-BEL alone induces some, albeit marginal, levels of p38, p53 and p21 expression supports this hypothesis. Further, *R*-BEL does decrease cell growth in several cell types as does iPLA$_2\gamma$ siRNA, just not as effectively as *S*-BEL (Saavedra et al, 2006). The differential effects of iPLA$_2\gamma$ inhibition, compared to iPLA$_2$ β, may result from the exclusive membrane location of iPLA$_2\gamma$, which is confined to the endoplasmic reticulum, the mitochondria and peroximomes (Kinsey et al, 2005; Kinsey et al 2007; Kinsey et al, 2008). Thus, iPLA$_2\beta$'s cytosolic expression may allow it greater access to cellular membrane, especially the plasma and nuclear membrane, which may account for the greater effect of *S*-BEL. It is also possible that the specific localization of iPLA$_2\gamma$ may result in activation of a differential set of signaling pathways, the identity of which are the subject of future studies.

Based on the pharmacological data with *R*- and *S*-BEL, and on our previous studies, we chose to focus the present study on iPLA$_2$ β. Molecular knockdown of iPLA$_2$ β using siRNA decreased cell growth in both LNCaP and PC-3 cells. The results were confirmed pharmacologically using BEL, and directly demonstrate roles for iPLA$_2$ β in prostate cancer cell growth. Further, these results also demonstrate that p53 is not required for iPLA$_2$ inhibition to

induce cytostasis. Such results are promising as a majority of malignant prostate tumors are negative or mutant for p53 (Eastham et al, 1995).

Work reported above also demonstrates the novel finding that $iPLA_2$ inhibition induces p38 activation in two different human prostate cancer cell models. To our knowledge this is the first report demonstrating that $iPLA_2$ inhibitors increase p38 in any cancer cell. This result is pertinent because p38 is often involved in cell death and senescence (Krishna et al, 2008). Further, the data suggest that $iPLA_2$ may regulate p38 MAPK.

The ability of $iPLA_2$ inhibitors to activate p38 in prostate cancer cells leads to questions about its function under these conditions. The ability of either SB202190 or SB203580 to decrease BEL-induced p53 phosphorylation (Ser15) and p53 expression in LNCaP cells suggests that p38 is being used to activate this tumor suppressor protein. The decrease in p21 expression induced by p38 inhibitors in the presence of BEL is most likely a result of p53 inhibition. Decreases in either p53 or p21 are mostly likely the cause of alterations in cell cycle in cells treated with SB202190 or SB203580 prior to BEL exposure.

Neither SB203580 nor SB202190 completely blocked BEL induction of p53. This suggests that other pathways for p53 activation exist during $iPLA_2$ inhibition. This hypothesis is supported by a recent study reporting that ATR mediates $iPLA_2$ inhibition-induced p53 induction in insulinoma cells (Zhang et al, 2008). Interestingly, we found that SB202190 plus caffeine, an ATR inhibitor blocked BEL-activated p53, while neither of those two totally reversed p53 by themselves (**Fig. 4.4 D**). These data suggest that both ATR and p38 may mediate p53 activation in prostate cancer cells.

Pretreatment of LNCaP cells with SB202190 also attenuated the increase of cells in G1 induced by BEL. The ability of SB202190 alone to increase cells in G1 apparently is not

associated with p53 as it did not induce p53 alone. Reasons why BEL attenuates the effect of SB202190 on cell cycle alterations are not currently known. One hypothesis is that $iPLA_2$ may also act as a downstream effecter of p38 via a negative feedback mechanism (Yellaturu et al, 2003; Beckett et al, 2006).

Reactive species (RS), including those containing oxygen, are considered as a major stimulator of p38 (Krishna et al, 2008). The ability of NAC to inhibit BEL-induced increase in RS, in correlation to p38 activation, suggests that $iPLA_2$ induces p53 using RS-mediated activation of p38. This hypothesis is supported by the fact NAC inhibited BEL-induced decrease in Mdm2 in correlation with p53 expression.

How exactly $iPLA_2$ inhibition induces RS, and what type of species is induced, is under study. Inhibition of $iPLA_2$ increases lipid peroxidation in several cell models (Kinsey et al, 2005; Kinsey et al, 2008; Cummings et al, 2002). Thus, lipid peroxides may be mediating the cascades of signaling events seen during inhibition. Another possibility is that BEL inactivates cys/thiol groups near the active site of $iPLA_2$, which mediates cellular redox regulation (Song et al, 2006). This action may increase thiol oxidation. This hypothesis is supported by the fact that NAC, but not ASA, altered BEL-induced cell signaling and cytostasis; however, it should be pointed out that NAC may also decrease lipid peroxidation as well.

It should be noted that cysteines are not directly targeted by BEL (Song et al, 2006). In fact, BEL itself does not interact with cysteine in $iPLA_2$. Rather, the specific reaction of BEL with cysteine bonds in $iPLA_2$ results from the ring opening of BEL, caused by serine-mediated hydrolysis. This is believed to form a specific reactive-bromoketone that alkylates cysteines located in $iPLA_2$ (Song et al, 2006).

To our knowledge, the finding that NAC significantly attenuates the growth inhibition effect of $iPLA_2$ inhibition is a novel finding. Several studies have attempted to reverse $iPLA_2$-inhibition induced cytostasis with only moderate success. For example, neither LPA nor lyso-phosphatidylcholine, metabolites of phospholipid metabolism by $iPLA_2$, reversed the effect of BEL on INS-1 cell proliferation (Zhang et al, 2006). Another study in ovarian cancer cells demonstrated that LPA only had a "weak" reversal effect on BEL-induced decreases in cell proliferation, and did not release cells from BEL-induced G2/M arrest (Song et al, 2007). Unpublished studies from our laboratory determined that p53 inhibition, calcium chelation, ER calcium depletion or epidermal growth factor activation also failed to reserve the effect of BEL on cell growth in prostate cancer cells (data not shown). Similarly, arachidonic acid, LPA and lyso-phosphocholines gave negative results as well (see details in Chapter 5).

The above data, in combination with the robust effect of NAC on reactive species, p38, p53 and p21, support the hypothesis that inhibition of $iPLA_2$ decreases cell proliferation via mechanisms that are not directly related to the production of mitogenic lipid signals. Rather, we propose that inhibition of $iPLA_2$ increases RS that initiate a broad series of cell signaling events including MAPK, p53 and p21 activation. The nature of the RS is probably thiol based due to the ability of NAC, but not ascorbic acid, to alter these signaling events and cell growth. The p53-independent mechanisms used by $iPLA_2$ inhibitors to decrease PC-3 cell growth remain undetermined, but may also involve p38 and RS, which also increased in PC-3 cells. As mentioned above, p38 is a stress-induced kinase and has multiple targets other than p53, including many pro-apoptotic proteins located in the mitochondria, mTOR and ER stress proteins (Pommery et al, 2005; Berti-Mattera et al, 2001). $iPLA_2$ is expressed at or translocates

to both the ER and mitochondria, so it's possible that $iPLA_2$ inhibition decreases cell growth by ER or mitochondrial dysfunctions.

Interestingly, aside from p38 MAPK, BEL induced a transient P-ERK1/2 increase in PC-3 cells but not in LNCaP cells. Further, $iPLA_2$ siRNA also slightly increased P-ERK1/2 in PC-3 cells. Reasons for the differential induction of P-ERK1/2 in these two cells are still unknown. One explanation is that PC-3 cells express a higher basal level of ERK1/2 (**Figure 4.3 A and B**). The role of ERK1/2 activation may be as a survival signal to resist the stress of $iPLA_2$ depletion. This hypothesis is supported by data demonstrating that the ERK1/2 selective inhibitor PD98059 intensified BEL induced cell cytostasis (**Figure 4.7 A**).

Data reported above suggest that inhibition of $iPLA_2$ activates ERK1/2 using EGFR pathways. This hypothesis is supported by the fact that BEL activates EGFR, and that the EGFR inhibitor AG1478 totally blocks BEL-induced ERK1/2 phosphorylation. GM6001, an inhibitor of MMP, also inhibited BEL-induced EGFR and ERK1/2 activation. MMP, especially MMP-3 and -9, stimulate release of endogenous heparin-binding EGF-like growth factor, which activates EGFR (Ongusaha et al, 2004). This pathway is commonly used for self-proliferation in several types of cancer cells. Thus, $iPLA_2$ inhibitors may function at the level of MMP to alter EGFR activity in PC-3 cells.

In conclusion, this study used both molecular and pharmacological techniques to demonstrate that $iPLA_2$ inhibition induced cytostasis in prostate cancer cell and demonstrated the novel finding that p38 is activated under these conditions, while ERK1/2 is transiently and differentially activated only in PC-3 cells. Inhibition of p38 altered cell cycle arrest induced by $iPLA_2$ inhibition, and decreased activation of p53 and p21 in LNCaP cells. Activation of p38 correlated to RS formation, which was inhibited by NAC, but not ascorbic acid. NAC reversed

the effect of BEL on cell proliferation. $iPLA_2$ inhibition activated a MMP/EGFR/ERK1/2 pathway in PC-3 cells and inhibition of ERK1/2 potentiates cytostatic effect of BEL. These data support the hypothesis that $iPLA_2$ mediates cell growth in prostate cancer cells, and identify novel MAPK signaling pathways mediated by this protein, and suggest that thiol-based RS may be involved.

CHAPTER 5

INHIBITION OF $iPLA_2$ ALTERS PHOSPHOLIPID PROFILES DURING CYTOSTASIS[3]

[3] Bin Sun, Xiaoling Zhang, and Brian S. Cummings. Manuscript in preparation.

Introduction

Phospholipids are building blocks of biological membrane, and play important roles in cell signaling, especially during cancer cell growth and metastasis. Phospholipids are precursors of several important molecules that control cell growth such as lypophospholipids and polyunsaturated fatty acids and lysophosphatidic acid (Meyer et al, 2007; Pandalai et al, 1996; Rose et al, 1988; Rose et al, 1991; Cave et al, 1991).

There is a strong association between metastasis and choline phospholipid metabolism. Increases in phosphatidylcholine (PtdCho) levels positively correlate to invasiveness of brain, prostate and breast cancer cells (Glunde et al, 2006). They also positively correlate to loss of p53 in colon cancer cells (Mori et al, 2004).

PtdCho were first thought to be critical in cancer when it was observed that the nuclear membrane of normal rat liver cells contain the highest levels of polyunsaturated fatty acids among phospholipid species (Khandwala et al, 1971). This study suggested the importance of PtdCho containing polyunsaturated fatty acids in the function of the nuclear membrane. The functions of these polyunsaturated PtdCho are believed to be in regulation of fluidity of nuclear membranes, which profoundly affects nuclear function, such as the timing of DNA replication. In support of this hypothesis, changing the membrane fluidity of vascular smooth muscle cells alters their DNA synthesis (Sachinidis et al, 1999).

Phosphatidylethanolamine (PtdEtn) is also essential to cell growth. Epithelial cells need ethanolamine to proliferate. Decreasing the content of PtdEtn of epithelial cells decreases cell growth. If PtdEtn is reduced to 50% or lower, the function of epidmeral growth factor receptor and protein kinase C activation is suppressed (Kano-Sueoka et al, 1993; Kano-Sueoka et al, 1990).

Lysophospholipids (LPs) and their metabolites, especially lysophosphatidic acid (LPA), are a group of bioactive phospholipids metabolites produced by PLA_2 and other phospholipases. LPA regulates cancer cell proliferation, survival, migration, adhesion and invasion (Van Corven et al, 1989; Moolenaar et al, 2004). LPA acts through specific G-protein-coupled receptors (GPCRs) including LPA1 through LPA4 (Choi et al, 2010).

Fatty acids, another metabolite of PLA_2, are also involved in cell growth. The most important fatty acids involved in cancer cell growth and metastasis are polyunsaturated fatty acids. Interestingly, omega-6 polyunsaturated fatty acids, such as arachidonic acid, promote cancer cell growth, including those of prostate cancer (Pandalai et al, 1996; Rose et al, 1988; Rose et al, 1991). In contrast, omega-3 polyunsaturated fatty acids, such as docosahexaenoic acid (DHA) and eicosapentaenoic acid (EPA), inhibit prostate cancer cell growth (Cave et al, 1991; Pandalai et al, 1996; Rose et al, 1991). This dichotomy exists because fatty acids activate differential pathways. For example omega-3 polyunsaturated fatty acids, such as DHA and EPA are agonist of PPARγ (Fajas et al, 2003) and inhibit cell growth. In contrast, omega-6 polyunsaturate fatty acids, such as arachidonic acid (AA) and linoleic acid (LA) activate lipoxygenases (Ghosh et al, 1997) or cycloxoxygenases (Attiga et al, 2000), which promote cell proliferation, invasiveness and metastasis (Vijayakrishnan, 2009). Although $cPLA_2$ has been demonstrated to play predominant roles in AA and LPA release and the sequelae of these events (Hirabayashi et al, 2005), in some circumstances, $iPLA_2$ are suggested to participate in the production of AA (Perez et al 2004; Yellaturu et al, 2003; Xu et al, 2003) and LPA (Senguota et al, 2003).

Phospholipid remodeling, which is mediated by the Lands Cycle, refers to rapid deacylation/reacylation of cellular phospholipids (Lands, 1965). In this cycle, PLA_2 generate

lysophospholipids (LPs) and free fatty acids, which are then recycled by acyltransferases to produce new or altered patterns of phospholipids. Phospholipid remodeling plays an important role in cell proliferation and apoptosis. For example, inhibition of acyltransferases such as CoA-independent acyltransferase blocks arachidonate phospholipid remodeling and subsequently decreases cell proliferation and induces apoptosis in neoplastic cells (Surette et al, 1996; Winkler et al, 1996; Surette et al, 1999).

$iPLA_2$ are reported to be crucial in phospholipid remodeling, particularly in the incorporation of arachidonic acid (Bao et al, 2005) into new phospholipids. We and others have shown that inhibition of $iPLA_2$ decreases cell proliferation in both cancerous and non-cancerous cells (Saavedra et al, 2006; Zhang et al, 2006; Song et al, 2007; Herbert et al, 2006). While we have demonstrated roles for several cell signaling proteins in these events, we have never identified the specific targets of $iPLA_2$, namely the phospholipids themselves.

This chapter tests the hypothesis that $iPLA_2$ inhibition alters phospholipid profiles during cytostasis in prostate cancer cells. These data are used to test the hypothesis that cytostasis induced by $iPLA_2$ inhibition is mediated by alterations of phospholipids or lysophospholipids and fatty acids.

Results

Effect of lysophospholipids and polyunsaturated fatty acids on $iPLA_2$ inhibition-induced cytostasis.

In order to test the hypothesis that $iPLA_2$ inhibition induced prostate cancer cell cytostasis is mediated by bioactive metabolites of $iPLA_2$, the effects of exogenous bioactive lipids and their metabolites, including LPA (18:1), arachidonic acid (AA), linoleic acid (LA) and prostglandin

E2 PGE_2, on $iPLA_2\beta$ siRNA-induced cytostasis was determined. Briefly, PC-3 and LNCaP cells were transfected with siRNA against $iPLA_2\beta$ for 6 hr, washed and media was replaced with that containing LPA (18:1), AA, linoleic acid (LA) and PGE_2. As previously shown, transfection of cells with siRNA against $iPLA_2\beta$ decreased Sulforhodamine B (SRB) staining or CellTiter Blue (CTB) staining 50% compared to cells transfected with negative control siRNA (**Fig. 5.1 A** and **B**). Treatment of cells with LPA, AA LA and PGE_2 did not reverse cytostasis induced by $iPLA_2\beta$ siRNA.

Effect of lysophospholipids and polyunsaturated fatty acids on p53 activation induced by $iPLA_2$ inhibition.

To confirm that the bioactive lipids studied above do not reverse cytostasis induced by $iPLA_2$ inhibition we used immunoblot to test the effects of those bioactive lipids on p53 pathway signaling pathways activated by BEL. LNCaP cells were treated with BEL (10 μM) in the presence and absence of LPA (18:1), AA, LA and PGE_2 for 8 hr prior to analysis of p53 and p21 expression (**Fig. 5.2 A** and **B**). As expected, BEL induced P-p53, p53 and p21; however, none of the lipid species tested reversed the ability of BEL to increase p53 and p21 expression. These data suggest that cytostasis and cell signaling induced by $iPLA_2$ inhibition is not mediated by inhibition of LPA or AA/PGE_2 pathways.

Effect of inhibition of $iPLA_2$ on cellular phospholipids.

Because our data suggested that cytostasis induced by $iPLA_2$ inhibition was not mediated by LPA or AA, we tested hypothesis that cytostasis correlated to alterations in phospholipid profiles. To achieve this goal, we treated prostate cancer cells with BEL for 0, 6 and 24 hr, and

extracted total lipids using Bligh-Dyer extraction protocols. Following lipid isolation we separated lipids using two dimensional high performance thin layer chromatography (2D-HP-TLC), and identified lipids using electrospray ionization mass spectrometry (ESI/MS). As seen in **Fig. 5.3,** 2D-HP-TLC successfully separated the three most abundant types of phospholipids; phosphotidylcholine (PtdCho), phosphotidylserine (PtdSer) and phosphotidylethanolamine (PtdEtn) in LNCaP cells. 2D-HP-TLC did not reveal any distinctive differences in individual levels of these three phospholipids between control LNCaP cells and BEL-treated cells (**Fig. 5.3**). Similar results were seen in PC-3 cells (data not shown).

Effects of $iPLA_2$ inhibition on individual PtdCho species.

2D-HP-TLC results did not show any differences in total levels of PtdCho, PtdEtn or PtdSer after BEL exposure, however it did successfully separate these three major phospholipids groups. Thus, we followed up 2D-HP-TLC with ESI/MS/MS to assess the effect of BEL on individual PtdCho species. 2D-HP-TLC-ESI/MS has two major advantages compared to traditional direct ESI/MS analysis. The first is that it avoids ion overlap from different phospholipid groups (Karlsson et al, 1996). The second is that it prevents ion suppression induced by PtdCho, which interferes with the ionization of other phospholipids (Petkovic et al, 2001).

Typical ESI/MS Spectra of PtdCho in PC-3 and LNCaP cells are shown in **Fig. 5.4 A** and **B**. The most abundant peak in both cells corresponded to that with an *m/z* value of 760. To confirm that 2D-HP-TLC separation was successful, we used a triple quadrupole ESI/MS to conduct tandem MS on the lipid isolated at *m/z* 760 ion **(Fig. 5.4 C)**. This resulted in a product

ion with a *m/z* of 184, which corresponds to a phosphocholine group, a typical fragment ion of PtdCho (Cole et al, 1991).

We next analyzed individual phospholipid species and normalized their intensity to total ion count in each sample. We identified several hundred different *m/z* values representing PtdCho, PtdEtn and PtdSer; however, we are only showing the species whose abundance significantly changed compared to control after treatment with BEL (**Figure 5.5-5.7)**. Specific PtdCho species decreased by BEL treatment in LNCaP cells included 30:2, 30:0, and 32:0 PtdCho (**Fig. 5.5 A**). PtdCho species increased in LNCaP cells in the presence of BEL included 36:1, 38:6, 38:2, 38:1, 40:4 and 40:5 PtdCho (**Fig. 5.6**). On the other hand, BEL treatment decreased the abundance of 30:0, 32:0 and 40:0 PtdCho in PC-3 cells (**Fig. 5.5 B**), while increasing the abundance of 34:3, 36:4, 38:3 and 40:4 PtdCho (**Fig. 5.7**). Thus, BEL treatment predominantly altered PtdCho by increasing phospholipids containing polyunsaturated fatty acyl chains (PUFA), and decreasing the abundance of PtdCho phospholipids containing saturated fatty acids (SFA).

Effect of iPLA$_2$ inhibition on PtdSer and PtdEtn levels.

We also used 2D-HP-TLC-ESI/MS to assess the effect of BEL on PtdEtn and PtdSer. As above, only those phospholipids whose levels significantly changed compared to control are shown. Only a few PtdEtn and PtdSer species were altered by BEL treatment in either cell line (**Fig. 5.8**). The three PtdEtn species containing PUFA that increased after BEL treatment in LNCaP cells were 30:2; 33:2; 40:2. The only PtdEtn species containg PUFA that increased in PC-3 cells after BEL treatment was 40:3. In contrast, two PtdEtn species (36:0; 38:1) containing SFA or MUFA were decreased after BEL exposure in PC-3 cells.

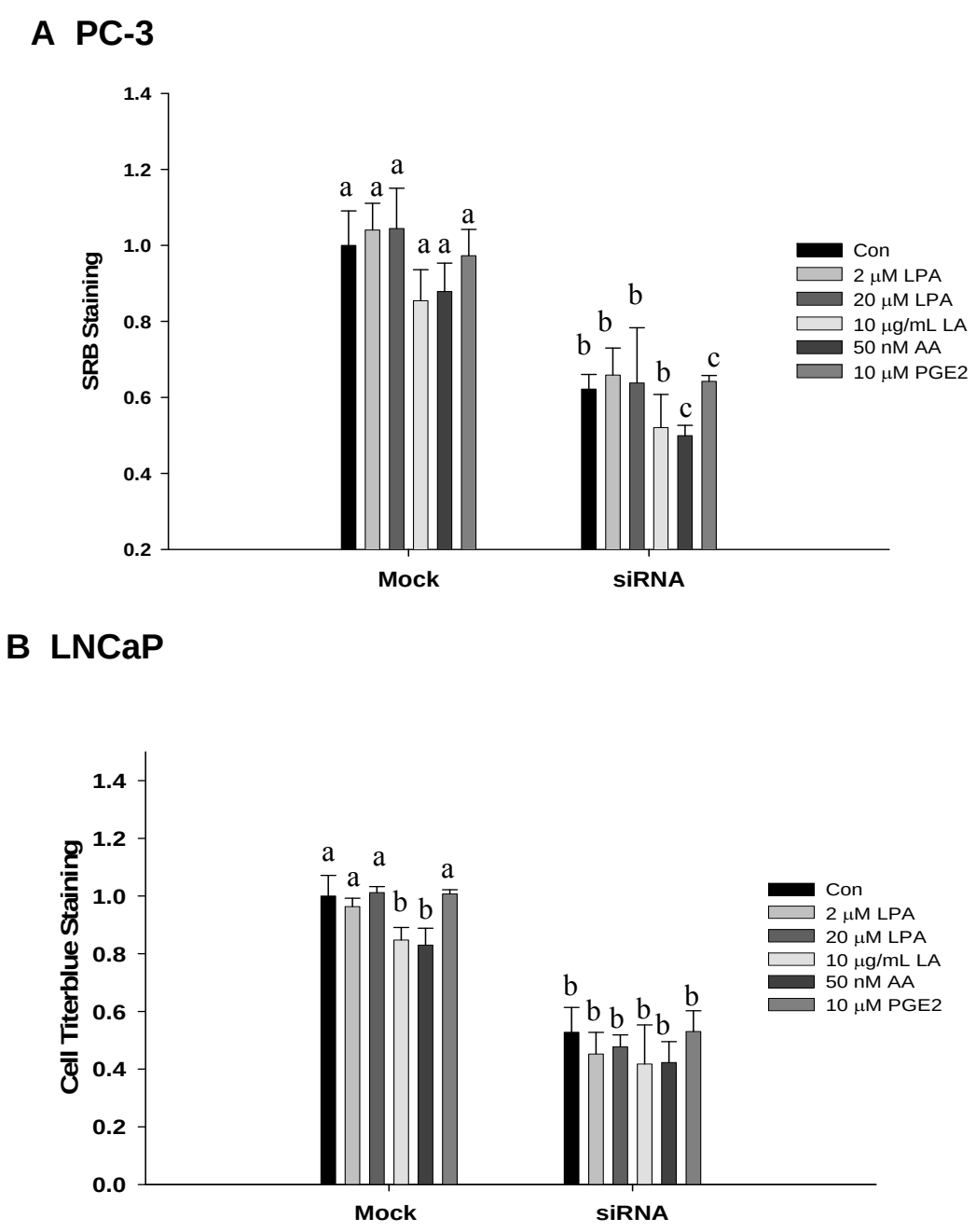

Figure 5.1 The effects of exogenous lysophosphatidic acid (LPA), LA AA and PGE_2 on $iPLA_2$ inhibition-induced cytostasis in prostate cancer cells. PC-3 (**A**) and LNCaP (**B**) cells were treated with siRNA against $iPLA_2\beta$ or negative control siRNA for 6 hr. After treatment, siRNA containing media was replaced with fresh media containing 50 nM AA, 10 μg/mL LA, 10 μM PGE_2 2 μM or 20 μM LPA. After 72 hr, cell viability was assessed either by SRB or cell titer blue. Data are presented as the mean ± SD of at least 3 (n = 3) separate experiments. Means with different subscripts are significantly different ($P < 0.05$) from each other.

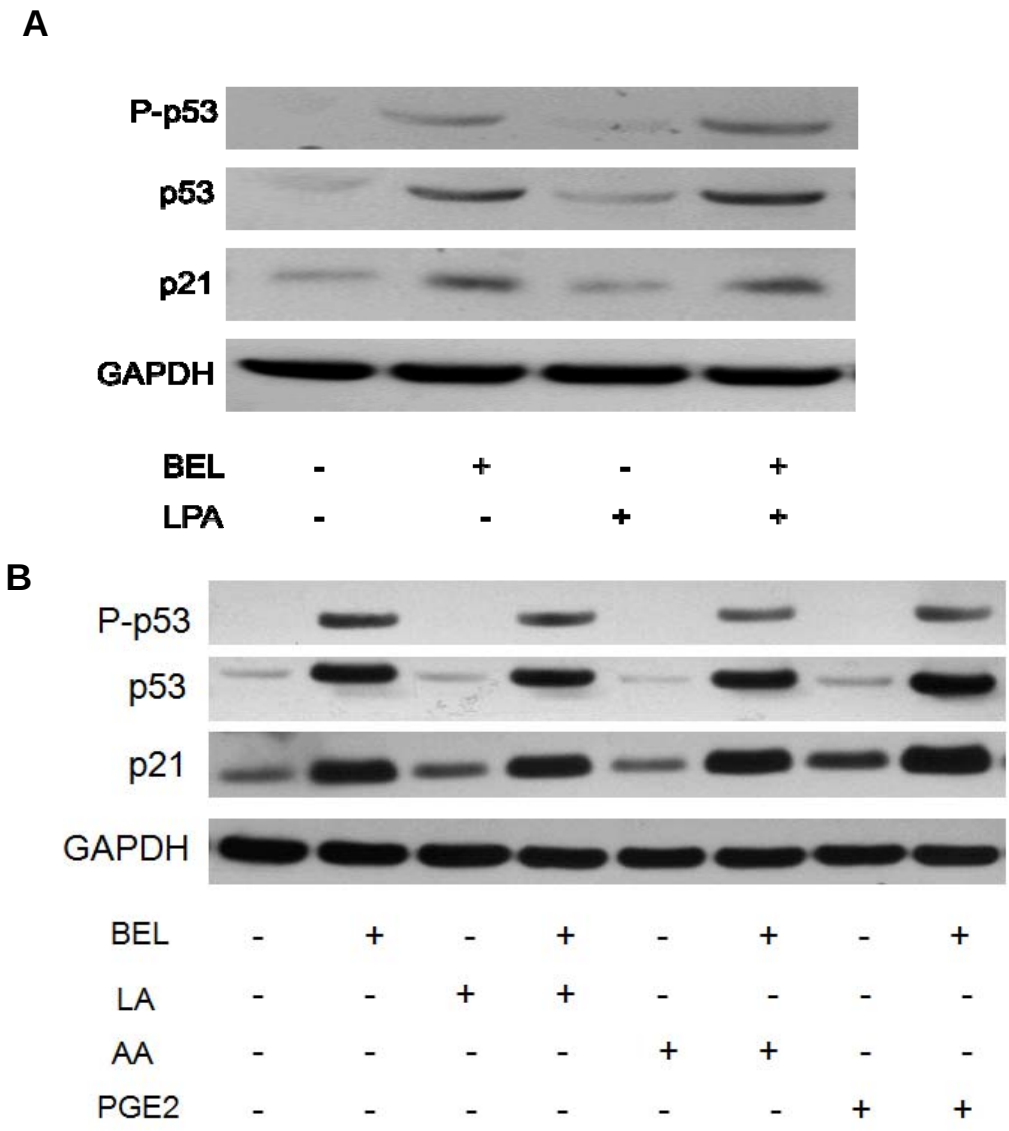

Figure 5.2 The effect of exogenous lysophosphatidic acid (LPA) AA and PGE_2 on $iPLA_2$ inhibition induced cell signaling in prostate cancer cells. LNCaP cells were pretreated with 2 μM LPA (**A**), 100 μg/mL LA, 50 nM AA or 100 μM PGE_2 (**B**) for 30 min and then exposed to 10 μM BEL. After exposure for 8 hr, P-p53, p53 and p21 were assessed using immunoblot analysis. GAPDH was used as loading control. All blots are representative of at least three different experiments.

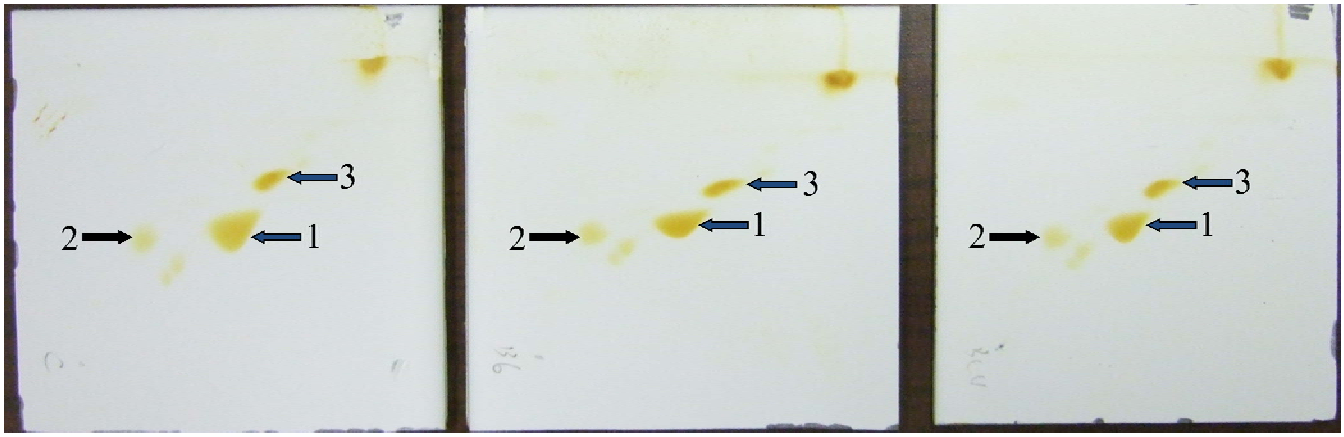

Con **BEL 6 hr** **BEL 24 hr**

1. **Phosphatidylcholine**
2. **Phosphatidylethanolamine**
3. **Phosphatidylserine**

Figure 5.3 The effect of inhibition of $iPLA_2$ on phospholipids in LNCaP cells. Cells were treated with 10 μM BEL for either 6 or 24 hr and total lipids were extracted using Bligh-Dyer methods. Inorganic phosphorous assay were used to determine the total phospholipids levels in each individual sample. Total lipids (100 nMole) were loaded onto a HP-TLC plate that was developed in two dimensions. The first solvent system was chloroform/methanol/28% ammonium hydroxide (65:25:5, v/v) and the second one contained chloroform/acetone/methanol/glacial acetic acid/water (50:20:10:10:5, v/v). After developing, the TLC plates were dried and stained using iodine to visualize lipid spots.

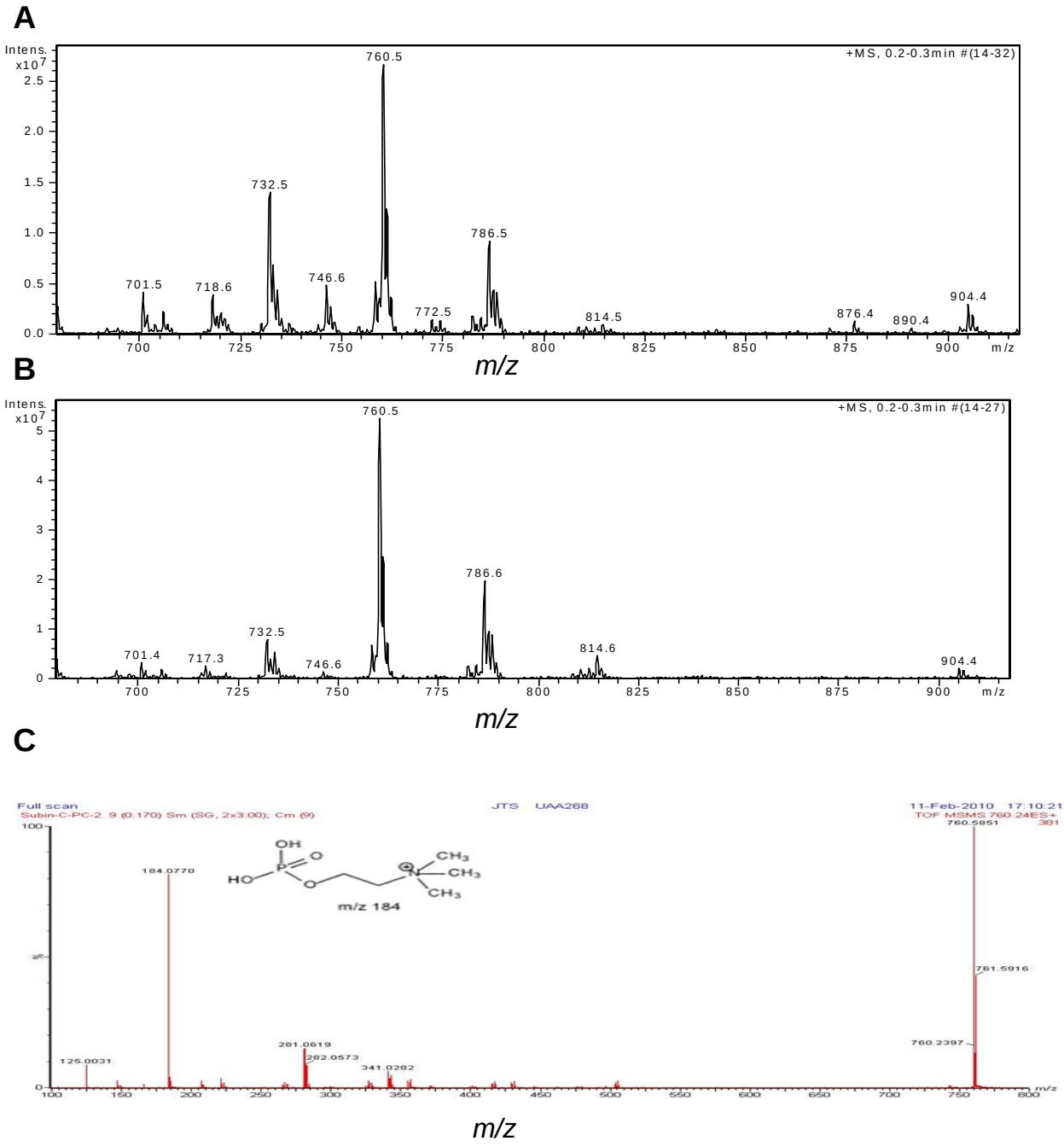

Figure 5.4 Mass Spectra of PtdCho in prostate cancer cells. PtdCho from cell exposed to BEL (10 μM) were separated on HP-TLC plates, scraped and re-extracted using Bligh-Dyer extraction. An Agilent Ion-Trap ESI/MS was then used to assess individual PtdCho species. The typical mass spectra of PtdCho in PC-3 and LNCaP cells are shown in **A** and **B**. Note the peak at *m/z* value 760, indicating 16:0 18:1 PtdCho, which is the most abundant species in both cell types. **C.** MS/MS analysis of the *m/z* 760, which generated a *m/z* 184 peak representing a phospho-choline group, the typical daughter ion of PtdCho.

A LNCaP

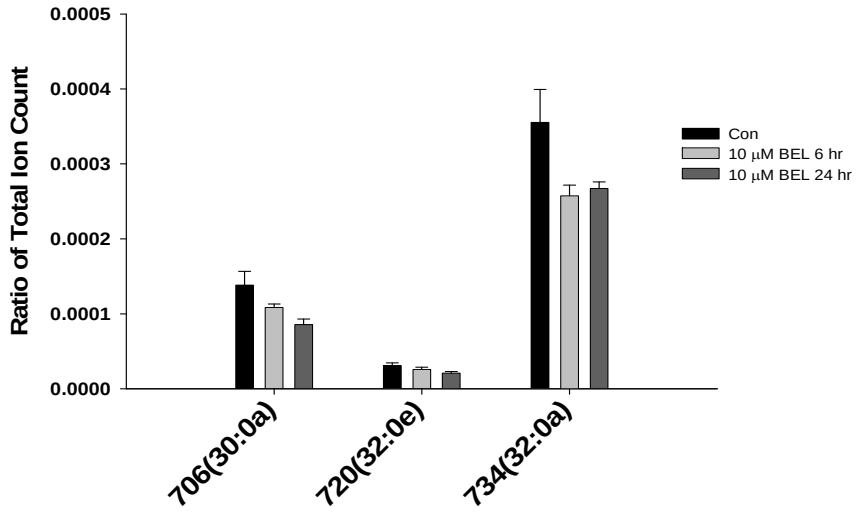

B PC-3

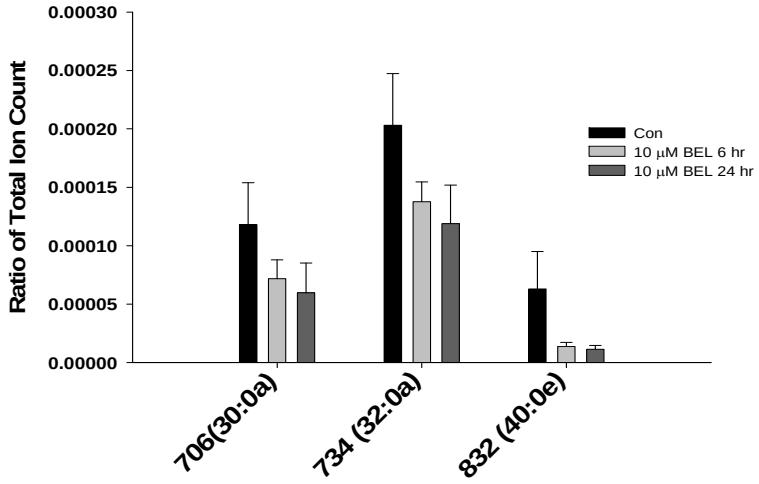

Figure 5.5 Effect of $iPLA_2$ inhibition on saturated PtdCho. LNCaP (**A**) and PC-3 (**B**) and were exposed to BEL (10 μM) for 6 and 24 hr prior to analysis of PtdCho using 2D-HP-TLC-ESI/MS/MS. Individual species of saturated PtdCho were quantified based on their intensities and normalized to the total ion count for each spectrum. Only those that had significant changes compared to control are shown. Data are presented as the mean ± SD of five separate experiments. All species shown possess significant difference between control and BEL treatment ($P<0.05$).

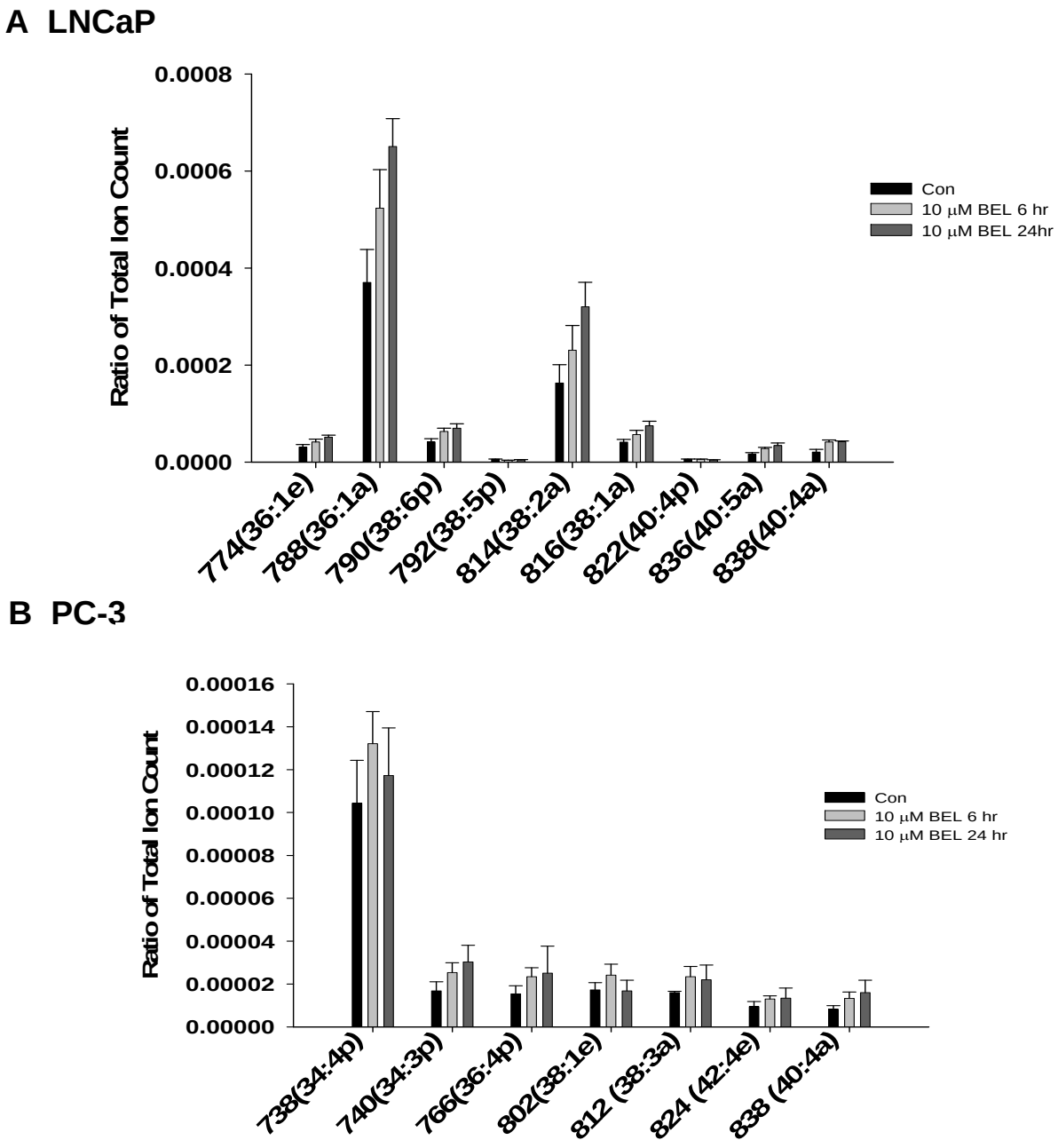

Figure 5.6. Effect of $iPLA_2$ inhibition on unsaturated PtdCho. LNCaP (**A**) and PC-3 (**B**) and were exposed to BEL (10 μM) for 6 and 24 hr prior to analysis of PtdCho using 2D-HP-TLC-ESI/MS/MS. Individual species of unsaturated PtdCho were quantified based on their intensities and normalized to the total ion count for each spectrum. Only those that had significant changes compared to control are shown. Data are presented as the mean ± SD of five separate experiments. All species shown possess significant difference between control and BEL treatment ($P<0.05$).

A. LNCAP

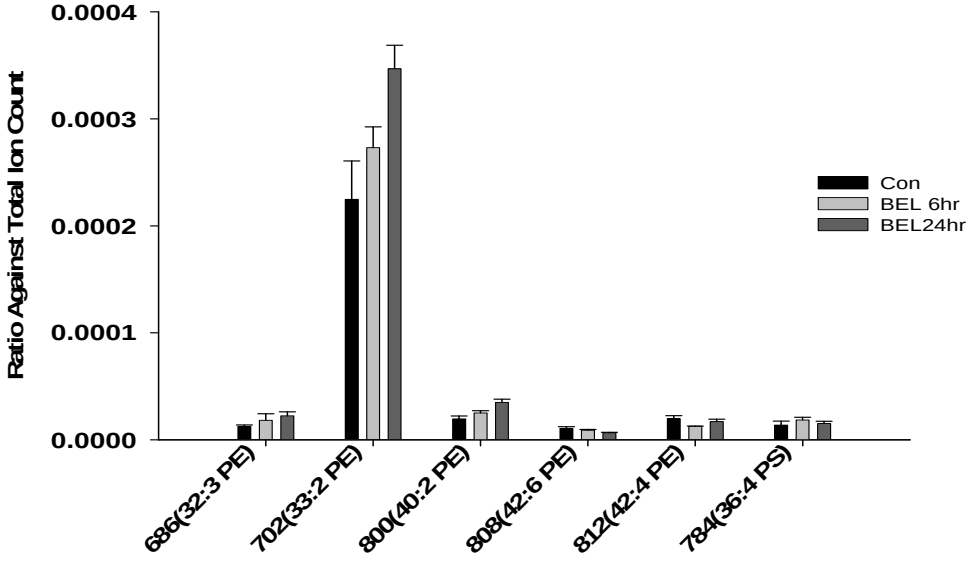

B. PC-3

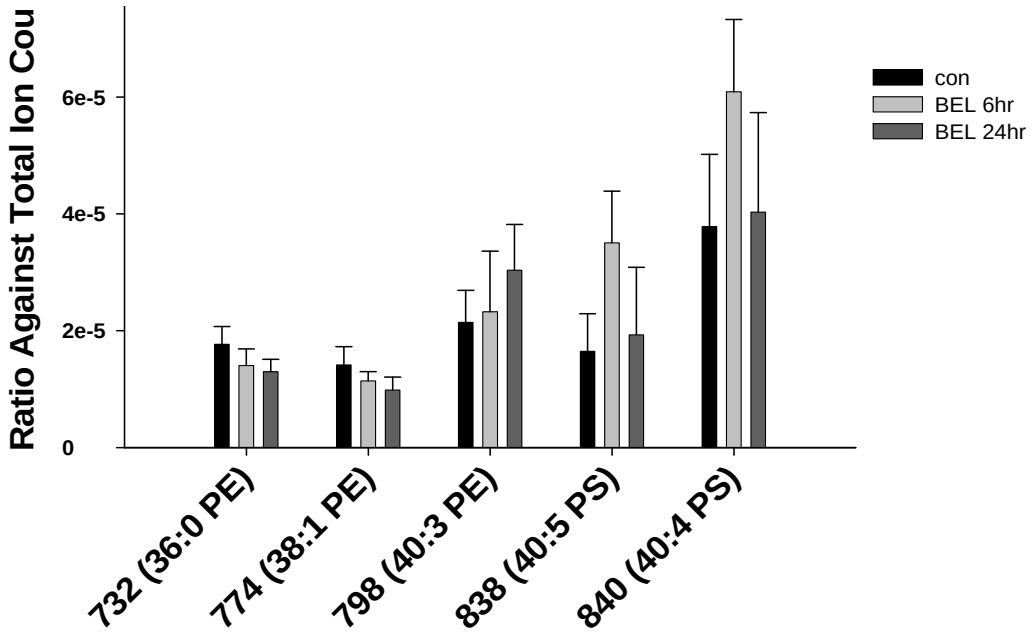

Figure 5.7 Effect of $iPLA_2$ inhibition on PtdEtn and PtdSer. LNCaP (**A**) and PC-3 (**B**) and were exposed to BEL (10 μM) for 6 and 24 hr prior to analysis of PtdEtn and PtdSer using 2D-HP-TLC-ESI/MS/MS. Individual phospholipids were quantified based on their intensities and normalized to the total ion count for each spectrum. Only those that had significant changes compared control are shown. Data are presented as the mean ± SD of five separate experiments. All species shown possess significant difference between control and BEL treatment ($P<0.05$).

Discussion

Phospholipids were historically considered as only building blocks of cellular membranes. However, in the last few decades, phospholipids have been found to be bioactive molecules. They can act as donors of several cell signaling lipids such as omega-3 and omega-6 polyunsaturated fatty acids (Daniel et al, 1981) and lysophospholipids. Altering the composition of phospholipids, either the head groups or fatty acyl chains, alters DNA synthesis, cell signaling, cell growth and cancer cell invasiveness (Khandwala et al, 1971; Sachinidis et al, 1999; Kano-Sueoka et al, 1990; Kano-Sueoka et al, 1993). More recently, phospholipids such as glycerophospholipids and sphingomyelin are demonstrated to be important component of lipid rafts, regulating cell signaling initiated by membrane associated receptors (Simons et al, 2000).

Two of the most important bioactive metabolites of phospholipids are lysophosphatidic acid (LPA) and arachidonic acid (AA), either of which has the ability to stimulate cell growth (Van Corven et al, 1989 and Moolenaar et al, 2004). To test the hypothesis that $iPLA_2$ inhibition induced cytostasis is caused by inhibition of LPA or AA production, we treated cells with exogenous 18:1 LPA, AA, LA and PGE_2 in cells in which $iPLA_2\beta$ was inhibited using siRNA. The results showed that none of these lipids significantly altered cytostasis induced by $iPLA_2\beta$ siRNA. This suggests that cytostasis induced by $iPLA_2\beta$ inhibition is not mediated by LPA or AA/PGE_2 pathways.

In the absence of effect of LPA or fatty acids, we tested the hypothesis that $iPLA_2$ inhibition decreases prostate cancer cell growth by altering phospholipid profiles using 2D-HP-TLC-ESI/MS. These data suggest that BEL treatment predominantly alters PtdCho by increasing PUFA containing phospholipids and decreasing abundance of SFA containing PtdCho phospholipids. The fact that BEL only slightly alters a few PtdEtn and PtdSer species in either

cell line suggest that $iPLA_2$ is not primarily involved in the regulation of these phospholipids in these cells. This finding is significant because $iPLA_2$ is reported to have little preference for specific head groups in cell-free systems (Tang et al, 1997; Yang et al, 1999). Thus, additional regulatory systems may exist in cancer cells controlling the specific targeting of PtdCho by BEL.

Collectively, these data show that treatment of PC-3 and LNCaP cells with classic lipid mitogens does not reverse cytostasis induced by inhibition of $iPLA_2$. These data also show that $iPLA_2$ inhibition alters the phospholipid profiles of these cells, predominately those lipid containing choline head groups. It is still unclear how increasing PUFA-containing PtdCho mediates cytostasis, and it is also unknown if changes in PtdCho are occurring at specific organelles, such as the nucleus. It is possible that the increase in PUFA containing PtdCho in cancer cells occurs at the nucleus, which may slow down DNA synthesis (Sachinidis et al, 1999). It is also possible that increasing PUFA-containing PtdCho alters the structures and functions of lipid rafts, which subsequently attenuates certain growth factor receptors-mediated signaling, such as EGFR (Schley et al, 2007). Further studies are needed to address these hypotheses.

CHAPTER 6

SUMMARY

The overall hypothesis of this research was that inhibition of $iPLA_2$ decreased prostate cancer cell proliferation. A three-fold research plan was undertaken to test this hypothesis. The first part of research determined that $iPLA_2$ inhibition induced cytostasis, but not cell death, through p53-dependent and -independent pathways in prostate cancer cells. The second part demonstrated that activation of a RS/p38MAPK/p53 pathway mediated cytostasis induced by $iPLA_2$ inhibition. The last part assessed the lipid singling molecules targeted by $iPLA_2$ inhibition and identified the specific phospholipids altered during cytostasis.

This study demonstrates, for the first time, the expression and activity of $iPLA_2\gamma$ and $iPLA_2\beta$ in LNCaP and PC-3 human prostate cancer cell lines. This report also demonstrated the novel finding that $iPLA_2$ inhibition induced cytostasis in a p53-independent manner. Inhibition of $iPLA_2$ activity was achieved through the use of the pharmacological inhibitor, bromonenol lactone (BEL) or molecular inhibitor, $iPLA_2\beta$ siRNA.

Inhibition of $iPLA_2$ decreased prostate cancer cell growth by inducing cytostasis, not cell death. Cytostasis correlated to a p53/p21-dependent G1 cell cycle arrest in LNCaP cells, but a p53-independent G2/M arrest in PC-3 cells. Further, selective inhibition of $iPLA_2\beta$ using *S*-BEL induced greater decreases in cell growth compared to that seen when $iPLA_2\gamma$ was inhibited using the $iPLA_2\gamma$ inhibitor *R*-BEL. This suggested that $iPLA_2\beta$ plays a more important role in prostate

cancer cell growth than iPLA$_2$γ. The role of iPLA$_2$β in growth in these cells was validated using small interference RNA (siRNA) against iPLA$_2$β.

Studies assessing MAPK activation demonstrated that iPLA$_2$ inhibition activated p38 and ERK, but not JNK in prostate cancer cells. Interestingly, p38 was consistently induced by iPLA$_2$ inhibition in both cell lines while ERK1/2 was transiently activated only in PC-3 cells. Use of selective pharmacological inhibitors against p38 and ERK1/2 demonstrated that p38 mediated p53 phosphorylation and activation in LNCaP cells. In contrast, the activation of ERK1/2 in PC-3 cells appeared to be a protective mechanism. Studies investigating the mechanisms of p38 and ERK1/2 activation showed that iPLA$_2$ inhibition-induced RS that were blocked by pretreatment with N-acetylcysteine (NAC). NAC subsequently attenuated p38, p53 and p21 activation induced by iPLA$_2$ inhibition. This suggests the novel finding that a RS/p38/p53/p21 pathway is involved in cytostasis induced by iPLA$_2$ inhibition. Subsequent studies also suggest that ERK1/2 activation is dependent on EGFR and MMP. The schematic summary of p38 and ERK pathways activated by iPLA$_2$ inhibition is shown in **Figure 6.1**.

Our studies also demonstrate that p38 plays a partial role in cytostasis induced by iPLA$_2$ inhibition. Thus, we tested the hypothesis that iPLA$_2$ inhibition induced cytostasis by altering the generation of bioactive lipids or by altering lipid profiles. In doing so we demonstrated that LPA, AA, LA or PGE$_2$ did not reverse cytostasis induced by iPLA$_2$ inhibition, nor did they alter p53 induction. This suggests that the cytostasis induced by iPLA$_2$ inhibition does not result from a decrease in production of these lipids. Assessment of the lipidomic profile of these cells in the presence and absence of BEL indicated that iPLA$_2$ inhibition tended to increase the abundance of PtdCho containing polyunsaturated fatty acids, while decreasing the abundance of PtdCho

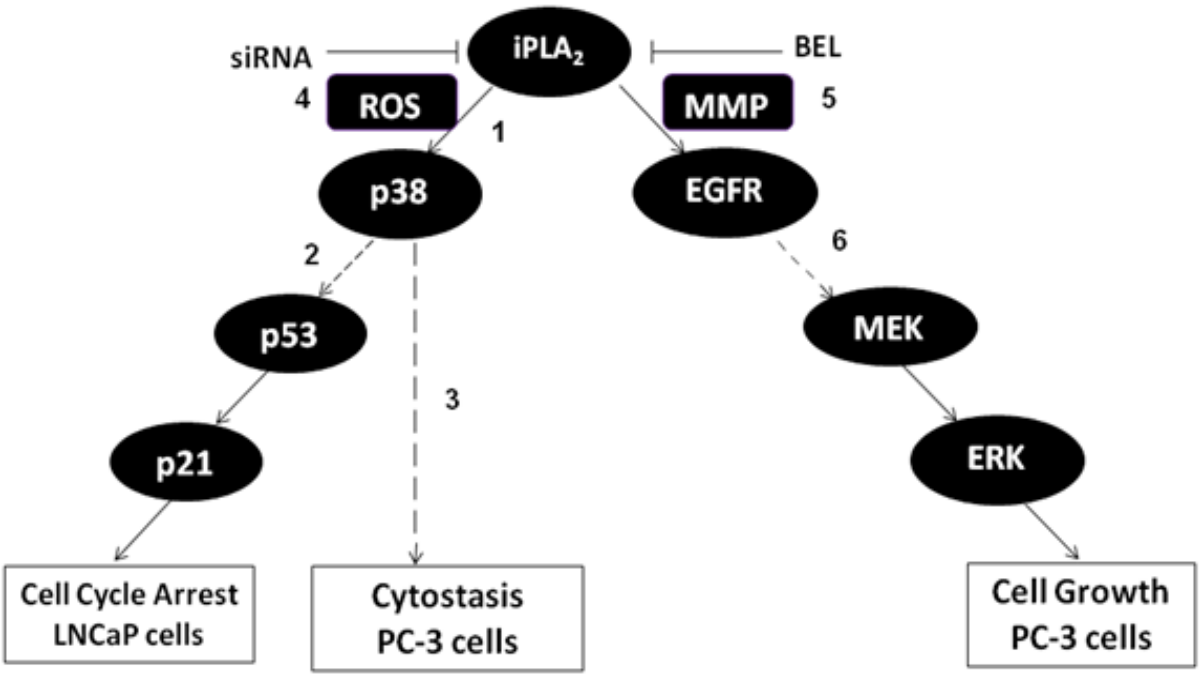

Figure 6.1 Proposed pathways for activation of MAPK in prostate cancer cells during $iPLA_2$ inhibition. **1.** Inhibition of $iPLA_2$ using either BEL or siRNA results in activation of p38 in both LNCaP and PC-3 cells. **2.** Activation of p38 in LNCaP cells increases the expression of p53 and p21 and induces cell cycle arrest. **3.** In PC-3 cells p38 activation correlates to cytostasis. **4.** RS may be involved in BEL induced p38 activation. **5.** Inhibition of $iPLA_2$ in PC-3 cells activates EGFR using mechanisms possibly involving MMP. **6.** EGFR activation mediates activation of ERK1/2 using MEK. The dashed lines represent possible indirect interactions.

containing saturated fatty acids; however the physiological significance of these events remains undetermined.

Collectively, these studies support the hypothesis that $iPLA_2$ mediates prostate cancer cell growth and that it is a potential therapeutic target for both early-stage and late-stage prostate cancer. These data also demonstrate that $iPLA_2$ primarily regulates phospholipids profiles in these cells, as opposed to being a major producer of bioactive metabolites, such as AA and LPA.

Future studies will include a two-aim research plan. The first aim will be an *in vivo* study testing the hypothesis that $iPLA_2$ inhibition decreases xenograft prostate tumor growth. The second aim will focus on further lipidomic analysis assessing the lipidomics of both subcellular membrane fractions and lipid rafts.

REFERENCES

Ackermann EJ, Conde-Frieboes K and Dennis EA (1995). Inhibition of macrophage Ca(2+)-independent phospholipase A2 by bromoenol lactone and trifluoromethyl ketones. *J Biol Chem* **270**: 445-50.

Ackermann EJ, Kempner ES and Dennis EA (1994). Ca(2+)-independent cytosolic phospholipase A2 from macrophage-like P388D1 cells. Isolation and characterization. *J Biol Chem* **269**: 9227-33.

Adibhatla RM, Hatcher JF, Larsen EC, Chen X, Sun D and Tsao FH (2006). CDP-choline significantly restores phosphatidylcholine levels by differentially affecting phospholipase A2 and CTP: phosphocholine cytidylyltransferase after stroke. *J Biol Chem* **281**:6718-25.

Aoki J (2004). Mechanisms of lysophosphatidic acid production. *Semin Cell Dev Biol* **15**:477-89.

Aoki J, Taira A, Takanezawa Y, Kishi Y, Hama K, Kishimoto T, Mizuno K, Saku K, Taguchi R and Arai H (2002). Serum lysophosphatidic acid is produced through diverse phospholipase pathways. *J Biol Chem* **277**: 48737-44.

Aoto M, Shinzawa K, Suzuki Y, Ohkubo N, Mitsuda N, Tsujimoto Y (2009). Essential role of p38 MAPK in caspase-independent, iPLA$_2$-dependent cell death under hypoxia/low glucose conditions. *FEBS Letters* **583**: 1611-18.

Aparicio Gallego G, Díaz Prado S, Jiménez Fonseca P, García Campelo R, Cassinello Espinosa J, Antón Aparicio LM (2007). Cyclooxygenase-2 (COX-2): a molecular target in prostate cancer. *Clin Transl Oncol* **9**:694–702

Attiga FA, Fernandez PM, Weeraratna AT, Manyak MJ, Patierno SR (2000). Inhibitors of prostaglandin synthesis inhibit human prostate tumor cell invasiveness and reduce the release of matrix metalloproteinases *Cancer Res* **60**:4629–37.

Atsumi G, Tajima M, Hadano A, Nakatani Y, Murakami M and Kudo I (1998). Fas-induced arachidonic acid release is mediated by Ca2+-independent phospholipase A2 but not cytosolic phospholipase A2, which undergoes proteolytic inactivation. *J Biol Chem* **273**: 13870-7.

Avruch J, Zhang XF, and Kyriakis JM (1994). Raf meets Ras: completing the framework of a signal transduction pathway. *Trends Biochem Sci* **19**: 279-83,

Bae IH, Kang SW, Yoon SH, Um HD (2006). Cellular components involved in the cell death induced by cisplatin in the absence of p53 activation. *Oncol Rep* **15**: 1175-80.

Balboa MA and Balsinde J (2002). Involvement of calcium-independent phospholipase A2 in hydrogen peroxide-induced accumulation of free fatty acids in human U937 cells. *J Biol Chem* **277**: 40384-89.

Balboa MA, Balsinde J, Jones SS and Dennis EA (1997). Identity between the Ca2+-independent phospholipase A2 enzymes from P388D1 macrophages and Chinese hamster ovary cells. *J Biol Chem* **272**: 8576-80.

Balboa MA, Varela-Nieto I, Killermann Lucas K and Dennis EA (2002). Expression and function of phospholipase A(2) in brain. *FEBS Lett* **531**: 12-7.

Balsinde J (2002A). Roles of various phospholipases A2 in providing lysophospholipid acceptors for fatty acid phospholipidincorporation and remodelling. *Biochem J* **364**: 695–702.

Balsinde J and Balboa MA (2005). Cellular regulation and proposed biological functions of group VIA calcium-independent phospholipase A2 in activated cells. *Cell Signal* **17**: 1052-62.

Balsinde J, Balboa MA and Dennis EA (1997A). Antisense inhibition of group VI Ca2+-independent phospholipase A2 blocks phospholipid fatty acid remodeling in murine P388D1 macrophages. *J Biol Chem* **272**: 29317-21.

Balsinde J, Balboa MA, Insel PA and Dennis EA (1999). Regulation and inhibition of phospholipase A2. *Annu Rev Pharmacol Toxicol* **39**: 175-89.

Balsinde J, Bianco ID, Ackermann EJ, Conde-Frieboes K and Dennis EA (1995). Inhibition of calcium-independent phospholipase A2 prevents arachidonic acid incorporation and phospholipid remodeling in P388D1 macrophages. *Proc Natl Acad Sci U S A* **92**: 8527-31.

Balsinde J and Dennis EA (1996). Bromoenol lactone inhibits magnesium-dependent phosphatidate phosphohydrolase and blocks triacylglycerol biosynthesis in mouse P388D1 macrophages. *J Biol Chem* **271**: 31937-41.

Balsinde J and Dennis EA (1997B). Function and inhibition of intracellular calcium-independent phospholipase A2. *J Biol Chem* **272**:16069-72.

Balsinde J, Winstead MV and Dennis EA (2002B). Phospholipase A(2) regulation of arachidonic acid mobilization. *FEBS Lett* **531**: 2-6.

Bao S, Bohrer A, Ramanadham S, Jin W, Zhang S and Turk J (2006). Effects of stable suppression of Group VIA phospholipase A2 expression on phospholipid content and composition, insulin secretion, and proliferation of INS-1 insulinoma cells. *J Biol Chem* **281**: 187-98.

Bao S, Miller DJ, Ma Z, Wohltmann M, Eng G, Ramanadham S, Moley K and Turk J (2004). Male mice that do not express group VIA phospholipase A2 produce spermatozoa with impaired motility and have greatly reduced fertility. *J Biol Chem* **279**: 38194-200.

Barbour SE, Kapur A and Deal CL (1999). Regulation of phosphatidylcholine homeostasis by calcium-independent phospholipase A2. *Biochim Biophys Acta* **1439**: 77-88.

Baburina I and Jackowski S (1999). Cellular Responses to Excess Phospholipid. *J Biol Chem* **274**: 9400-8

Beckett CS, Pennington K, McHowat J (2006). Activation of MAPKs in thrombin-stimulated ventricular myocytes is dependent on Ca2+-independent PLA2. *Am J Physiol Cell Physiol* **290**: C1350-4.

Berti-Mattera LN, Harwalkar S, Hughes B, Wilkins PL, Almhanna K (2001). Proliferative and morphological effects of endothelins in Schwann cells: roles of p38 mitogen-activated protein kinase and Ca(2+)-independent phospholipase A2. *J Neurochem* **79**:1136-48.

Bevers EM, Comfurius P, Dekkers DW, Harmsma M and Zwaal RF (1998). Transmembrane phospholipid distribution in blood cells: control mechanisms and pathophysiological significance. *J Biol Chem* **379**: 973-86.

Bhat, N. R. and Zhang, P (1999). Hydrogen peroxide activation of multiple mitogen-activated protein kinases in an oligodendrocyte cell line: role of extracellular signal-regulated kinase in hydrogen peroxide-induced cell death. *J Neurochem*, **72***:* 112-19.

Bligh EG and Dyer WJ (1959). A rapid method of total lipid extraction and purification. *Can J Biochem Physiol* **37**: 911-17.

Bortner CD and Cidlowski JA (1999). Caspase independent/dependent regulation of K(+), cell shrinkage, and mitochondrial membrane potential during lymphocyte apoptosis. *J Biol Chem* **274**: 21953-62.

Bradham C, McClay DR (2006). p38 MAPK in development and cancer. *Cell Cycle* **5**: 824-8.

Brown L, Benchimol S (2006). The involvement of MAPK signaling pathways in determining the cellular response to p53 activation: cell cycle arrest or apoptosis. *J Biol Chem* **281**:3832-40.

Campbell, S. L., Khosravi-Far, R., Rossman, K. L., Clark, G. J., and Der, C. J (1998). Increasing complexity of Ras signaling. *Oncogene* **17**: 1395-413.

Capper EA and Marshall LA (2001). Mammalian phospholipases A(2): mediators of inflammation, proliferation and apoptosis. *Prog Lipid Res* **40**:167-97.

Cave WT Jr (1991). Dietary n-3 polyunsaturated fatty acid effects on animal tumorigenesis. *FASEB J* **5:** 2160-6

Chang HL, Wu YC, Su JH, Yeh YT, Yuan SS (2008). Protoapigenone, a novel flavonoid, induces apoptosis in human prostate cancer cells through activation of p38 mitogen-activated protein kinase and c-Jun NH2-terminal kinase 1/2. *J Pharmacol Exp Ther* **325**: 841-9.

Chen Z, Gibson TB, Robinson F, Silvestro L, Pearson G, Xu B (2001). MAP kinases. *Chem Rev* **101**:2449-76.

Choi, JW et al (2010). LPA receptors: subtypes and biological actions. *Annu. Rev. Pharmacol. Toxicol* **1781**: 531–9.

Clark JD, Lin LL, Kriz RW, Ramesha CS, Sultzman LA, Lin AY, Milona N and Knopf JL (1991) A novel arachidonic acid-selective cytosolic PLA2 contains a Ca(2+)-dependent translocation domain with homology to PKC and GAP. *Cell* **65**: 1043-51.

Cole MJ and Enke CG (1991). Direct determination of phospholipidstructures in microorganisms by fast bombardment triple quadrupole mass spectrometry, *Anal Chem.* **63**: 1032-38.

Cui Z and Houweling M (2002). Phosphatidylcholine and cell death. *Biochim Biophys Acta* **1585**: 87-96.

Cummings BS, Gelasco AK, Kinsey GR, McHowat J and Schnellmann RG (2004). Inactivation of endoplasmic reticulum bound Ca2+-independent phospholipase A2 in renal cells during oxidative stress. *J Am Soc Nephrol* **15**: 1441-51.

Cummings BS, McHowat J and Schnellmann RG (2000). Phospholipase A(2)s in cell injury and death. *J Pharmacol Exp Ther* **294**: 793-9.

Cummings BS, McHowat J and Schnellmann RG (2002). Role of an endoplasmic reticulum Ca(2+)-independent phospholipase A(2) in oxidant-induced renal cell death. *Am J Physiol Renal Physiol* **283**: F492-498.

Cummings BS and Schnellmann RG (2002). Cisplatin-induced renal cell apoptosis: caspase 3-dependent and -independent pathways. *J Pharmacol Exp Ther* **302**: 8-17.

Daniel LW, King L and Waite M (1981). Source of Arachidonic Acid for Prostaglandin Synthesis in Madin-Darby Canine Kidney Cel *J. Biol Chem* 256: 12830-35.

Das S, Castillo C and Stevens T (2001). Phospholipid remodeling/generation in Giardia: the role of the Lands cycle. *Trends in Parasitology* **17**: 316-319.

Dennis EA (1994). Diversity of group types, regulation, and function of phospholipase A2. *J Biol Chem* **269**: 13057-60.

Dennis EA (1997). The growing phospholipase A2 superfamily of signal transduction enzymes. *Trends Biochem Sci* **22**: 1-2.

Diez E, Chilton FH, Stroup G, Mayer RJ, Winkler JD and Fonteh AN (1994). Fatty acid and phospholipid selectivity of different phospholipase A2 enzymes studied by using a mammalian membrane as substrate. *Biochem J* **301**: 721-6.

Dong Q, Patel M, Scott KF, Graham GG, Russell PJ, Sved P (2006). Oncogenic action of phospholipase A2 in prostate cancer. *Cancer Lett* **240**: 9-16.

Eastham JA, Stapleton AM, Gousse AE, Timme TL, Yang G, Slawin KM (1995). Association of p53 mutations with metastatic prostate cancer. *Clin Cancer Res* **1:**1111-8.

Fan M, Chambers TC (2001). Role of mitogen-activated protein kinases in the response of tumor cells to chemotherapy. *Drug Resist Updat* **4**: 253-67.

Fajas L, Egler V, Reiter R, Miard S, Lefebvre AM, Auwerx J (2003). PPARγ controls cell proliferation and apoptosis in an RB-dependent manner. *Oncogene* **22**: 4186–93

Farooqui AA, Litsky ML, Farooqui T and Horrocks LA (1999). Inhibitors of intracellular phospholipase A2 activity: their neurochemical effects and therapeutical importance for neurological disorders. *Brain Res Bull* **49**: 139-53.

Fuentes L, Perez R, Nieto ML, Balsinde J and Balboa MA (2003). Bromoenol lactone promotes cell death by a mechanism involving phosphatidate phosphohydrolase-1 rather than calcium-independent phospholipase A2. *J Biol Chem* **278**: 44683-90.

Ghosh J., Myers C. E (1997). Arachidonic acid stimulates prostate cancer cell growth: critical role of 5-lipoxygenase. *Biochem Biophy. Res Commun* **235***:* 418-423.

Gijon MA, Spencer DM, Kaiser AL and Leslie CC (1999). Role of phosphorylation sites and the C2 domain in regulation of cytosolic phospholipase A2. *J Cell Biol* **145**:1219-32.

Gioeli D, Mandell JW, Petroni GR, Frierson (Jr.) HF, Weber MJ (1999). Activation of mitogen-activated protein kinase associated with prostate cancer progression. *Cancer Res* **59:**279-284.

Glaser KB (1995). Regulation of phospholipase A2 enzymes: selective inhibitors and their pharmacological potential. *Adv Pharmacol* **32**: 31-66.

Glunde K, Ackerstaff E, Mori N, Jacobs MA, and Bhujwalla ZM (2006). Choline Phospholipid Metabolism in Cancer:Consequences for Molecular Pharmaceutical Interventions. *Mol Pharmaceutics* **3**: 496-506

Graff JR, Konicek BW, Deddens JA, Chedid M, Hurst BM, Colligan B, Neubauer BL, Carter HW and Carter JH (2001). Expression of group IIa secretory phospholipase A_2 increases with prostate tumor grade. *Clin. Cancer Res* **7**: 3857–3861.

Green JT, Orr SK, Bazinet RP (2008). The emerging role of group VI calcium-independent phospholipase A2 in releasing docosahexaenoic acid from brain phospholipids. *J Lipid Res* **49**: 939-44.

Hassan S, Carraway RE (2006). Involvement of arachidonic acid metabolism and EGF receptor in neurotensin-induced prostate cancer PC3 cell growth. *Regulatory Peptides* **133**: 105-14.

Han WK, Sapirstein A, Hung CC, Alessandrini A, Bonventre JV (2003). Cross-talk between cytosolic phospholipase A2 alpha (cPLA2 alpha) and secretory phospholipase A2 (sPLA2) in hydrogen peroxide-induced arachidonic acid release in murine mesangial cells: sPLA2 regulates cPLA2 alpha activity that is responsible for arachidonic acid release. *J Biol Chem* **278**:24153-63.

Hazen SL, Stuppy RJ and Gross RW (1990). Purification and characterization of canine myocardial cytosolic phospholipase A2. A calcium-independent phospholipase with absolute f1-2 regiospecificity for diradyl glycerophospholipids. *J Biol Chem* **265**: 10622-30.

Hazen SL, Zupan LA, Weiss RH, Getman DP and Gross RW (1991). Suicide inhibition of canine myocardial cytosolic calcium-independent phospholipase A2. Mechanism-based discrimination between calcium-dependent and -independent phospholipases A2. *J Biol Chem* **266**: 7227-32.

Herbert SP, Walker JH (2006). Group VIA calcium-independent phospholipase A2 mediates endothelial cell S phase progression. *J Biol Chem* **281**: 35709–16.

Hiraoka M, Abe A and Shayman JA (2002). Cloning and characterization of a lysosomal phospholipase A2, 1-O-acylceramide synthase *J Biol Chem* **277**: 10090 – 99.

Hiraoka M, Abe A, Lu Y, Yang K, Han X, Gross RW and Shayman JA (2006). Lysosomal phospholipase A2 and phospholipidosis, Mol. Cell. Biol. 26 6139–48.

Hirabayashi T, Murayama T and Shimizu T (2005). "Regulatory mechanism and physiological role of cytosolic phospholipase A2." *Biol. Pharm. Bull.* **27**: 1168–73.

Iwashita A, Maemoto T, Nakada H, Shima I, Matsuoka N and Hisajima H (2003). A novel potent radical scavenger, 8-(4-fluorophenyl)-2-((2E)-3-phenyl-2-propenoyl)-1,2,3,4-tetrahydropyrazol o[5,1-c] [1,2,4]triazine (FR210575), prevents neuronal cell death in cultured primary neurons and attenuates brain injury after focal ischemia in rats. *J Pharmacol Exp Ther* **307**: 961-8.

Jarvi K, Langlais J, Gagnon C and Roberts KD (1993). Platelet-activating factor acetylhydrolase in the male reproductive tract: origin and properties. *Int J Androl* **16**: 121–127.

Jenkins CM, Han X, Mancuso DJ and Gross RW (2002). Identification of calcium-independent phospholipase A2 (iPLA2) beta, and not iPLA2gamma, as the mediator of arginine vasopressin-induced arachidonic acid release in A-10 smooth muscle cells. Enantioselective mechanism-based discrimination of mammalian iPLA2s. *J Biol Chem* **277**: 32807-14.

Jenkins CM, Mancuso DJ, Yan W, Sims HF, Gibson B and Gross RW (2004). Identification, cloning, expression, and purification of three novel human calcium-independent phospholipase A2 family members possessing triacylglycerol lipase and acylglycerol transacylase activities. *J Biol Chem* **279**: 48968-75.

Jenkins CM, Yan W, Mancuso DJ and Gross RW (2006). Highly selective hydrolysis of fatty acyl-CoAs by calcium-independent phospholipase A2beta. Enzyme autoacylation and acyl-CoA-mediated reversal of calmodulin inhibition of phospholipase A2 activity. *J Biol Chem* **281**: 15615-24.

Jing Q, Xin S-M, Cheng Z-J, Zhang W-B, Zhang R and Qin Y-W (1999). Activation of p38 Mitogen-Activated Protein Kinase by Oxidized LDL in Vascular Smooth Muscle Cells : Mediation via Pertussis Toxin–Sensitive G Proteins and Association With Oxidized LDL-Induced Cytotoxicity. *Circ Res* **84**: 831-39.

Kano-Sueoka T, King DM and Fisk HA (1990). Binding of epidermal growth factor to its receptor is affected by membrane phospholipid environment. *J. Cell. Physiol.* **145:** 543-8.

Kano-Sueoka, T.; Nicks, M. E (1993). Abnormal function of protein kinase C in ceils having phosphatidylethanolamine-deficient and phosphatidylcholineexcess membranes. *Cell Growth Differ* **4**: 533-37.

Karlsson AÅ, Michelsen P, Larsen Å, and Odham G (1996). Normal-phase Liquid Chromatography Class Separation and Species Determination of Phospholipids Utilizing Electrospray Mass Spectrometry/Tandem Mass Spectrometry *Rapid Commun. Mass Spectrom* **10**: 775-780

Kell PJ, Creer MH, Crown KN, Wirsig K and McHowat J (2003). Inhibition of platelet-activating factor (PAF) acetylhydrolase by methyl arachidonyl fluorophosphonate potentiates PAF synthesis in thrombin-stimulated human coronary artery endothelial cells. *J Pharmacol Exp Ther* **307**: 1163–70.

Khandwala AS. and Kasper CB (1971). The fatty acid composition of individual phospholipids from rat liver nuclear membrane and nuclei. *J Biol Chem* **246**: 6242-6.

Kim BJ, Ryu SW and Song BJ (2006). JNK- and p38 kinase-mediated phosphorylation of Bax leads to its activation and mitochondrial translocation and to apoptosis of human hepatoma HepG2 cells. *J Biol Chem* **281**: 21256-65.

Kinsey GR, Cummings BS, Beckett CS, Saavedra G, Zhang W, McHowat J and Schnellmann RG (2005). Identification and distribution of endoplasmic reticulum iPLA2. *Biochem Biophys Res Commun* **327**: 287-293.

Kinsey GR, Blum JL, Covington MD, Cummings BS, McHowat J and Schnellmann RG (2008). Decreased iPLA2gamma expression induces lipid peroxidation and cell death and sensitizes cells to oxidant-induced apoptosis. *J Lipid Res* **49**: 1477-87.

Krishna M and Narang H (2008). The complexity of mitogen-activated protein kinases (MAPKs) made simple. *Cell Mol Life Sci* **65**: 3525-44.

Kyriakis JM, Banerjee P, Nikolakaki E, Dai T, Rubie EA and Ahmad MF (1994). The stress-activated protein kinase subfamily of c-Jun kinases. *Nature* **369**:156-60.

Lands WE (1965). Lipid Metabolism. *Annu Rev Biochem* **34**:313-346.

Larsson Forsell PK, Kennedy BP and Claesson HE (1999). The human calcium-independent phospholipase A2 gene multiple enzymes with distinct properties from a single gene. *Eur J Biochem* **262**: 575-585.

Lio YC, Reynolds LJ, Balsinde J and Dennis EA (1996). Irreversible inhibition of Ca(2+)-independent phospholipase A2 by methyl arachidonyl fluorophosphonate. *Biochim Biophys Acta* **1302**: 55-60.

Loeffler M and Kroemer G (2000). The mitochondrion in cell death control: certainties and incognita. *Exp Cell Res* **256**: 19-26.

Lu X, Ma O, Nguyen TA, Jones SN, Oren M, and Donehower LA (2007) The Wip1 phosphatase acts as a gatekeeper in the p53-Mdm2 autoregulatory loop. *Cancer Cell* **12**: 342–354.

Ma Z, Ramanadham S, Kempe K, Chi XS, Ladenson J and Turk J (1997). Pancreatic islets express a Ca2+-independent phospholipase A2 enzyme that contains a repeated structural motif homologous to the integral membrane protein binding domain of ankyrin. *J Biol Chem* **272**: 11118-27.

Ma Z, Wang X, Nowatzke W, Ramanadham S and Turk J (1999). Human pancreatic islets express mRNA species encoding two distinct catalytically active isoforms of group VI phospholipase A2 (iPLA2) that arise from an exon-skipping mechanism of alternative splicing of the transcript from the iPLA2 gene on chromosome 22q13.1. *J Biol Chem*; **274**: 9607–16.

Ma Z, Ramanadham S, Wohltmann M, Bohrer A, Hsu FF and Turk J (2001). Studies of insulin secretory responses and of arachidonic acid incorporation into phospholipids of stably transfected insulinoma cells that overexpress group VIA phospholipase A2 (iPLA2beta)

indicate a signaling rather than a housekeeping role for iPLA2beta. *J Biol Chem* **276**: 13198-208.

Mancuso DJ, Abendschein DR, Jenkins CM, Han X, Saffitz JE, Schuessler RB and Gross RW (2003). Cardiac ischemia activates calcium-independent phospholipase A2beta, precipitating ventricular tachyarrhythmias in transgenic mice: rescue of the lethal electrophysiologic phenotype by mechanism-based inhibition. *J Biol Chem* **278**: 22231-36.

Mancuso DJ, Jenkins CM and Gross RW (2000). The genomic organization, complete mRNA sequence, cloning, and expression of a novel human intracellular membrane-associated calcium-independent phospholipase A(2). *J Biol Chem* **275**: 9937-9945.

Mancuso DJ, Jenkins CM, Sims HF, Cohen JM, Yang J and Gross RW (2004). Complex transcriptional and translational regulation of iPLAgamma resulting in multiple gene products containing dual competing sites for mitochondrial or peroxisomal localization. *Eur J Biochem* **271**: 4709-24.

Manguikian AD and Barbour SE (2004). Cell cycle dependence of group VIA calcium-independent phospholipase A2 activity. *J Biol Chem* **279**: 52881-92.

Marshall M (1995). Interactions between Ras and Raf: key regulatory proteins in cellular transformation. *Mol Reprod Dev* **42**: 493-499.

Martinez J and Moreno JJ (2001). Role of Ca2+-independent phospholipase A2 on arachidonic acid release induced by reactive oxygen species. *Arch Biochem Biophys* **392**: 257-262.

McHowat J, Kell PJ, O'Neill HB, and Creer MH (2001). Endothelial cell PAF synthesis following thrombin stimulation utilizes Ca2+-independent phospholipaseA2. *Biochemistry* **40**: 14921–14931.

Meyer AM, Dwyer-Nield LD, Hurteau GJ, Keith, RL, O'Leary E and You M (2004). Decreased lung tumorigenesis in mice genetically deficient in cytosolic phospholipase A2. *Carcinogenesis* **25**: 1517–1524.

Meyer HD and Jakobs KH (2007). "Lysophospholipid receptors: signalling, pharmacology and regulation by lysophospholipid metabolism". *Biochim Biophys Acta* **1768**: 923–40.

Moolenaar WH, van Meeteren LA and Giepmans BN(2004), The ins and outs of lysophosphatidic acid signaling, *Bioessays* **26:** 870–812.

Mori N, Delsite R, Natarajan K, Kulawiec M, Bhujwalla Z M and Singh KK (2004). Loss of p53 function in colon cancer cells results in increased phosphocholine and total choline. *Mol. Imagine* **3**: 319-23.

Morrison DK and Cutler RE (1997). The complexity of Raf-1 regulation. *Curr Opin Cell Biol* **9**: 174-9.

Murrant CL and Reid MB (2001). Detection of reactive oxygen and reactive nitrogen species in skeletal muscle. *Microscopy Research and Technique* **55:** 236-48.

Murakami M, Masuda S, Ueda-Semmyo K, Yoda E, Kuwata H, Takanezawa Y, Aoki J, Arai H, Sumimoto H, Ishikawa Y, Ishii T, Nakatani Y and Kudo I (2005). Group VIB Ca2+-independent phospholipase A2gamma promotes cellular membrane hydrolysis and prostaglandin production in a manner distinct from other intracellular phospholipases A2. *J Biol Chem* **280**: 14028-41.

Nakano T, Inoue I, Shinozaki R, Matsui M, Akatsuka A, Takahashi S, Tanaka K, Akita M, Seo M, Hokari S, Katayama S and Komoda T (2009). A possible role of lysophospholipids produced by calcium-independent phospholipase A2 in membrane-raft budding and fission. *Biochimica et Biophysica Acta* **1788**: 2222-8.

Oh-Hashi K, Maruyama W and Isobe K (2001). Peroxynitrite induces GADD34, 45, and 153 VIA p38 MAPK in human neuroblastoma SH-SY5Y cells. *Free Radic Biol Med* **30**: 213-21.

Ongusaha PP, Kwak JC, Zwible AJ, Macip S, Higashiyama S, Taniguchi N, Fang L, and Lee SW (2004). HB-EGF is a potent inducer of tumor growth and angiogenesis. *Cancer Res* **64:** 5283-90.

Oyama Y, Hayashi A, Ueha T and Maekawa K (1994). Characterization of 2',7'-dichlorofluorescin fluorescence in dissociated mammalian brain neurons: estimation on intracellular content of hydrogen peroxide. *Brain Research* **635:** 113-7.

Pandalai PK, Pilat MJ, Yamazaki K, Naik H and Pienta KJ (1996). The effects of omega-3 and omega-6 fatty acids on in vitro prostate cancer growth. *Anticancer Res* **16:** 815-20.

Patel MI, Singh J, Niknami M, Kurek C, Yao M, Lu S, Maclean F, King NJ, Gelb MH, Scott KF, Russell PJ, Boulas J and Dong Q (2008). Cytosolic phospholipase A2-alpha: a potential therapeutic target for prostate cancer. *Clin Cancer Res.* **14**: 8070-9

Perez R, Melero R, Balboa MA and Balsinde J (2004). Role of group VIA calcium-independent phospholipase A2 in arachidonic acid release, phospholipid fatty acid incorporation, and apoptosis in U937 cells responding to hydrogen peroxide. *J Biol Chem* **279**: 40385-91.

Peterson B, Knotts T and Cummings BS (2007). Involvement of Ca(2+)-independent phospholipase A(2) isoforms in oxidant-induced neural cell death. *Neurotoxicology* **28**: 150-160.

Peterson B (2007). Roles of Ca(2+)-independent phospholipase A(2) isoforms in oxidant-induced neural cell death. *PhD Disseration University of Georgia* **2**: 23

Petkovic M, Schiller J, Muller M, Benard S, Reichl S, Arnold K and Arnhold J (2001). Detection of individual phospholipids in lipid mixtures by matrix-assisted laser desorption/ionization time-of-flight mass spectrometry: phosphatidylcholine prevents the detection of further species. *Anal Biochem* **289**: 202–216.

Pickard RT, Chiou XG, Strifler BA, DeFelippis MR, Hyslop PA, Tebbe AL, Yee YK, Reynolds LJ, Dennis EA, Kramer RM and Sharp JD (1996). Identification of essential residues for the catalytic function of 85-kDa cytosolic phospholipase A2. Probing the role of histidine, aspartic acid, cysteine, and arginine. *J Biol Chem* **271**:19225-31.

Pommery N, Henichart JP (2005). Involvement of PI3K/Akt pathway in prostate cancer--potential strategies for developing targeted therapies. *Mini Rev Med Chem* **5**: 1125-32.

Pulfer M and Murphy RC (2003). Electrospray mass spectrometry of phospholipids. *Mass Spectrom Rev* **22**: 332-64.

Ramanadham S, Yarasheski KE, Silva MJ, Wohltmann M, Novack DV and Christiansen B (2008). Age-related changes in bone morphology are accelerated in group VIA phospholipase A2 (iPLA2beta)-null mice. *Am J Pathol* **172**: 868–81.

Ramanadham S, Hsu FF, Bohrer A, Ma Z and Turk J (1999). Studies of the role of group VI phospholipase A2 in fatty acid incorporation, phospholipid remodeling, lysophosphatidylcholine generation, and secretagogue-induced arachidonic acid release in pancreatic islets and insulinoma cells. *J Biol Chem* **274**: 13915-27.

Reinhardt HC, Aslanian AS, Lees JA and Yaffe MB (2007). p53-deficient cells rely on ATM- and ATR-mediated checkpoint signaling through the p38MAPK/MK2 pathway for survival after DNA damage. *Cancer Cell* **11**:175-89.

Rordorf G, Uemura Y and Bonventre JV (1991). Characterization of phospholipase A2 (PLA2) activity in gerbil brain: enhanced activities of cytosolic, mitochondrial, and microsomal forms after ischemia and reperfusion. *J Neurosci* **11**: 1829-36.

Rose DP and Cohen LA (1988). Effects of dietary menhaden oil and retinol acetate on the growth of DU145 human prostatic adenocarcinoma cells transplanted into athymic nude mice. *Carcinogenesis* **9:** 603-5

Rose DP, Connolly JM (1991). Effects of fatty acids and eicosanoid synthesis inhibitors on the growth of two human prostate cancer cell lines. *Prostate* **18:** 243-54

Roshak AK, Capper EA, Stevenson C, Eichman C and Marshall LA (2000). Human calcium-independent phospholipase A2 mediates lymphocyte proliferation. *J Biol Chem* **275**: 35692-8.

Saavedra G, Zhang W, Peterson B and Cummings BS (2006). Differential Roles for Cytosolic and Microsomal Ca2+-Independent Phospholipase A2 in Cell Growth and Maintenance of Phospholipids 10.1124/jpet.106.105650. *J Pharmacol Exp Ther* **318**: 1211-9.

Sabbatini M, Santillo M, Pisani A, Paterno R, Uccello F, Seru R, Matrone G, Spagnuolo G, Andreucci M, Serio V, Esposito P, Cianciaruso B, Fuiano G, and Avvedimento EV (2006). Inhibition of Ras/ERK1/2 signaling protects against postischemic renal injury. *Am J Physiol Renal Physiol* **290**: F1408-15.

Sachinidis A, Carniel M, Seewald S, Seul C, Gouni-Berthold, I., Ko, Y. and Vetter, H. (1999). Lipid-induced changes in vascular smooth muscle cell membrane fluidity are associated with DNA synthesis. *Cell Prolif.* **32:** 101-5.

Schaloske RH, Dennis EA (2006). The phospholipase A2 superfamily and its group numbering system. *Biochimica et Biophysica Acta* **1761**: 1246 – 59.

Schley PD, Brindley DN and Field CJ (2007). (*n*−3) PUFA alter raft lipid composition and decrease epidermal growth factor receptor levels in lipid rafts of human breast cancer cells. *J Nutr* **137**: 548–53.

Seegers HC, Gross RW and Boyle WA (2002). Calcium-independent phospholipase A(2)-derived arachidonic acid is essential for endothelium-dependent relaxation by acetylcholine. *J Pharmacol Exp Ther* **302**: 918-23.

Seger R and Krebs EG (1995). The MAPK signaling cascade. *Faseb J* **9**:726-35.

Seleznev K, Zhao C, Zhang XH, Song K and Ma ZA (2006). Calcium-independent phospholipase A2 localizes in and protects mitochondria during apoptotic induction by staurosporine. *J Biol Chem* **281**: 22275-88.

Senguptas S, Xiao YJ and Xu Y(2007). A novel laminin-induced LPA autocrine loop in the migration of ovarian cancer cells. *FASEB Journal* **17**: 1570-72

Simons K, and Toomre D (2000). Lipid rafts and signal transduction. *Nat Rev Mol Cell Biol* **1**: 31-9

Song H, Bao S, Ramanadham S, and Turk J (2006A). Effects of biological oxidants on the catalytic activity and structure of group VIA phospholipase A2. *Biochemistry* **45**: 6392-406.

Song H, Ramanadham S, Bao S, Hsu F and Turk J (2006B). A Bromoenol Lactone Suicide Substrate Inactivates Group VIA Phospholipase A2 by Generating a Diffiusible Bromomethyl Keto Acid That Alkylates Cysteine Thiols. *Biochemistry* **45**: 1061-73.

Song H, Wohltmann M, Bao S, Ladenson J, Semenkovich C and Turk J (2010). Mice Deficient in Group VIB Phospholipase A_2 (iPLA2g) Exhibit Relative Resistance to Obesity and Metabolic Abnormalities Induced by a Western Diet. *Am J Physiol Endocrinol Metab* **298**: E1097 – E1114.

Song K, Zhang X, Zhao C, Ang NT and Ma ZA (2005). Inhibition of Ca2+-independent phospholipase A2 results in insufficient insulin secretion and impaired glucose tolerance. *Mol Endocrinol* **19**: 504-15.

Stewart A, Ghosh M, Spencer DM and Leslie CC (2002). Enzymatic Properties of Human Cytosolic Phospholipase A2 gamma. *J Biol Chem.* **277**: 29526-36.

Su X, Mancuso DJ, Bickel PE, Jenkins CM and Gross RW (2004). Small interfering RNA knockdown of calcium-independent phospholipases A2 beta or gamma inhibits the hormone-induced differentiation of 3T3-L1 preadipocytes. *J Biol Chem* **279**: 21740-48.

Sun GY, Xu J, Jensen MD, Yu S, Wood WG, Gonzalez FA, Simonyi A, Sun AY and Weisman GA (2005) Phospholipase A2 in astrocytes: responses to oxidative stress, inflammation, and G protein-coupled receptor agonists. *Mol Neurobiol* **31**: 27-41.

Surette ME, Winkler JD, Fonteh AN and Chilton FH (1996). Relationship between arachidonate-phospholipid remodeling and apoptosis. *Biochemistry* **35**: 9187–96.

Surette ME, Fonteh AN, Bernatchez C, Chilton FH. (1999). Perturbations in the control of cellular arachidonic acid levels block cell growth and induce apoptosis in HL-60 cells. *Carcinogenesis* **20**: 757-63.

Sved P, Scott KF, McLeod D, King N, Singh J, Tsatralis T, Niloloc B, Boulas J, Nallan L, Gelb MH, Sajinovic M, Graham G, Russel PJ, Dong Q (2004). Oncogenic action of secreted phospholipase A2 in prostate cancer. *Cancer Ree* **64**: 6934-40

Taguchi R, Hayakawa J, Takeuchi Y and Ishida M (2000). Two-dimensional analysis of phospholipids by capillary liquid chromatography/electrospray ionization mass spectrometry. *J Mass Spectrom* **35**: 953-966.

Tanaka H, Takeya R and Sumimoto H (2000). A novel intracellular membrane-bound calcium-independent phospholipase A(2). *Biochem Biophys Res Commun* **272**: 320-6.

Tang J, Kriz RW, Wolfman N, Shaffer M, Seehra J and Jones SS (1997). A novel cytosolic calcium-independent phospholipase A2 contains eight ankyrin motifs. *J Biol Chem* **272**: 8567-75.

Teslenko V, Rogers M and Lefkowith JB (1997). Macrophage arachidonate release via both the cytosolic Ca(2+)-dependent and -independent phospholipases is necessary for cell spreading. *Biochim Biophys Acta* **1344**: 189-199.

Van Corven EJ, Groenink A, Jalink K, Eichholtz T and Moolenaar WH (1989). Lysophosphatidate-induced cell proliferation: identification and dissection of signaling pathways mediated by G proteins. *Cell* **59**: 45–54.

Vijayakrishnan R (2009). Dual LOX/COX inhibitors: potential novel anti-cancer drugs. Irish *Journal of Medical Science* **178**: 517.

Wang X, Martindale JL, and Holbrook NJ (2000). Requirement for ERK activation in cisplatin-induced apoptosis. *J Biol Chem* **275**: 39435-43.

Wenk MR (2005). "The emerging field of lipidomics". *Nat Rev Drug Discov* **4**: 594–610

Wilkins WP 3rd and Barbour SE (2008). Group VI phospholipases A2: homeostatic phospholipases with significant potential as targets for novel therapeutics. *Curr Drug Targets* **9**: 683-97.

Williams NG and Roberts TM (1994). Signal transduction pathways involving the Raf proto-oncogene. *Cancer Metastasis Rev* **13:** 105-16.

Winkler JD, Eris T, Sung CM, Chabot-Fletcher M, Mayer RJ, Surette ME and Chilton FH (1996). Inhibitors of CoA-independent transacylase induce apoptosis in human HL-60 cells. *J Pharmacol Exp Therapeut* **279**: 956–66.

Woo KJ, Lee TJ, Lee SH, Lee JM, Seo JH, Jeong YJ, et al (2007). Elevated gadd153/chop expression during resveratrol-induced apoptosis in human colon cancer cells. *Biochem Pharmacol* **73**: 68-76.

Xu J, Weng YI, Simonyi A, Krugh BW, Liao Z, Weisman GA and Sun GY (2002) Role of PKC and MAPK in cytosolic PLA2 phosphorylation and arachadonic acid release in primary murine astrocytes. *J Neurochem* **83**:259-270.

Xu J, Yu S, Sun AY and Sun GY (2003). Oxidant-mediated AA release from astrocytes involves cPLA(2) and iPLA(2). *Free Radic Biol Med* **34**:1531-43.

Xu KP, Yin J, and Yu FS (2007). Lysophosphatidic acid promoting corneal epithelial wound healing by transactivation of epidermal growth factor receptor. *Invest Ophthalmol Vis Sci* **48***:* 636-43.

Yan W, Jenkins CM, Han X, Mancuso DJ, Sims HF, Yang K and Gross RW (2005). The highly selective production of 2-arachidonoyl lysophosphatidylcholine catalyzed by purified calcium-independent phospholipase A2gamma: identification of a novel enzymatic mediator for the generation of a key branch point intermediate in eicosanoid signaling. *J Biol Chem* **280**: 26669-79.

Yang HC, Mosior M, Ni B and Dennis EA (1999). Regional distribution, ontogeny, purification, and characterization of the Ca2+-independent phospholipase A2 from rat brain. *J Neurochem* **73**:1278-1287.

Yong Q, Chen et al (2007). "Modulation of prostate cancer genetic risk by omega-3 and omega-6 fatty acids". *The Journal of Clinical Investigation* **117**: 1866–75.

Zhang L, Peterson BL and Cummings BS (2005). The effect of inhibition of Ca2+-independent phospholipase A2 on chemotherapeutic-induced death and phospholipid profiles in renal cells. *Biochem Pharmacol* **70**: 1697-706.

Zhang XH, Zhao C, Seleznev K, Song K, Manfredi JJ, and Ma ZA (2006). Disruption of G1-phase phospholipid turnover by inhibition of Ca2+-independent phospholipase A2 induces a p53-dependent cell-cycle arrest in G1 phase. *J Cell Sci* **119:** 1005–15.

Zhao Y, He D, Saatian B, Watkins T, Spannhake EW, Pyne NJ and Natarajan V(2006). Regulation of lysophosphatidic acid-induced epidermal growth factor receptor transactivation and interleukin-8 secretion in human bronchial epithelial cells by protein kinase Cdelta, Lyn kinase, and matrix metalloproteinases. *J Biol Chem* **281**: 19501-11.

Zhou X and Arthur G (1992). Improved procedures for the determination of lipid phosphorus by malachite green. *J Lipid Res* **33**: 1233-6.